1-1-2017

Design, Evaluation, and Particle Size Characterization of an In-Duct Flat Media Particle Loading Test System for Nuclear-Grade Asme Ag-1 Hepa Filters

Matthew Christopher Wong

Design, evaluation, and particle size characterization of an in-duct flat media particle loading test system for nuclear-grade ASME AG-1 HEPA filters

By

Matthew C. Wong

A Thesis
Submitted to the Faculty of
Mississippi State University
in Partial Fulfillment of the Requirements
for the Degree of Master of Science
in Mechanical Engineering
in the Department of Mechanical Engineering

Mississippi State, Mississippi

May 2017

Design, evaluation, and particle size characterization of an in-duct flat media particle loading test system for nuclear-grade ASME AG-1 HEPA filters

By

Matthew C. Wong

Approved:

_____

Heejin Cho
(Major Professor)

_____

Charles A. Waggoner
(Minor Professor/Committee Member)

_____

Pedro J. Mago
(Committee Member)

_____

Yucheng Liu
(Graduate Coordinator)

_____

Jason M. Keith
Dean
Bagley College of Engineering

Name: Matthew C. Wong

Date of Degree: May 5, 2017

Institution: Mississippi State University

Major Field: Mechanical Engineering

Major Professor: Dr. Heejin Cho

Title of Study: Design, evaluation, and particle size characterization of an in-duct flat media particle loading test system for nuclear-grade ASME AG-1 HEPA filters

Pages in Study: 207

Candidate for Degree of Master of Science

The design and performance evaluation of in-duct, isokinetic samplers capable of testing flat sheet, nuclear-grade High Efficiency Particulate Air (HEPA) filters simultaneously with a radial filter testing system is discussed in this study. Evaluations within this study utilize challenge aerosols of varying particle diameters and masses such as hydrated alumina, Arizona test dust, and flame-generated acetylene soot. Accumulated mass and pressure drop for each in-duct sampler is correlated to the full-scale radial filter accumulated mass from initial to 10 in w. c. of loading. SEM imaging of samples at 25%, 50%, 75% and 100% loading verifies particle sizes with instrumentation used, revealing filter clogging resulting from particle impaction and interception. The U.S Department of Energy requires prototype nuclear-grade HEPA filters to be qualified under ASME AG-1 standards. The data obtained can be used to determine baseline performance characteristics on pleated radial filter medium for increased loading integrity and lifecycle endurance.

DEDICATION

This work is dedicated to my mother, whom supported my upbringing until her passing in July 2004 and to my father, for supporting me afterwards until I reached higher education. To my family friends whom have supported me in the best and worst times, I dedicate this work to show how far I have gone because of your support.

ACKNOWLEDGEMENTS

I would like to thank my advisor Dr. Heejin Cho for his support and guidance through this project. Gratitude goes to the test stand team lead, John Wilson, and his testing crew, and QA coordinator, Jaime Rickert, at The Institute for Clean Energy Technology for additional supervision on the project. Thanks, to Coralie Rose for providing laboratory procedure guidance and development of the gravimetric analysis procedure. Deep appreciation goes to the undergraduate student workers Tyler Covin, Brandon Bogle, and Ryan Denney for providing additional assistance in performing gravimetric analysis and maintaining tidiness in the laboratories. Special thanks go to Amanda Lawrence and her staff at the MSU Institute for Imaging and Analytical Technologies for their support and guidance with the scanning electron microscope

TABLE OF CONTENTS

LIST OF TABLES

LIST OF FIGURES

CHAPTER I

INTRODUCTION

1.1 Introduction

During the Second World War the British sent gas masks acquired from German soldiers to the United States Army Chemical Warfare Service Laboratories (CWS) in Edgewood, Maryland [1]. Once World War II ended, the utilization and research of "absolute filters" (now called high efficiency air (HEPA) filters) began in 1950. The research of absolute filters was classified technology following World War II. Arthur Little, Inc. was commissioned by the U.S. Atomic Energy Commission (AEC) to be a supplier of an equivalent or better filter medium than the media used in German gas masks during World War II. The investigations conducted by Little Inc. led to using coarse glass fibers as a substitute for the filtration media materials used in the German gas masks. Little, Inc. also began the commercialization of absolute filters by three manufacturers by 1957.

The initial name of HEPA filters extended from the name "absolute filter" for their unusually high particle retention efficiency. HEPA filters became the more widely accepted name after Humphrey Gilbert coined the term in 1961 in his report titled *High-Efficiency Particulate Air Filter Units, Inspection, Handling, Installation* [2]. This report provided the definition of a HEPA filter. A HEPA filter was defined as a throwaway, extended-medium, dry-type filter with: (1) a minimum particle removal efficiency of

99.95 percent (later raised to 99.97 percent) for a 0.3-µm monodisperse particle cloud; (2) a maximum resistance (when clean) of 1 inches water gauge (in.wg) when operated at rated airflow capacity; and (3) a rigid frame extending the full depth of the medium. Throughout the 1960's the development of HEPA medium capable of flame and smoke resistance were studied. These developments led to the modification of MIL-SPEC standards in 1968 which were initially focused filter medium resistance to radiation [1].

The development of the American Society of Mechanical Engineers (ASME) AG-1 - Code on Nuclear Air and Gas Treatment was initiated in 1978. The proposed code was to outline the requirements for all essential ventilation and air cleaning equipment used in containment ventilation systems of nuclear facilities [3]. The AG-1 Code was finished in 1985 and was endorsed by the Nuclear Regulatory Commission (NRC). The AG-1 code is based on the two standards: ASME N509 and ASME N510. ASME N509 focuses on the design, construction, and qualification and acceptance testing of air-cleaning units and components for HEPA and gas treatment systems in nuclear power plants. ASME N510 covers the development of test programs for HEPA cleaning systems for nuclear power plants and related applications.

1.2 Statement of Need

Radial flow HEPA filters are classified as a type of special HEPA filter under ASME AG-1 Section FK. Primary advantages of using these radial flow filters include the use of pleated media for greater dust loading capacity. A major disadvantage of using pleated media is the reduction of filtering efficiency when pleats are formed. The introduction of pleating causes imperfections that introduces a higher potential of failure along pleats of filter media during particulate mass loading. Other disadvantages for these

types of HEPA include manufacturing difficulties, escalated costs, and increased susceptibility to leakage [4]. The design potential of radial type HEPA filters has grown through the decades because of the effective method of pleating filter media.

The advancement of modern technology and qualification standards under ASME Nuclear Quality Assurance- 1 (NQA-1) and ASME AG-1 brought improvements in filter designs and testing methodologies in the nuclear air and gas treatment industry. Higher strength, dimple pleated filter media and separator/separatorless designs had been implemented into the radial filter designs under Section FK. The capability of testing under elevated conditions called for high strength filter media falling under Section FM. Section FM is under development and will require evaluation of filter media for the establishment of test codes and standards.

The implementation of updated HEPA media and designs, multiple factors within the full-filter package can make the slightest change in pressure drop, loading capacity, filter efficiency, and effective media velocity. Therefore, a need for interpreting these factors for the optimization in filter media and full filter design must be performed to alleviate these design issues and reduce overall production costs.

1.3 Literature Review

Development of AG-1 code depend on the design basis event (DBE) tests performed for prototype filters. The continuous development and qualification of nuclear-grade HEPA filters under ASME AG-1 Section FK take place at the U.S. Army's Edgewood Chemical Biological Center (ECBC) in Maryland. The establishment of test stands capable of performance evaluation of HEPA filter designs in spanning multiple sections of AG-1 code have been developed at the MSU Institute for Clean Energy

Technology (ICET). Construction of a Section FK test stand capable of performance evaluations tests under DBE conditions for full-scale radial flow HEPA filters have been conducted by former personnel [5, 6]. The design systems at MSU ICET have been constructed with harsh DBE loading conditions in mind. Pressure drops up to 50 in. w.c. have been obtained with radial flow HEPA filters with alumina powders and carbon black with varying temperatures and relative humidity up to 80% RH [7]. The effects of pressure drop and mass loading were observed for pleated filter media for various testing conditions on Section FK radial flow filters.

The study of mass loading effects on HEPA filter media and filters have been conducted by many researchers in the past for remote and safe change radial flow filter types, axial filters, and flat sheet HEPA filter mats under ambient relative humidity conditions. Multiple testing stands and orientations have been created to observe these effects using multiple types of aerosols. Studies Loughborough University have considered effects of mass loading on fibrous, flat sheet HEPA filters. The tests at Loughborough University have utilized a test setup involving a NaCl atomizer as a submicron aerosol generator to observe the relationship of collection efficiency as pressure drop increased throughout the loading process [8]. An experimental apparatus for filter loading used by Japuntich et al. studied multiple types of fibrous filters to observe the behavior of depth loading of particles with monodisperse particles [9].

Other studies by Endo et al. and Lee et al. involved test rigs utilizing polydisperse aerosol generation to observe the dust caking formation of general air filters. They utilized a mixture of alumina and Arizona Road Dust challenge aerosols [10, 11]. Endo et al. studied the bi-modal dust cake structure formation on filters as a function of pressure

drop and filtration flow rate in real time. Lee et al. studied bi-modal particulate mass loading for gas cleaning industrial HEPA filters using alumina and Arizona Road dusts similar to challenge aerosols used at MSU ICET. Both Endo and Lee found that pressure drop slopes increase when the ratio of finer particles of alumina increase when mixed with coarse Arizona Road dust particles. They found that a denser filter cake formation results and a greater specific resistance to gas flow occurs.

Aerosol sampling instrumentation and Environmental Protection Agency (EPA) stack testing used by personnel in workplace environments have been studied under isokinetic conditions to improve the representative results associated with filters. The emphasis of studying particulate matter under isokinetic conditions has been stressed in both research and industry sampling studies concerning personnel particulate matter intake. Studies by Carter et al. [12] and Baron et al. [13] have used isokinetic samplers in the National Institute for Occupational Safety and Health (NIOSH) to study effects of filter deposits in fiber sampling cassettes. However, these isokinetic samples were performed on 25 mm diameter asbestos fiber media and similar fiber types with filter cassettes for EPA applications. In addition, previous studies by Belyaev et al. included isoaxial testing of thin-walled samplers to observe the effects of distortion of particle diameter and number concentrations at the inlets of sampling nozzles by [14]. Regarding particulate size distributions, Pena et al. performed studies with an isokinetic sampler for continuous flow through airborne aerosol instrumentation used on research aircraft [15].

The effects of dust caking are important in understanding how mass loading affects pressure drop in a HEPA filter. The loading curve increases during the initial stages is linear due to depth loading of challenge aerosol. The stages of loading affect the

restriction of airflow through the porous media and accumulation of loaded particles. Studies conducted by Thomas et al. were performed to experimentally observe influences of filter clogging and penetration due to solid particles [16]. Parameters such as air velocity, particle size, number concentration, and filter characteristics were also considered in his studies to develop a mathematical model to describe influences based on filter clogging. Particle sizing verification was also performed by using scanning electron micro-graphs. Filter clogging studies performed with flat and pleated media by Bourrous et al. focused on the measurement of nanoparticle distribution for the two types of media. He mentions that for pleated filter media depth loading characteristics are identical to flat sheet media [17]. For pleated filters under the event of filter clogging, the behavior of pleating does not occur at the same point as done in the flat sheet media. The difficulty in studying the mass loading effects is difficult due to dendritic bridging within the pleating during loading. Therefore, a need to study the effect of mass loading in simultaneity with pleated media should be performed using flat sheet media.

1.4 Objectives

The development and research of ASME AG-1 Section FK nuclear-grade HEPA filters are underway. the utilization of fibrous, At the MSU ICET, the study of in-place, isokinetic samplers have been performed with a full-scale radial filter test stand to understand the baseline characteristics of a nuclear-grade, radial flow HEPA filter. The combination of isokinetic samplers and nuclear-grade HEPA filters can be used to improve nuclear-grade HEPA filter designs based on the mass loading effects on pressure drop. Data obtained from the in-place, isokinetic sampling system can assist in the design optimization of the full-filter. The design optimization of the: media velocity, pressure

drop, mass loading capacity, and filter parameters such as HEPA media fiber diameter, thickness and pleat count can benefit from the collected isokinetic sampler data. The isokinetic samplers contain flat sheet HEPA media of the same type that is found in the full-filter being evaluated. The use of the same HEPA media by both the isokinetic sampler and full-filter allow the correlation of mass loading and pressure drop to that filter pack.

The use of measuring and testing equipment to collect the particle number concentration and particle size distribution is essential in validating the results of such system. The mass accumulated on the HEPA media samples will be correlated to the mass concentration obtained from an aerodynamic particle sizer (APS). The cumulative mass will be estimated for each isokinetic sampler interval using the APS. Particle size data obtained from a scanning mobility particle sizer (SMPS) and aerodynamic particle sizer (APS) will be used to correlate data obtained from a Pilat Mk. V cascade impactor. The cascade impactor data will present the mass mean diameter (MMD) of each type of challenge aerosol used during the loading tests. The jet stages from the cascade impactor with the greatest mass accumulated will indicate the range of the MMD obtained from the impactor. This MMD range will be correlated to the MMD obtained from the APS.

The particle sizing data will also be correlated to images taken with scanning electron microscopy (SEM) from the MSU Institute for Imaging & Analytical Technologies (I2AT). The particulate matter will be imaged under SEM to provide additional method of verification for particle sizing. Particle sizing and morphology will follow methods outlined by the American Society for Testing and Materials (ASTM). The sizing and morphological shapes will be observed and implemented with the SMPS

and APS size ranges. The SMPS size range will be converted from an electric mobility diameter to an aerodynamic diameter range using the shape factor obtained from the morphological studies. This project is applied in simultaneity with the radial large scale test stand (RLSTS) located at MSU ICET, but is not limited solely to this test stand. Applications can be extended to various testing ductwork capable of accepting in-place isokinetic samplers.

CHAPTER II

TEST SYSTEM DESIGN

2.1 Isokinetic Test System Components

The isokinetic sampler system is composed of various components ranging from ductwork to electronic hardware. These components include the overall design, control, and sampling rate in the test duct. The description of each component will be described in detail. The design drawings can be found in the sections proceeding Test System Components and in the Appendix A.

2.1.1 Sampler Assembly

A critical component of the isokinetic sampler is the housing assembly. HEPA coupon media is contained in the sampler assemblies. These assemblies are designed to ensure a proper seal on the HEPA media coupon media during testing, while acquiring an evenly distributed loading pattern onto the coupon. Hines describes this type of filter housing design as an open-face filter holder for the collection of particulate matter [18]. He explains that for open-face filter holder designs ensure uniform particle distribution onto the filter surface. The filter holder designs are recommended for use with microscopic analysis. The possibility of inlet losses is minimized using this design. The following list identifies the six components required to assemble the isokinetic sampler coupon housing. Table 2.1 and Figure 2.1 presents the assembly order for the sampler assembly components.

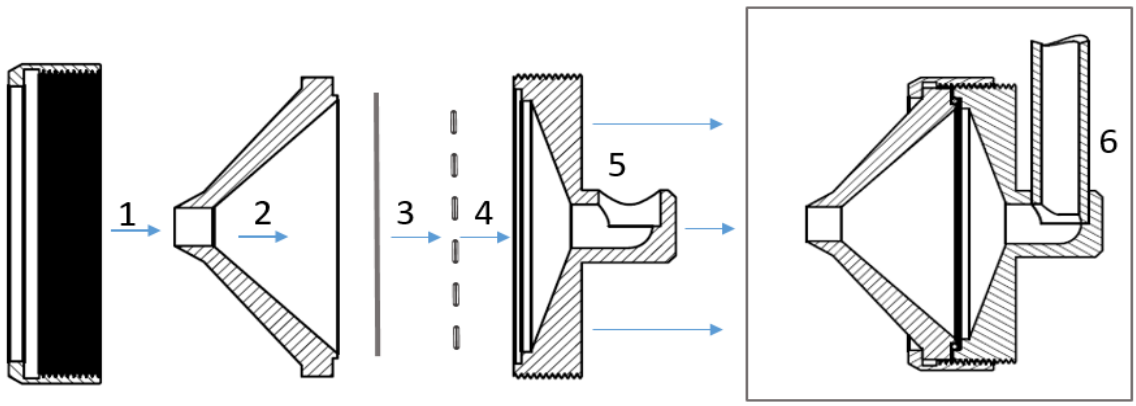

Figure 2.1 Assembly order for the isokinetic sampler components.

Table 2.1 List of isokinetic sampler assembly components.

Component number	Component
1	Knurled, threaded brass collar
2	Isokinetic sampling nozzle
3	Flat sheet, 60 mm (2.37”) dia. HEPA media coupon
4	Filter support plate
5	Sampler assembly base
6	Stainless steel vacuum tube

The boxed portion in Figure 2.1 represents the fully-assembled sampler assembly. In the original design concept an O-ring between the HEPA media coupon and the isokinetic sampling nozzle was intended to ensure higher confidence in vacuum sealing. The O-ring has shown to adhere and damage the coupon surface during removal after elevated humidity tests. The O-ring was removed in the current revision. The mating edge of the isokinetic sampling nozzle can provide thorough vacuum sealing without an O-ring. This is because the design tolerance between the sampling nozzle and HEPA media coupon is enough to provide sufficient sealing without damaging and introducing leaks.

After several preliminary tests the filter support plate was added to the design. The support plate is created from a sheet of punched metal of approximately 2 mm thickness. The perforations are 6 mm in diameter and allow sufficient airflow through the HEPA media coupon while providing additional support for the coupon during loading conditions. Further design details regarding the computer-aided drawings (CAD) of the sampler assembly can be found in the Appendix. The CAD drawing of the support screens were not created for the isokinetic sampler assembly because this component was not initially included in the original design.

2.1.2 Sampling Nozzles

The nozzles affixed onto the sampler assemblies are specifically designed to provide isokinetic sampling. The inlet diameter of the sampling nozzle was designed to be 0.325 inches to meet isokinetic sampling conditions. Figure 2.2 shows the isokinetic sampling nozzle and knurled retaining collar for the isokinetic sampler assembly.

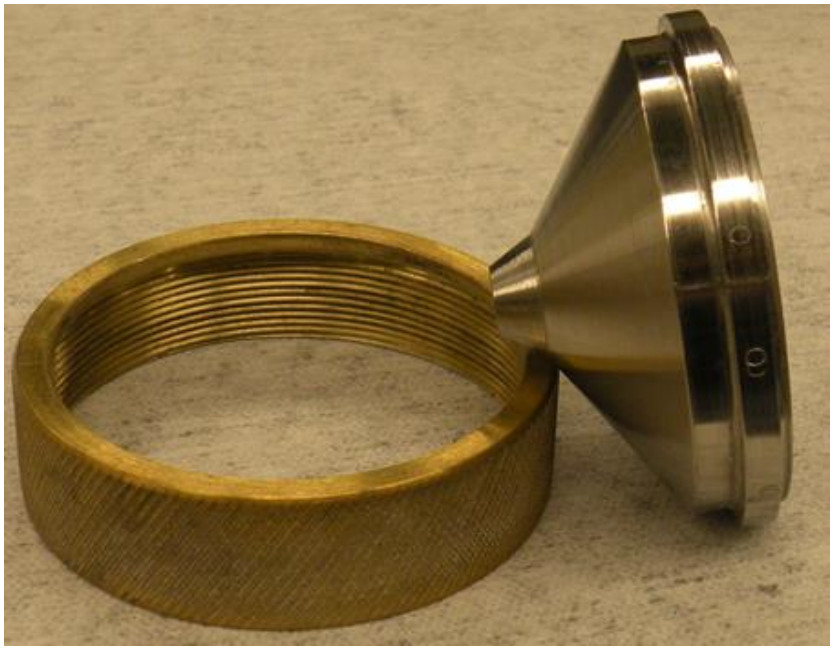

Figure 2.2 Isokinetic sampling nozzle and knurled retaining collar of the sampler.

The definition of isokinetic refers to achieving equivalent velocity entering through the sampling nozzle inlet and the free-stream velocity approaching the inlet. The volumetric flowrate across the sampler coupon and full size test filter must be proportional with respect to their filter cross-sectional areas. In terms of the sampling nozzle depth and divergence angle, the depth of the nozzle measures at 1.313 inches with an internal angle of divergence of 47 degrees to provide an even aerosol distribution onto the HEPA media coupon. Further details regarding the design calculations of the isokinetic sampling nozzle will be discussed in the Design Calculations section.

2.1.3 HEPA Media Coupon

The HEPA media coupons contained in the assembly are used to collect the challenge aerosol. The coupons are weighed before and after testing to determine the

differential mass. This value is paired with the differential pressure of the isokinetic sampler and of the radial full-filter. Nuclear grade HEPA media sheeting for this study was obtained from Lydall Inc. The filter media sheeting provided by Lydall Inc. comes in three types designated as: Lydall 3398 L0W, L1W, and L2W. The HEPA media coupons must correspond with the same filter media used in the radial full-filter package for the differential pressure data to be useful. Table 2.2 provides the filter designations and short descriptions for each type of filter type. Figure 2.3 shows the three types of HEPA filter media provided by Lydall Inc.

Table 2.2 List of Lydall HEPA media used with the isokinetic samplers.

Lydall HEPA Filter Designations		
Designation	**Filter Scrim Support**	**Description**
3398 L0W	**No**	**Conventional nuclear grade HEPA filter medium**
3398 L1W	**Yes, single side**	**HEPA filter medium with scrim support on one side of the filter media**
3398 L2W	**Yes**	**HEPA filter medium with scrim backing on both sides of the filter media**

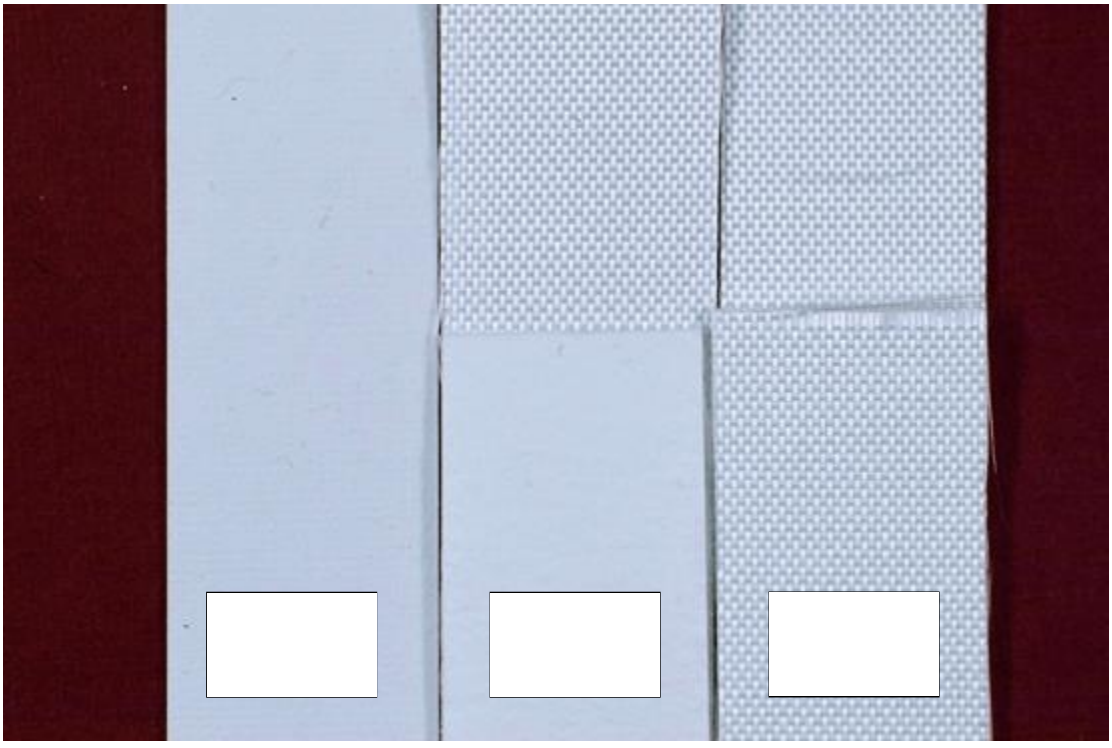

Figure 2.3 Lydall 3398 Flat Sheet Filter Media supplied by Lydall Inc.

The designation of L0W is the conventional nuclear grade HEPA filter medium. L1W features a woven fabric scrim backing adhered to one side of the filter medium to add rigidity and dramatically increase tensile strength. The scrim backing provides additional protection from moisture and microbes from weakening the fibrous microstructure during loading. L2W features scrim backing on both sides of the conventional L0W HEPA filter media to maximize protection from adverse loading conditions in extreme environments. The L2W scrim backing increases the tensile strength of the media, enduring pressure impulses capable of destroying non-reinforced filter media. Loading tests at ICET have primarily consisted of filters containing L0W and L2W for various loading conditions and challenge aerosols.

The creation of the HEPA media coupons is made by using a 59-mm arch punch. The HEPA media coupons are uniformly cut out and placed within glass petri dishes. Figure 2.4 shows the HEPA media coupons and the handheld arch punch in petri dishes.

Figure 2.4 59-mm coupon arch punch and flat sheet HEPA media coupons.

Glass petri dishes were used to minimize static charging effects encountered with plastic petri dishes. This is important when performing gravimetric analysis in accordance to HEPA-029-Gravimetric Analysis because static charging can affect the mass fluctuations on the analytical balance. This procedure can be found in Appendix B. Description of HEPA-029-Gravimetric Analysis is found in Section 3.1 Gravimetric Analysis Procedure.

2.1.4 Blinds/Flanges

The isokinetic sampler ductwork features modified flanges on the ductwork. The blinds used on the isokinetic sampling test section are eight-hole stainless steel, raised face blinds with ANSI rating at 150 lb/sq.in. The blinds are used to seal off the ports when the samplers are not in place. The isokinetic sampler ductwork blinds are exchanged with the modified sampling blinds on the six-inch test stand ports when elevating to testing conditions. These modified flanges were tapped and changed to accept stainless steel stems attached to the HEPA media coupon holders. Figure 2.5 represents a modified sampling flange with a disassembled coupon holder.

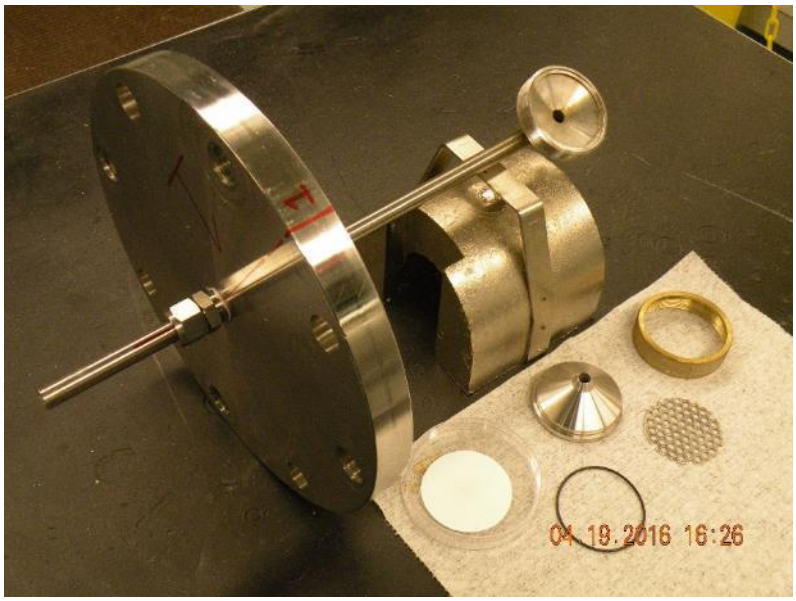

Figure 2.5 Modified flange equipped with HEPA media coupon holder

Please note that the revision used in testing does not use an O-ring.

The O-ring caused damage to the filter media upon removal due to compression and sticking to the media surface. The sampler base and nozzle were designed to provide enough sealing to clamp the HEPA media coupon sample between the mating surfaces without encountering leaks. This was verified by comparing differential pressure across the HEPA media coupon with and without the O-ring for all samplers. No changes in initial clean differential pressure were noticed between the tests with and without the O-ring.

The fittings on the flange allow the length of the sampler tubing and the angle of attack of the sampling nozzle to be adjusted. Nylon ferrules at the fittings of the sampler tubing allow the fitting to be tightened or loosened to provide ease of length adjustment. Markings on the flanges are used to ensure that the sampler nozzles are parallel to the axis of the duct. This ensures that sampling under anisoaxial conditions does not occur.

When sampling under anisoaxial conditions vortices may form depending on the angle of sampling.

2.1.5 Mass Flow Controllers

Mass flow controllers (MFCs) are used on the test system to manage the vacuum flow rate through the samplers. Four individual Alicat Scientific MFCs are used to regulate the air through the samplers. The MFCs can control the volumetric flowrates steadily and accurately within 1% of their setpoint values. Table 2.3 represents the operating parameters of the MFCs. Figure 2.6 represents the arrangement for the mass flow controllers and the differential pressure transmitters.

Table 2.3 Operating parameters of the Alicat MFCs on the isokinetic samplers.

	Controllable Flow Range	**Mass Reference Conditions**	**Operating Temperature**	**Humidity Range**
Alicat MC Series Mass Flow Controller	0 to 0.5 scfm	25 ^{o}C & 14.696 psia	-23 to 140 ^{o}F	0 to 100 % (non-condensing)

Figure 2.6 Mass flow controller and dP gauge arrangements for each sampler.

The MFCs were initially controlled with pre-determined sampling flow setpoints during preliminary design phases. The MFCs are now controlled from the test stand SCADA after the automation of the test system. This allows the volumetric flow to be automatically correlated with the measured filter media surface area of the radial full filter. Further details regarding the MFC automation can be found in Section 2.2.2 Test Stand SCADA.

2.1.6 Differential Pressure Transmitters

The collection of differential pressure data would not be possible without the differential pressure transmitters. The Endress+Hauser PMD75 differential pressure transmitter operates by obtaining the difference between the high and low pressure sides of the test stand and isokinetic sampler via two ports. PTFE vacuum tubing is used to connect the high and low side ports on the differential pressure transmitter to the isokinetic sampler system. The high side differential pressure is connected to the test stand, whereas the low side differential pressure is connected to the isokinetic sampler stem. The isokinetic sampler stem connects to a union tee fitting to split the low side pressure line and allow the flow of filtered air through the condenser units. Figure 2.6 in the previous section showed the setup for the differential pressure transmitters alongside the mass flow controllers.

The differential pressure range for these transmitters can reach a maximum limit of 50 in. w.c.. These transmitters were chosen to meet this specification because the pressure drop on the flat sheet HEPA media coupons can be measured within 50 in w.c. during the 10-in. w.c. loading procedure. The reason the flat sheet coupons achieves differential pressure this high is because the HEPA media is flat and does not include pleating. The pleating on the full filter makes a slower increase in pressure drop due to more surface area. The flat HEPA media is representative of an equivalent surface area on the radial full filter without pleating. Once 10-in. w.c. of loading is achieved on a full filter the pressure drop across a flat HEPA media sample may have achieved a pressure drop up to three times the differential pressure than the full filter.

2.1.7 Vacuum Pump and Air Ballast Tank

The flow source on the isokinetic samplers is produced by a vacuum pump located on the floor of the high bay between the upstream and downstream duct sections. The vacuum pump is rated at 3/4 horsepower and is activated by a toggle switch alongside the upstream ductwork. The vacuum pump is connected to a ballast tank rated for 2 gallons of air and 175 PSI. The ballast tank can support a total of six samplers. Figures 2.7 and 2.8 show the vacuum pump and ballast tank, respectively.

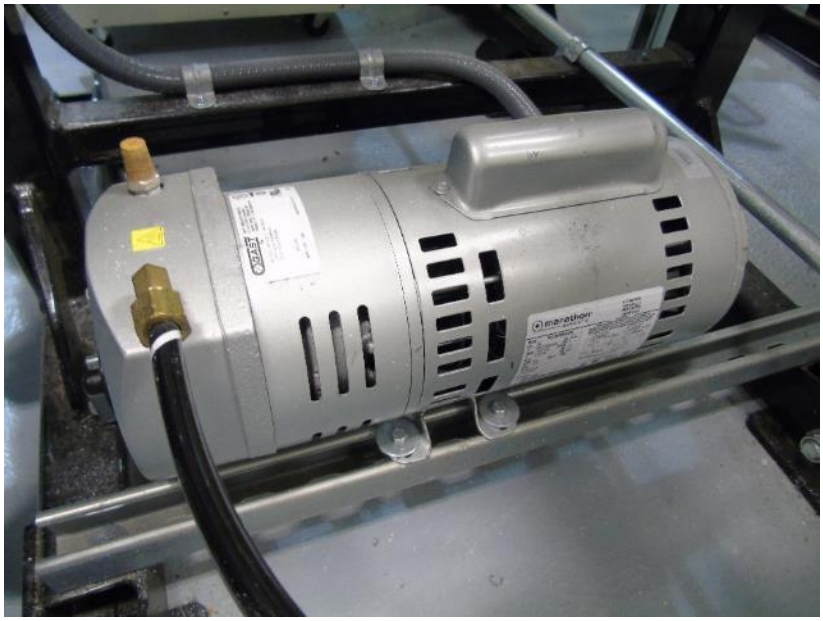

Figure 2.7 Vacuum source of the isokinetic samplers and Pilat impactor.

Figure 2.8 Ballast tank for the isokinetic samplers.

Figure 2.8 shows the ballast tank connected to the isokinetic sampler MFCs. The ballast tank is connected to each MFC regulating the volumetric flow through the individual isokinetic sampler lines and Mk. V Pilat Cascade Impactor. Plastic vacuum tubing is used to connect each MFC to the ballast tank to provide appropriate flow through each sampler. The tubing is rigid to safeguard against instances where softer tubing would tend to collapse under vacuum. A separate vacuum tank will be added to the test system to provide enough vacuum for up to eight samplers of simultaneous testing.

2.1.8 Heat Exchangers

The isokinetic samplers must operate with a heat exchanger stage to condense the moist, heated air for elevated condition testing in the RLSTS. The samplers operating at elevated temperatures and relative humidity can lead to condensation in sampling lines. Each sampler stem has a union tee splitting a pressure measurement to the pressure transmitter and the filtered air to a condenser unit. This allows the low side pressure port for the differential pressure sensor to obtain the differential pressure across the flat HEPA filter media while the condensate and moist air progresses towards the heat exchanger system. The condensate is collected within water collection capsules installed at the bottom of each condenser unit. The images of condenser units on the heat exchanger system are shown in Figure 2.9.

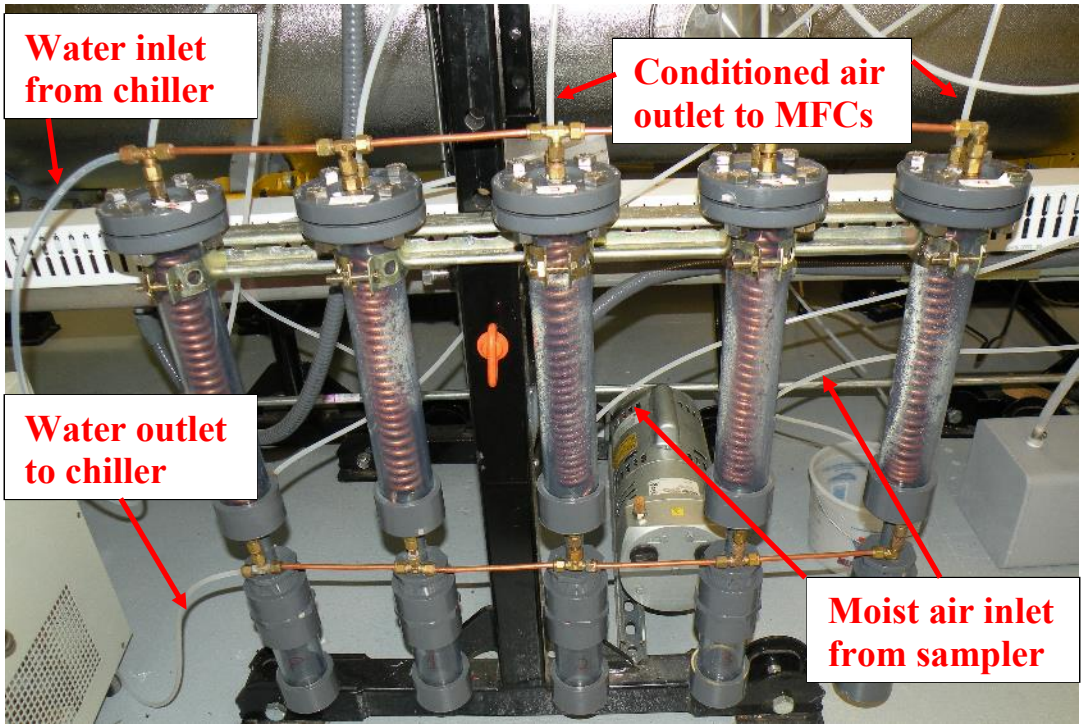

Figure 2.9 Heat exchanger stages connected to the isokinetic samplers.

Chilled de-ionized (DI) water is supplied by a standalone chiller unit which enters in through the top left tube fitting and is distributed throughout each of the heat exchangers. The chilled DI water flows from the top of each heat exchanger in a counter-flow orientation with the heated, moist air entering from the bottom of each heat exchanger unit. Condensed moisture from the process is collected in the removable collection capsules, located at the bottom of each heat exchanger unit. The return DI water then exits the heat exchanger system through the bottom left tube fitting and is recirculated through the chiller unit. The temperature of the DI water is regulated through the chiller at a range of 50 ^{o}F to 60 ^{o}F. Figure 2.10 shows the chiller unit connected to the heat exchanger units.

Figure 2.10 Chiller unit of the heat exchanger stages.

A simulation was performed during the design phase of the heat exchanger to ensure that the temperature of the chilled water circulating through the stage would condense the moisture from the hot air exiting the downstream test section. The Flow Simulation package for the student edition of Solidworks 2014 was used to simulate the conditioned air flowing through the heat exchanger stage. The preliminary design simulation was for a simple, straight piece of copper tubing. Figure 2.11 shows the Solidworks simulation model of the straight copper tube with hot air passing through the center.

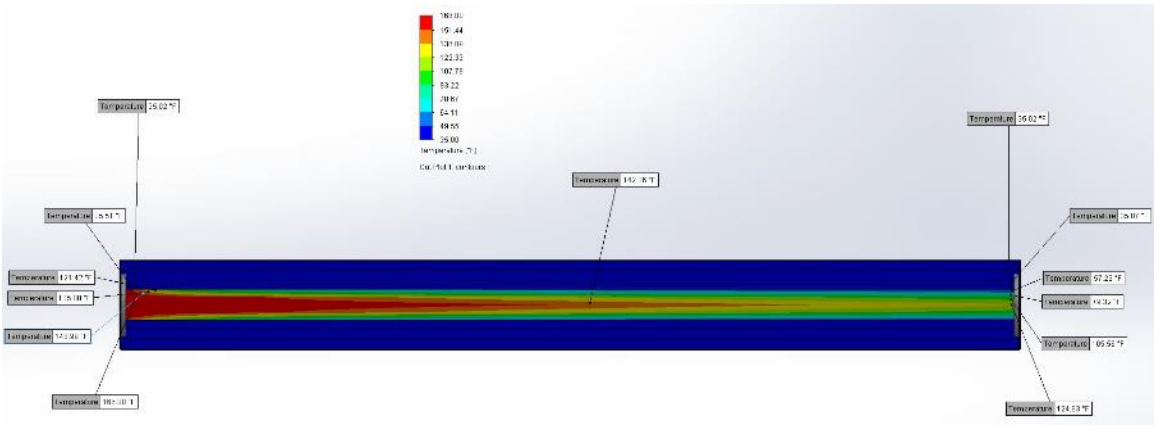

Figure 2.11 Preliminary design simulation of the heat exchanger using Solidworks.

The preliminary design simulation in Figure 2.11 shows a temperature gradient as the temperature at the inlet conditions on the left were assumed to be at 170^{o}F, and the exit temperature is approximately 79^{o}F. Probing the post-processed images provided insight on designing the physical model. A worst-case scenario was assumed, and temperature losses from the sampling lines were not considered. The temperature from the sampling lines would have decreased gradually as the fluid progressed towards the condenser units

since the working environment in the test area is air conditioned. The sampling lines are not thermally insulated.

2.1.9 Test Stand SCADA

A supervisory control and data (SCADA) system was designed to allow users to control, tune parameters, and monitor conditions for various testing activities. The control panel for the RLSTS and isokinetic samplers are located on the same screen on a control cabinet containing programmable logic controller (PLC) connections near the filter housing of the test stand. The SCADA controls the RLSTS and isokinetic sampler components. This includes the Pilat impactor and isokinetic sampler flow rates.

The interface of the SCADA contains an overall schematic of the upstream and downstream ductwork with real-time sensor and data monitoring capabilities. The sensors are representative of their installed locations on the RLSTS and are labeled on the control panel accordingly. The real-time trendline charts show the RLSTS flow, relative humidity and temperature of the upstream and downstream ducts, and differential pressure across the filter housing for a period of 30 minutes. The temperature and relative humidity are controlled by using the SCADA, as seen in Figure 2.12. Figure 2.13 provides the touchscreen control interface as seen on the test stand SCADA control cabinet.

Figure 2.12 The SCADA system for the RLSTS.

The SCADA for the RLSTS is on the monitor of the left cabinet door. The monitor on the right cabinet door controls a separate testing system.

Figure 2.13 RLSTS and isokinetic sampler touchscreen control interface on the SCADA.

The isokinetic sampler flow settings shown in Figure 2.13 can be controlled from 0.0 to 0.5 scfm by touching the white boxes in the grey box labeled “In-Duct” and entering the desired flow rates manually. The “In Duct – Auto” checkbox on the right-hand side of the controls is used to automatically control the flow rate for each sampler based on the filter media surface area of the full filter. The RLSTS must be in the “Start” position, and the radial full-filter area must be entered for the isokinetic samplers. The flow rate is calculated automatically adjust to optimal flow setpoints for each individual MFC. Description of the automatic flow calculations performed can be found in 2.2.2.1 Consideration of Moist Air Sampled During Elevated Conditions. The gray box located

on the middle left of the interface is the flowrate setpoint controls for the University of Washington Mk. V Pilat Cascade Impactor, furthermore stated as the Pilat Impactor.

The automation of the test system allows for easier control and more accurate results by using the SCADA rather than manually controlling the setpoints. For example, when the flow setpoint on the RLSTS is set to 2000 cfm, the flow in the sampler flowrates will automatically adjust to the change in flowrate through the filter housing when the full filter begins to increase in differential pressure. The induced draft fan will work harder to maintain the flowrate a consistent 2000 cfm through the full filter. The same phenomenon occurs for the MFC flow setpoints as loading increases on the isokinetic samplers. The SCADA will automatically update the flow setpoints when the differential pressure increases during loading. This automation allows the flow through the isokinetic nozzle to maintain at isokinetic flow conditions without having to change the flow setpoints manually.

2.2 Design Calculations

This section provides design calculations related to the development of the isokinetic sampler testing system. The design calculations include justification for the sampler nozzle design using fundamentals of fluid flow dynamics, as well as simulation software to validate designs prior fabrication.

2.2.1 Sampler Head Divergence Angle and Depth

The design of the sampler head divergence angle was created in consideration with uniform mass distribution onto the HEPA media coupon. A numerical study conducted by Sparrow et al. mentioned that for total angles of divergence less than five

degrees, flow separation will not occur [19]. In their case study, the downstream diameter and upstream diameter ratio was set at 4:1 for all simulation cases. The study also stated that for diffuser divergence angles of 10^o and 30^o, their numerical simulations showed that flow separation occurred on all their studies at low Reynolds numbers ranging from 500 to 33,000.

The calculated Reynolds numbers for a circular duct of 24 in. inner diameter at 2000 cfm (Category 2b and 2c) and 1200 cfm (Category 3) are approximately 93,000 and 56,500, respectively. The internal divergence angle of the sampler nozzle was designed to be 43^o and with a nozzle depth of 1.313". This design allows flow separation to occur at the higher Reynolds numbers mentioned for test categories 2b, 2c, and 3. The external divergence angle was designed at an angle to minimize turbulence downstream of the samplers. Since the TSI Aerodynamic Particle Sizer (APS) is located downstream of the isokinetic samplers, the reduction of flow vortices was taken into design consideration. Please refer to the Appendix A for design schematics of the sampler nozzle.

A computational fluid dynamics (CFD) simulation was performed to further validate the reduction of turbulence of the samplers. Solidworks simulation software was used to simulate the test conditions for Category 3, 2b, and 2c. The following figures show the simulation from the cross-sectional perspective to observe the effect of airstream laminarization prior reaching the APS sampling nozzle.

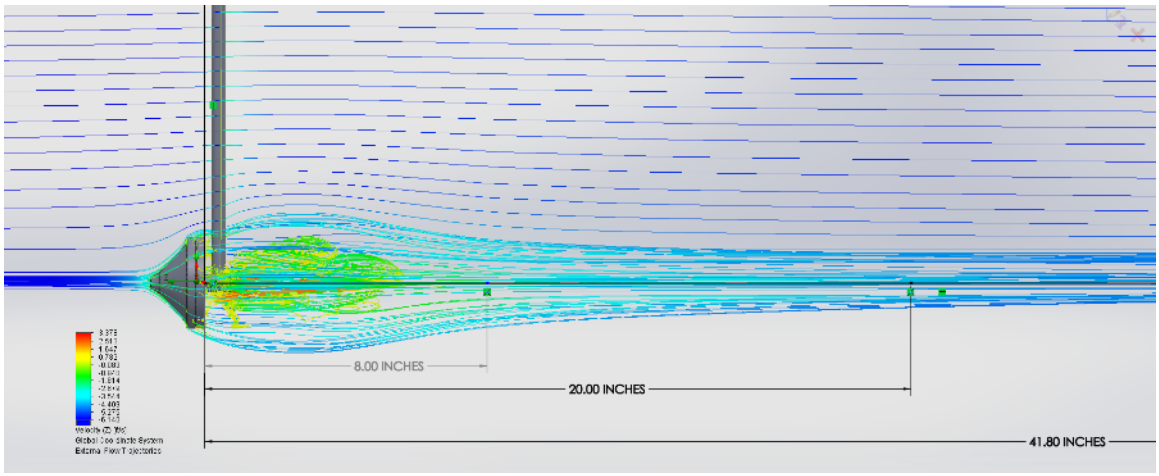

Figure 2.14 Solidworks Flow Simulation results for Category 3 test conditions.

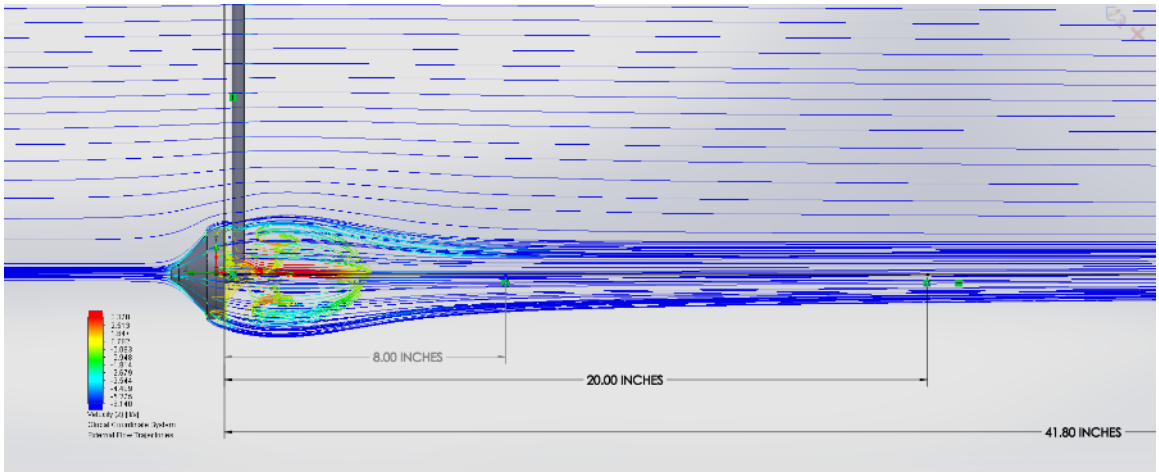

Figure 2.15 Solidworks Flow Simulation results for Category 2b and 2c test conditions.

The calculated Reynolds numbers of 56,500 (1200 cfm) and 93,000 (2000 cfm) were input for the simulated duct flow conditions seen in Figures 2.14 and 2.15, respectively. The length of the flow simulation downstream of the sampler was set to 41.80 inches, demonstrating the minimization of turbulence downstream. Figures 2.14 and 2.15 show that the reconnection of flow streamlines is slightly different for the two

testing flowrates of 1200 cfm and 2000 cfm. The flow streamlines are lengthened at a lower flowrate of 1200 cfm when simulating Category 3, whereas at 2000 cfm, the flow streamlines reconnect at approximately 8 inches past the sampler head base. It was not necessary to perform show two separate CFD flow simulations since Category 2b and 2c have testing flowrate of 2000 cfm. The only difference between Category 2b and 2c test conditions is a 10% increase in relative humidity. It would be interesting to study if flow straightening would occur before reaching downstream samplers. The current simulation results show that flow straightening can occur within 20 inches. The flow simulation for the addition of samplers downstream should be studied in future tests since sampler ports are located 22 inches downstream of the current sampler locations.

Apparent signs of uneven loading occurred on the surfaces of the HEPA media coupons after performing a series of loading tests. Noticeable buildup at the center of the coupon for samples representing 50% through 100% loading showed that the length of the sampling nozzle was not sufficient to provide enough flow separation for uniform aerosol loading. A prototype nozzle design was proposed to revise the original nozzle design, and was tested alongside the original sampling nozzle design to show a difference. Figure 2.16 shows the revised nozzle design installed onto isokinetic sampler base in the RLSTS for preliminary testing.

Figure 2.16 Prototype nozzle design installed onto isokinetic sampler base.

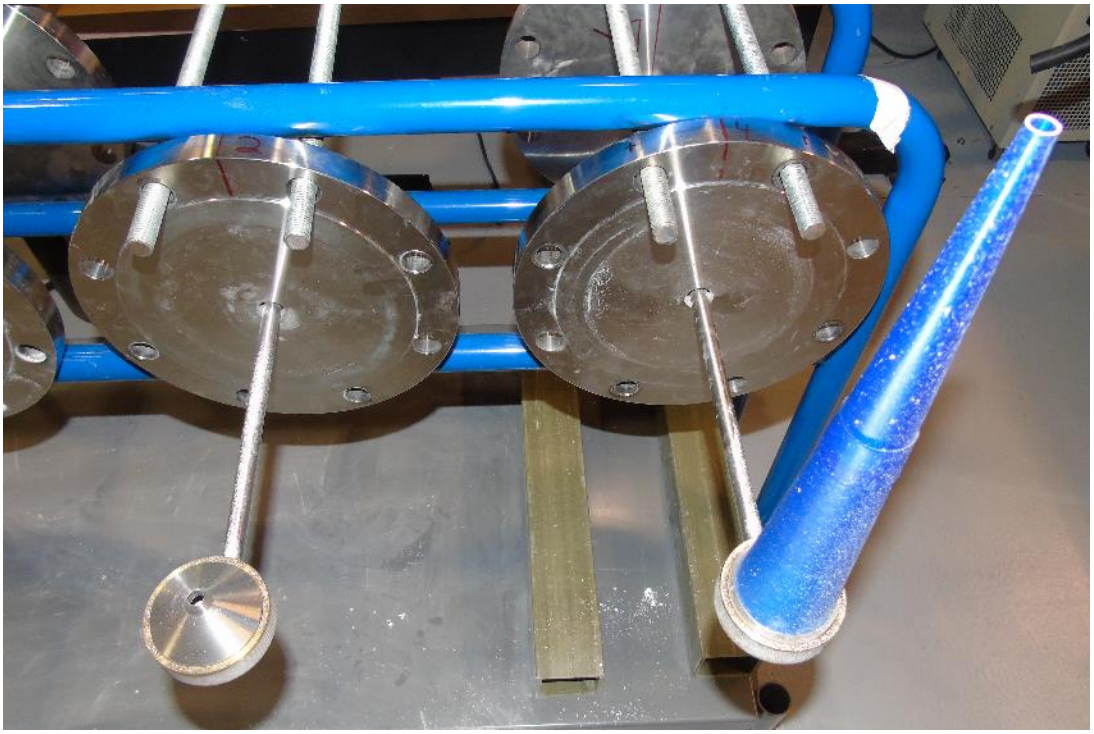

Figure 2.17 Length comparison of original nozzle design to the prototype nozzle design.

Figure 2.17 shows the difference in length of the prototype nozzle design compared to the original nozzle design. The prototype design shown is a preliminary design created from two pieces of 3D printed Polylactic Acid (PLA) designed from AutoCAD. The finalized designs for the new sampling nozzle design have not been finalized at the time this article was written. The new nozzle design will feature a longer, tapered length for the sampling nozzle, and it will be machined from stainless steel to withstand elevated testing conditions and to prevent triboelectric charging from occurring. The internal divergence angle will also be reduced to allow flow separation to occur as particulate matter travels within the nozzle to the HEPA media coupon. Figure 2.18 represents the comparison of the initial nozzle design and the prototype nozzle design.

Figure 2.18 Loading pattern using original vs. revised sampling nozzle design.

The loading pattern on the left image shows a dense formation of particles at the center of the coupon, whereas the image on the right shows an evenly distributed loading pattern.

The topography was examined cross-directionally with one sweep horizontal and the second sweep vertical at a rate of 2 mm per point using a Talysurf CLI 2000 surface profiler to determine the loading pattern. The sample tested with the prototype nozzle proved to more uniform throughout the center, without concentrating in a pile.

2.2.2 Isokinetic Flow

Isokinetic flow on the sampler is required to obtain representative samples of mass loading onto the flat sheet HEPA media coupons. Hines states that the conditions for isokinetic sampling is defined in Equation 2.1 [18].

$$U = U_0 \tag{2.1}$$

Where:

U = Sampling probe velocity
U_0 = Free-stream velocity

In terms of the free-stream velocity, U_0, and probe inlet velocity, U, both velocities must be equivalent for isokinetic conditions to be met. EPA Method 5 - Determination of Particulate Matter Emissions From Stationary Sources, states that for using alternative isokinetic metering systems, such as the mass flow controllers, the sampled flowrate must be within 10% of isokinetic flow and the determined sample volumes to be within 2% may be used [21]. The RLSTS SCADA was programmed to automatically set the sampler mass flow controllers to maintain an isokinetic volumetric flowrate based on the sampler filter area and the full-filter surface area. The following expression was programmed into the SCADA to maintain isokinetic flow for the sampler nozzle with respect to flow through the full filter.

$$\frac{Q_{IS}}{A_{IS}} = \frac{Q_{FF}}{A_{FF}} \quad (2.2)$$

Where:

Q_{IS} = Isokinetic sampler volumetric flowrate
Q_{FF} = The full-filter volumetric flowrate
A_{IS} = Effective surface area of the HEPA filter sample
A_{FF} = Effective surface area of the full-filter

Equation 2.2 shown above represents the equivalent ratio of isokinetic sampler volumetric flowrate (Q_{IS}) and effective surface area of the HEPA filter sample (A_{IS}) to the RLSTS full-filter volumetric flowrate (Q_{FF}) and the radial full-filter effective surface area (A_{FF}). The operators on the RLSTS must measure the effective full-filter surface area prior testing as according to pre-test procedures. The full filter effective surface area is entered onto the test stand control panel to ensure that the samplers are collecting at their adequate volumetric flowrate. The volumetric flowrate for the isokinetic samplers will be corrected for the flow at the full filter according to the ratio of the full-filter flowrate and surface area.

2.2.2.1 Consideration of Moist Air Sampled During Elevated Conditions

The flow of moist air through the isokinetic sampling nozzle inlet must be considered for testing in elevated conditions. The discrepancy of assuming dry air for all flow settings will cause the sampler to oversample, therefore, the differential mass obtained through gravimetric analysis procedure would not be representative of the elevated testing condition. EPA Method 4 – Determination of Moisture Content in Stack Gases, states that the determination of moisture content is made in the gas stream, assuming the gas stream is saturated, and a temperature is calculated based on average

stack temperature using a temperature sensor [22]. The moisture content in the isokinetic samplers are accounted for in the RLSTS SCADA control scheme based on ASHRAE definitions for psychrometric calculations. These calculations account for the change in density based on measurements from the temperature and relative humidity probe located at the location between the isokinetic samplers and RLSTS filter housing.

The process of calculation begins at the temperature and relative humidity probe. The SCADA calculates the corrected density of the airstream for every second based on the relative humidity and temperature obtained from the probe. The actual flow rate is determined and then converted to standard flow rate for the isokinetic samplers, as seen in the following figure.

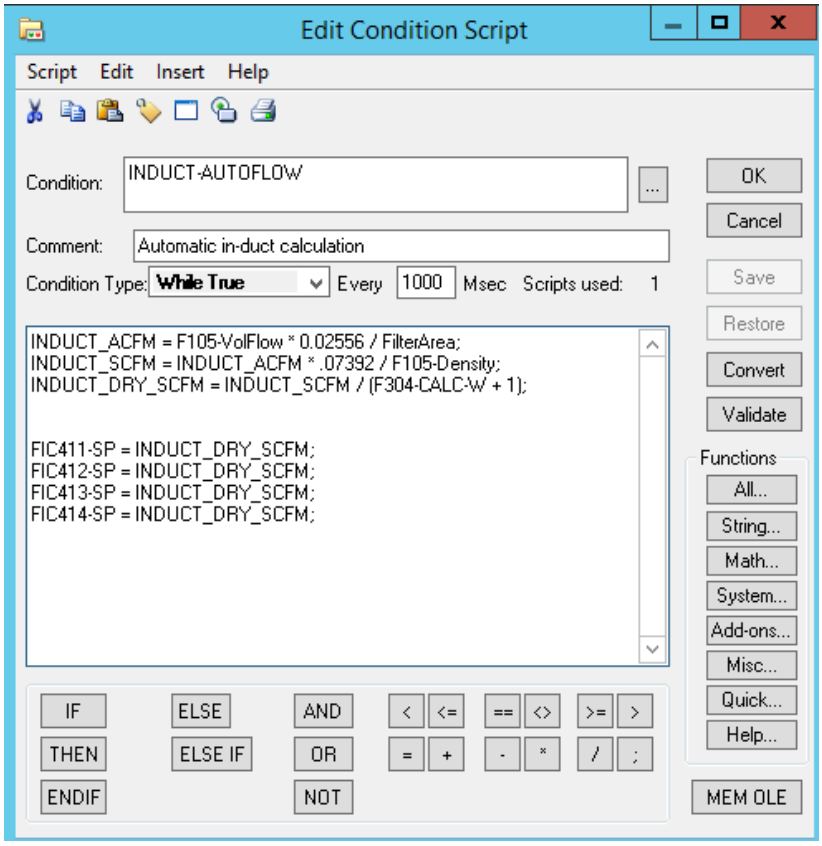

Figure 2.19 SCADA calculation loop for the isokinetic sampler inlet flow rate in consideration to elevated testing conditions.

The temperature and relative humidity in the upstream duct section is taken into consideration to calculate for the sampled air density, “F105-Density”, in the standard flow rate equation, “INDUCT_SCFM” as seen in Figure 2.19. The isokinetic sampler dry flow rate is then calculated for all samplers based on the calculated humidity ratio and standard flow rate. The “INDUCT_DRY_SCFM” variable is looped through each mass flow controller and updated every second to account for the variation in psychrometric parameters during elevated testing. A similar calculation to maintain isokinetic flow is also used in the mass flow controller assigned to the Pilat impactor as well. The following

figure shows a similar calculation in consideration for moist air when sampling through the inlet of the Pilat impactor.

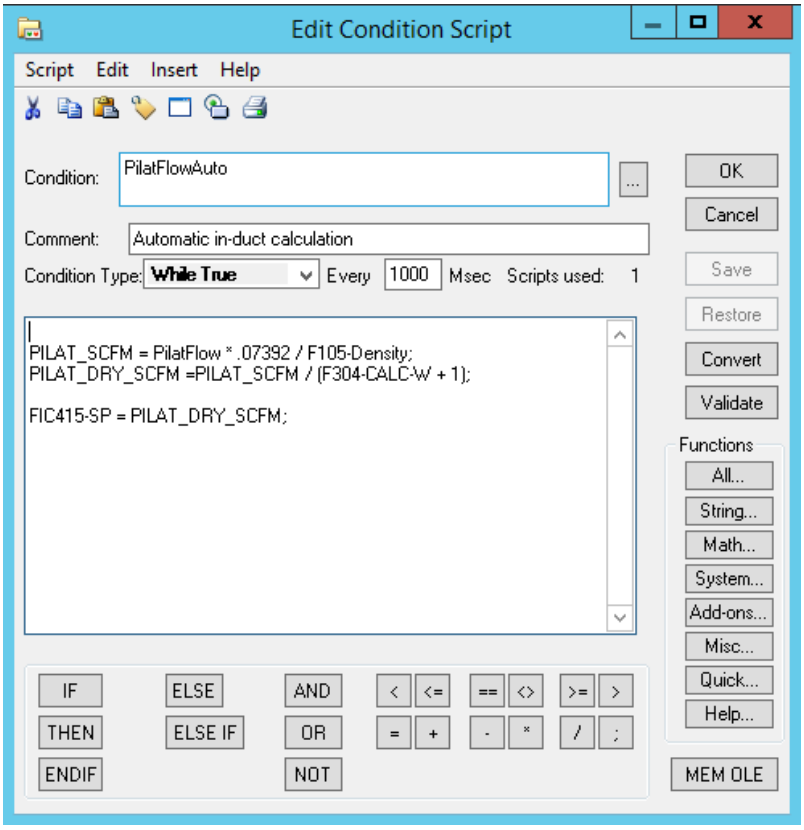

Figure 2.20 SCADA calculation loop for the Pilat impactor isokinetic flowrate for elevated testing conditions.

Figure 2.20 shows the use of "F105-Density" to calculate for the standard volumetric flowrate through the Pilat impactor inlet. The humidity ratio is also determined the same manner as the isokinetic samplers, and the parameter "PILAT_DRY_SCFM" is looped every second to account for the variation in psychrometric parameters during elevated condition testing.

2.3 Radial Large Scale Test Stand

MSU ICET has developed the RLSTS to perform full-scale filter pack loading tests under ambient and elevated conditions. The test stand was designed to evaluate filter performance under ASME AG-1 Section FK. The overall test stand is comprised of the following three base components: (1) induced-draft fan, (2) full-scale filter housing, and (3) the ductwork. The ductwork is composed of round 0.61 m (24 in.) inner diameter, schedule 10 304 L stainless steel duct. The ductwork prior the full-scale filter housing has been designed to evaluate filter performance under normal and upset conditions. The upstream duct section contains ports for installing isokinetic samplers and additional instrumentation. Figure 2.21 shows the upstream duct section on the RLSTS that contains ports for isokinetic sampler installation.

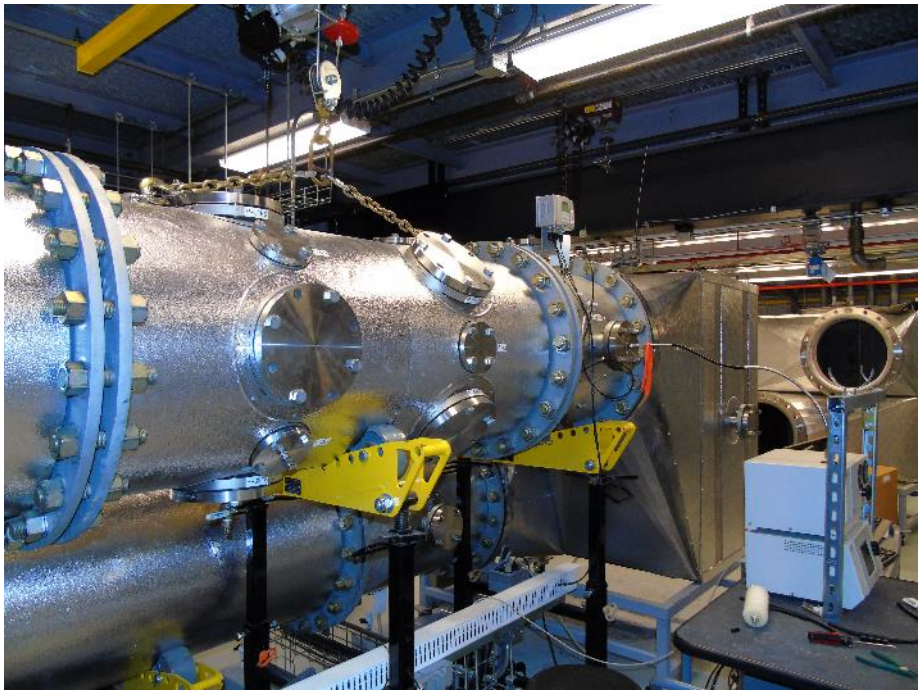

Figure 2.21 Isokinetic sampler duct section on the RLSTS.

The isokinetic sampler duct section is located on the upstream side before the full filter housing. The full filter housing is located midway into the test stand and is capable of interchanging housings for safe change or remote change radial filter testing. Figure 2.22 shows the ductwork of the RLSTS from the perspective of the aerosol injection site.

Figure 2.22 Configuration of the RLSTS with the isokinetic duct section installed.

The aerosol injection site is located upstream of the filter housing where the challenge aerosol can properly mix before reaching the isokinetic samplers and full-scale filter. An induced draft fan is located at the end of the downstream section and can maintain a volumetric flowrate up to 113.25 m^3/min (4000 cfm) +/- 0-10% for radial filters rated at 50 inches water column (in w.c.). The upstream ductwork of the test stand

has been electrically grounded to minimize aerosol clinging due to electrostatic attraction. The inlet of the test stand is located outdoors of the ICET high bay walls and utilizes a series of medium efficiency air filters commonly seen in HVAC applications. This series of filters are used to prevent undesired macroscopic particulate matter from entering the test system from the outdoor environment. The medium efficiency filter minimizes the chance for outdoor airborne particles from entering the sampling instrumentation, allowing data collection results to be more experimentally controlled. Elevated temperature and humidity conditions are generated by using resistance coil heaters and steam injection nozzles located upstream, prior to the aerosol injection site.

2.3.1 Ductwork

The test stand ductwork section where the isokinetic samplers are located is a modified duct section of the RLSTS. As with the RLSTS, the section ductwork is composed of a five-foot long, 24-inch diameter, schedule 10 304 L stainless steel duct. The section contains multiple sampling ports of varying sizes for accommodating temperature and relative humidity sensors, static pressure sensors, additional isokinetic sampling flanges, and a cascade impactor. The modified duct section is seen in Figure 2.23.

Figure 2.23 Modified duct section for the isokinetic samplers.

Figure 2.23 shows the modified duct section removed from the ductwork. The entire ductwork section for the isokinetic samplers and RLSTS is insulated with thermal foam and an exterior layer of stainless steel sheeting covering the foam to retain heat during elevated condition testing. A total of eight, six-inch ports are used to affix the isokinetic samplers, and a total of eight, two-inch ports are used for the installation of sampling nozzles for sampling instrumentation. The aerosol instrumentation used on this test stand includes the: TSI Scanning Mobility Particle Sizer (SMPS), Aerodynamic Particle Sizer (APS), and Laser Aerosol Spectrometer (LAS). Figure 2.4 shows the two-inch port equipped with plumbing (marked with orange tape) reserved for the Mk. V Pilat Cascade Impactor. Images of the Pilat Impactor can be found in Chapter III, Section 3.5.3 Mk. V Pilat Cascade Impactor. The isokinetic sampler section features an electrical crane

hoist to bring the modified section down during periods of maintenance or design revisions. Figure 2.24 shows the electrical crane hoist.

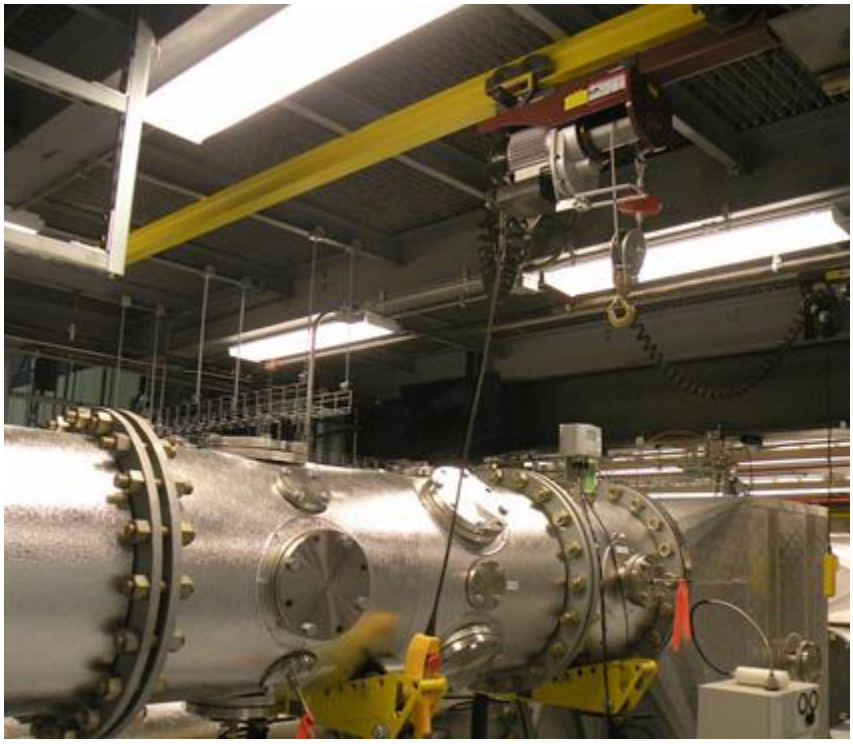

Figure 2.24 Electrical crane hoist for the modified duct section.

The new addition of a recirculatory duct was added to connect the test stand inlet and exit at the induced draft fan. This addition proved useful when testing at elevated conditions to reduce losses in temperature and relative humidity ranges in the upstream portion of the duct. Most of the base components of the RLSTS have remained the same, previous work presenting the initial construction, design, and procedure of the RLSTS can be found in Giffin et al., 2012 [5].

2.3.2 Sampler Locations

The isokinetic samplers are located within the ductwork approximately 20 feet downstream from the aerosol injection site, preceding the radial full filter housing. This location was chosen because of the criteria stated within *Method 1 – Sample and Velocity Traverses for Stationary Sources*. The EPA Method states that ideal aerosol sampling locations of a circular duct must be eight duct diameters downstream from a flow disturbance and two duct diameters preceding a flow disturbance, such as the radial full filter housing [20]. Further, details regarding the airflow characterization of the test section is described in Section 4.1 Test System Characterization. The sampler assemblies are extended to where the center of the sampling nozzles are 7.5 inches from the internal duct walls. In Figure 2.25 the isokinetic sampler testing location is shown in the CAD drawing. Figure 2.26 shows the samplers installed into the test stand at their described sampler depths from a downstream perspective.

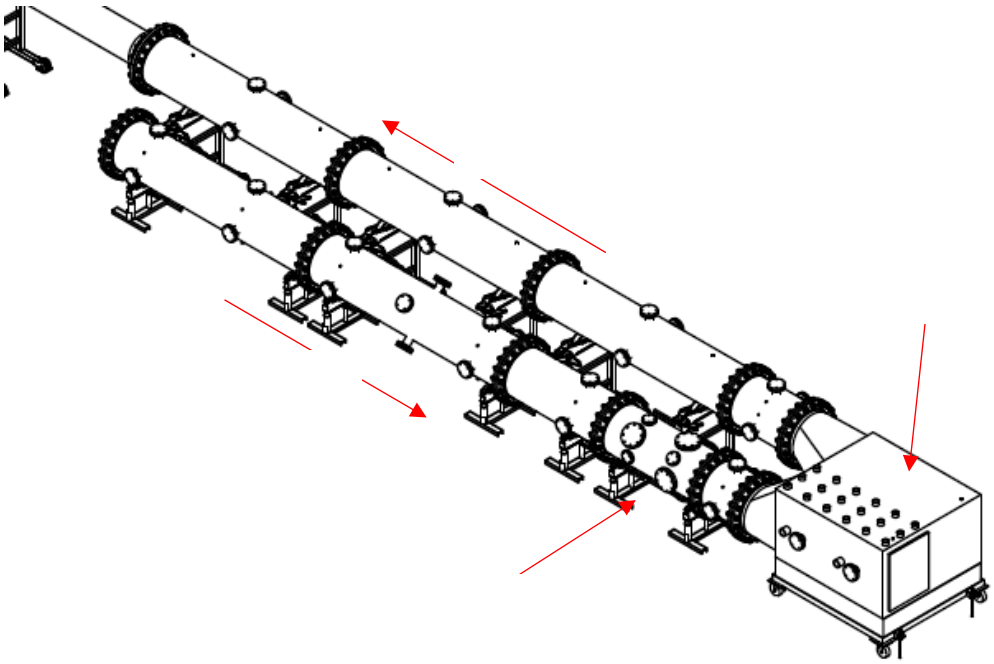

Figure 2.25 Isokinetic samplers testing location in respect to the RLSTS upstream duct.

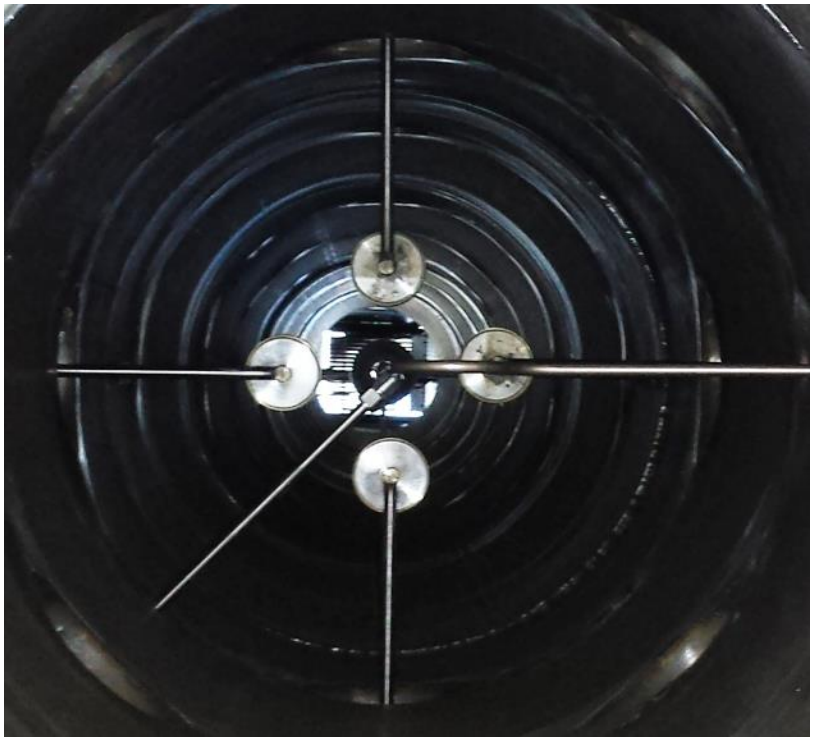

Figure 2.26 Installed isokinetic samplers within the RLSTS test duct.

The upstream sampling nozzle for aerosol sampling equipment and Pilat Impactor sampling line can also be seen in Figure 2.26 in the right-side and bottom-left of the duct, respectively. The aerosol instrumentation sampling nozzle is placed at an adequate distance away from the isokinetic samplers where flow is stabilized. Further sections will discuss the considerations and design aspects to reduce turbulence flow within the isokinetic test duct section.

2.3.3 Test System Performance Criteria

The isokinetic sampler test system must meet the performance criteria set within the test plan. The isokinetic samplers are used to determine how efficiently the pleating preserves loading capacity and pressure drop. Sampling simultaneously in the same duct allows the differential pressure and loaded masses from the isokinetic samplers to be correlated with the performance of the full-scale radial filter. In Table 2.4, the isokinetic samplers undergo the same loading and elevated temperature and humidity conditions as experienced by the radial filter tested within the RLSTS.

Table 2.4 Isokinetic sampler system performance criteria.

Isokinetic Sampler System Performance Criteria	
Compatibility	Capable of sampling simultaneously with the RLSTS without hindering the full filter results
Sampler Capacity	Up to eight HEPA media coupon samplers.
Condition Measurement	Relative humidity (RH) and temperature probes measure conditions relative to the samplers. (0 to 100% RH and -94 to +356 ^{o}F)
Aerosol Measurement	Capable of testing with all aerosols (i.e. powders, sprays, soot, etc.) accepted by the full filter.
Elevated Conditions	Capable of testing at same elevated conditions as the RLSTS up to +200 ^{o}F and 95% RH.
Volumetric Flowrate	Manually controllable volumetric flowrates from 0.1 to 0.5 scfm. Automatic flowrate control settings are implemented via the SCADA to maintain isokinetic flow conditions.
Differential Pressure	Capable of measuring differential pressures up to 50 in. w.c. for each individual sampler.

The isokinetic sampler coupons are removed at scheduled differential pressure goals of 2.5, 4.0, 6.0, and 10 in w.c. to capture the mass loading effects on the HEPA media coupons. The accumulated mass on these HEPA media coupons can be examined to further understand how the effects of aerosol mass loading, particle diameter, and number concentration can affect the filter integrity of the full-scale radial filter. The

isokinetic samplers are used as supplemental instruments to simultaneously test radial filters. The baseline performance parameters of the radial filter pleated media can be obtained from the loaded flat HEPA filter coupons.

Currently only four samplers are utilized during sampling of the HEPA media coupons. The differential pressure for each HEPA filter coupon is measured independently with separate differential pressure sensors. Moist, warm air collected during testing is condensed through the individual condenser units to remove any moisture from damaging or causing flow disruptions in the mass flow controllers. Further details regarding the collection of condensate from moisture laden air and design of the condenser units are found in Section 2.1.8 Heat Exchangers. The consideration of isokinetic sampling in high relative humidity is discussed in Section 2.2.2.1 Consideration of Moist Air Sampled During Elevated Conditions. The following sections will describe the isokinetic test system components in further detail.

CHAPTER III

TEST METHODOLOGIES

3.1 Gravimetric Analysis Procedure

The determination of differential mass for the isokinetic samples are performed using a gravimetric analysis procedure. Procedure HEPA-029-Gravimetric Analysis includes textile testing standards from the Technical Association of the Pulp and Paper Industry (TAPPI), American Society for Testing and Materials International (ASTM), and the International Organization for Standardization – Guide to the Expression of Uncertainty in Measurement (ISO GUM). These standards selected from the listed organizations are used to correct for air buoyancy, relative humidity, temperature, barometric pressure, as well as account for user handling errors during weighing methods for mitigating static of the sample during weighing. Methodologies from ASTM D6552-06(2011) and ISO GUM (1993) were implemented to account for errors in weighing uncertainties [23, 24]. Pre-conditioning chambers were used to control the temperature and humidity of the HEPA media coupon samples prior and after testing to ensure that weighing conditions were within industry standards. Methodologies from ASTM D5032 - 11 were used to create a controlled humidity environment using a glycerol solution to maintain relative humidity within a pre-conditioning chamber between 50% to 60% RH [25]. MSU ICET procedures for the gravimetric analysis can be found in Appendix B. Once the HEPA media coupons have been pre-weighed for testing, the MSU ICET

procedure HEPA-RLSTS-015 ICTS Removal and Installation procedure is followed to ensure mass accumulation during the installation and removal processes is minimized.

3.2 Testing Conditions

The testing conditions for the isokinetic samplers varied depending on the full size HEPA filter type and conditions being tested within the RLSTS filter housing. These conditions ranged from ambient conditions as seen in air-conditioned indoor environments with room temperature and humidity levels to elevated conditions operating at high temperature and strict relative humidity ranges. The operating flowrates, temperatures, and relative humidity varied depending on the requirements stated for testing the full filters within the test plan. These flowrates can range from 25 % rated flow to 100% rated flows, depending on the radial full filter design specifications. The RLSTS flowrate for the tests including the isokinetic samplers have been set at volumetric flowrates of 1200 and 2000 cfm. Table 3.1 represents the ambient and elevated testing conditions used to evaluate the flat media HEPA media coupons and radial full filter designs.

Table 3.1 Psychrometric testing conditions for the RLSTS.

Test Category	Test Condition Classification	Operating flowrates (cfm)	Temperature Ranges (^{o}F)	Relative Humidity Ranges (%)
N/A	Ambient	2000	60 - 80	40 - 60
3	Elevated	1200	166 - 171	50 - 55
2b	Elevated	2000	177 - 182	40 - 45
2c	Elevated	2000	177 – 182	50 - 55

The elevated test conditions are specified as seen in Table 3.1 prior the test. The capability of testing in ambient and elevated testing conditions can simulate a wide range of temperature and relative humidity effects on nuclear grade HEPA filter media under upset conditions.

3.3 Aerosol Generation

The generation of test aerosols is vital to the consistency of data collected. The use of aerosol generation equipment at MSU ICET range from powder feeders, in-house fabricated burner ports, and oil droplet generators. Powder feeders are used to disperse test powders by controlling the rate of aerosol injection into the test stand. The powder feeder is a mixer that uses twin screws to feed test powders through a compressed air vacuum nozzle. Burner ports have been created at MSU ICET to assist in generating acetylene soot particles. These ports are affixed at the same aerosol injection location as the powder feeder. Each burner is lit manually to a specific flame length before

performing the loading test. The powder feeder and burner ports will be discussed in this section. Oil droplet generators were not used in the loading procedure on the isokinetic samplers. The oil droplet generator is used only for distributing dioctyl phthalate (DOP) during the full filter efficiency tests after four in. w.c. and 10 in. w.c. of loading.

3.3.1 Powder Feeder

MSU ICET utilizes a twin screw, gravimetric powder feeder with continual agitation to ensure consistent powder generation rates for the dispersion of test dusts and powdered aerosols. A K-Tron Model K-MV-T20ID powder feeder is used for the generation of aluminum trihydroxide and Arizona Road Dust test powders at the aerosol injection site on the RLSTS. A compressed air line is attached to a resistance heating element to maintain heated air into the test duct when generating aerosols during elevated loading tests. The powder and heated air are combined at the Vaccon vacuum nozzle before being dispersed into the aerosol injection site. The following figure shows the powder feeder arrangement.

Figure 3.1 K-Tron powder feeder used for test dust generation on the RLSTS.

Figure 3.1 shows the installed powder feeder at the aerosol injection location on the upstream RLSTS ductwork. On the aluminum trihydroxide and Arizona Road Dust loading tests, the powder feeder is set to 1000 RPM whenever loading is performed. This setting has been pre-determined to allow consistent target particle concentrations ranging from 1E+5 to 1E+6 particles per cubic centimeter.

3.3.2 Burner Ports

The challenge aerosol including the acetylene soot is generated using modified burner ports. These modified flanges fabricated in-house at MSU ICET feature an open-port design that can adjust the flame casting height and depth into the port. The flame length is adjusted using the needle valve located on each burner port, where number concentration with all four burners set at seven inches of flame length can consistently

output 10E+5 to 10E+6 particles per cubic centimeter. An image of the burner ports installed onto the RLSTS can be seen below in Figure 3.2.

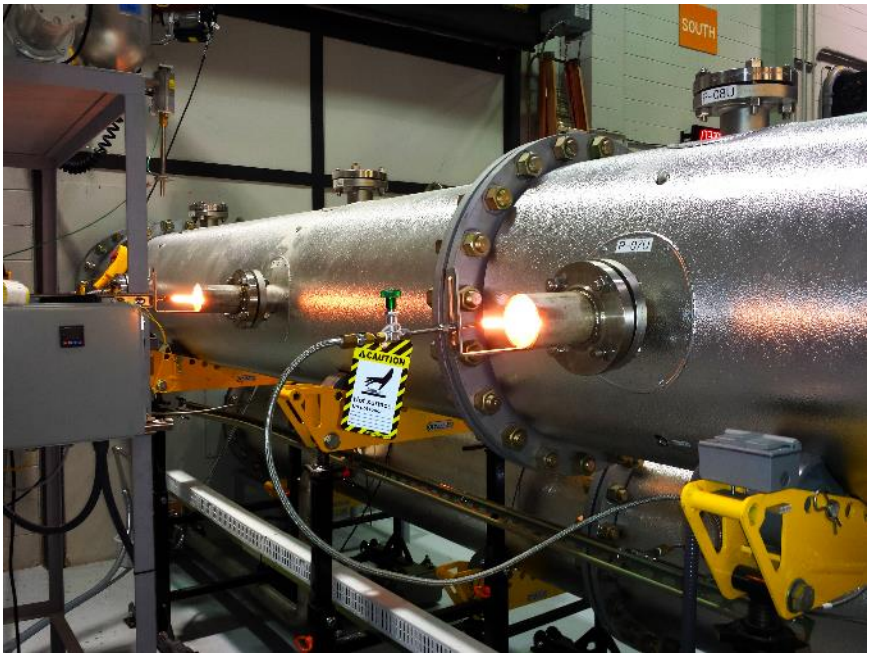

Figure 3.2 Modified burner ports installed onto the RLSTS.

Figure 3.2 shows the modified burner ports installed and set to a flame length of seven inches. This flame height provides a suitable number concentration for the aerosol instruments that will soon be discussed. The burners are connected to a single supply line coming from the canister of dissolved acetylene (not shown). A pressure regulator controls the outflowing gas. The burner ports have also been used to accommodate other gas types, such as conventional propane, butane, and methane, with modification of the flame outlet to correct for flame intensity and test stand vacuum from sucking out the flame. This study does not include data obtained from those observations.

3.4 Challenge Aerosols

A factor in the evaluation of the full filter is the challenge aerosol generated. The types of challenge aerosols used in the RLSTS tests, range from fine test powders to flame generated soot. Each test is performed with a polydisperse challenge aerosol to study the effects of pressure drop across the radial full filter and the HEPA media coupon samples.

Challenge aerosols used at MSU ICET typically consist of test powders used within industrial filtration tests and flame generated soot from various gaseous fuels, such as butane, propane, methane, and acetylene. Aluminum trihydroxide powder ($Al(OH)_3$), A-1 ultrafine Arizona test dust (Arizona Road Dust), and acetylene soot will be represented as the challenge aerosols evaluated in the RLSTS and isokinetic samplers.

Physical parameters vary between each challenge aerosol type include the aerosol hygroscopic properties, particle mass, particle size distribution, particle surface area, and morphology. Table 3.2 shows the bulk density, particle size distribution, geometric standard deviation (GSD), CMD, and MMD of each challenge aerosol used. These challenge aerosol statistics will be used to compare

Table 3.2 Statistical information of the challenge aerosols.

Challenge Aerosol	Bulk Density (g/cm^3)	Particle Size Distribution (μm)	GSD	CMD (μm)	MMD (μm)
$Al(OH)_3$	2.42	0.5 to 2.5	1.49	1.12	1.92
Arizona Road Dust	2.65	1 to 22	1.57	0.87	2.87
Acetylene Soot	2.0	0.07 to 17	2.09	0.63	5.67

3.4.1 Aluminum Trihydroxide

SpaceRite S-3 aluminum trihydroxide, abbreviated as $Al(OH)_3$, is used as a test powder for many of the tests at MSU ICET. The test powder commonly known as hydrated alumina has the notable characteristic to provide fire retardancy and smoke suppresant at high temperatures to about 180 ^oC (356 ^oF) until decomposition occurs. The aerosol is capable of releasing water vapors in the process of heating. The d50 particle size is 1.0 micron per the test dust manufacturer specifications, with most ultrafine particles being greater than 0.5 microns. The granular powder at this particle size distribution allows the challenge aerosol to be deposited within the filter media depth as loading increases via filtration mechanisms such as impaction and interception. Water droplets that are formed between the granular dendrites strengthen the aerosol caking characteristics as aerosol loading continues during elevated conditions. This challenge aerosol serves to evaluate filters with the provided characteristics for the cases of "worst case scenario" testing.

3.4.2 Arizona Road Dust

ISO 12103-1 A-1 Ultrafine Arizona test dust, also known as Arizona Road Dust (ARD), is another standard test dust used in filter evaluation tests at MSU ICET. The test dust is used to simulate an environment with a wide range of particle sizes commonly seen in deserts and dense cities from one micron to 20 microns in size, with an MMD of 5.0 microns. ARD is non-hygroscopic in nature much like alumina trihydrate. However, hygroscopic tendencies for particles to shrink have been shown to occur at higher relative humidity greater than 90% for particle sizes larger than 100 nm, as studied by Vlasenko et. al. [26]. The primary trait of this challenge aerosol is the particulate mass per unit volume. The effects of mass loading on HEPA filters can be studied effectively by using this as a challenge aerosol to simulate a natural loading condition on HEPA filters.

3.4.3 Acetylene Soot

Acetylene soot is generated from a canister of dissolved acetylene using the four modified burner ports affixed at the aerosol generation site of the RLSTS. This challenge aerosol is substantially smaller in particle size distribution than the generated powders. The particle size distribution has ranged from 40 nm to 200 nm. Agglomeration is likely to occur within the airstream and when in contact with other soot particles at the filter media due to the aliphatic nature of soot particles, as studied by Kim et. al. [27]. This characteristic, in combination to the small particle size distribution, contributes to a test filter to load much quicker due to clogging within the fiber depths without sufficient surface loading to occur.

3.5 Aerosol Instrumentation

Determination of the challenge aerosol particle size range, number concentration, and mass concentration during testing requires the use of precise instrumentation. Equipment such as the: (1) TSI Aerodynamic Particle Sizer (APS), (2) Scanning Mobility Particle Sizer (SMPS), and (3) Laser Aerosol Spectrometer (LAS) can effectively sample the challenge aerosol in the upstream and downstream ducts under elevated conditions. Diffusion dryers have been implemented to reduce the moisture from entering the instruments during sampling. A limited number of samples are made when sampling during elevated conditions to reduce the amount of moisture from building up in the diluter capillary tubes.

The SMPS and APS sample the particle size distribution, particle number concentration, and other parameters such as the MMD, count mean diameter (CMD) of the sampled distribution. The LAS samples the particle size distribution and particle number concentration. The following table summarizes the aerosol instrumentation used during the filter tests.

Table 3.3 Summary of aerosol instrumentation specifications.

Instrument	Min. Diameter	Max Diameter	Number Concentration Upper Limit (#/cc)
SMPS 3938	24 nm	1 μm	1E+7
APS 3321	1 μm	20 μm	1E+3
LAS 3340	90 nm	7.5 μm	1E+3 to 1E+4

The size range of the SMPS using the custom 95 cm differential mobility analyzer (DMA) is from 24 nm to 1 micron. The APS is capable of sampling particle size distributions from 0.5 micron to 20 microns. The APS minimum diameter samples as low as 0.37 μm. Due to Rayleigh scattering from sampled air and Mie scattering from the particles the effective minimum APS diameter at 1 μm. Light scattering from 0.1 μm to 1 μm affects the particleThe LAS is used to sample particles upstream and downstream during the filter efficiency tests on the full filter. It is ideal for filter efficiency tests but is not used as an instrument of the isokinetic sampler calculations.

The Mk. V Pilat Cascade Impactor (furthermore stated as the Pilat impactor) is an instrument used to correlate the combined SMPS and APS data with the particle size distribution collected by the cascade impactor. The Pilat impactor does not have real-time particle measurement instrumentation so the SMPS and APS data are used to validate the sampled Pilat impactor data. The SMPS particle size range must be converted to an aerodynamic diameter before being combined with the APS size range. The use of the

combined SMPS and APS data are essential in validating the challenge aerosol sampled by the Pilat impactor. The upstream sampling locations for the SMPS and APS are in the upstream duct between the isokinetic samplers and radial full filter housing. The downstream sampling location is located midway into the downstream duct. The Pilat Impactor is placed within the upstream ductwork just before the isokinetic samplers.

3.5.1 Aerodynamic Particle Sizer

The TSI aerodynamic particle sizer (APS) Model 3321 is used to accurately collect the mass concentration of the challenge aerosol using time-of-flight laser technique to size particles from 0.5 to 20 microns in size. The APS can detect particles as low as 0.37 microns using a separate light scattering technique. This option becomes a second method of measurement when the time of flight measurements are not sufficient. The APS determines the particle airborne behavior based on aerodynamic particle diameter when passing through two overlapping lasers to generate a signal and two crests. When the particle passes through these two lasers, the instrument analyzes the time of flight to provide the aerodynamic particle size.

Maximum particle number concentrations on the APS range from 1000 particles/cm^3 at 0.5 micron with <5% coincidence up to 10E+4 particles/cm^3 at 10 micron with <10% coincidence. A coincidence event occurs when there is more than one particle between the viewing volume of the lasers and is detected by the instrument. These events are classified as Event 1 – 4, and depending on the classified event, particle size distribution and light-scattering intensity results are recorded. The figure below from the TSI APS Model 3321 product information brochure describes each classified coincidence event [28].

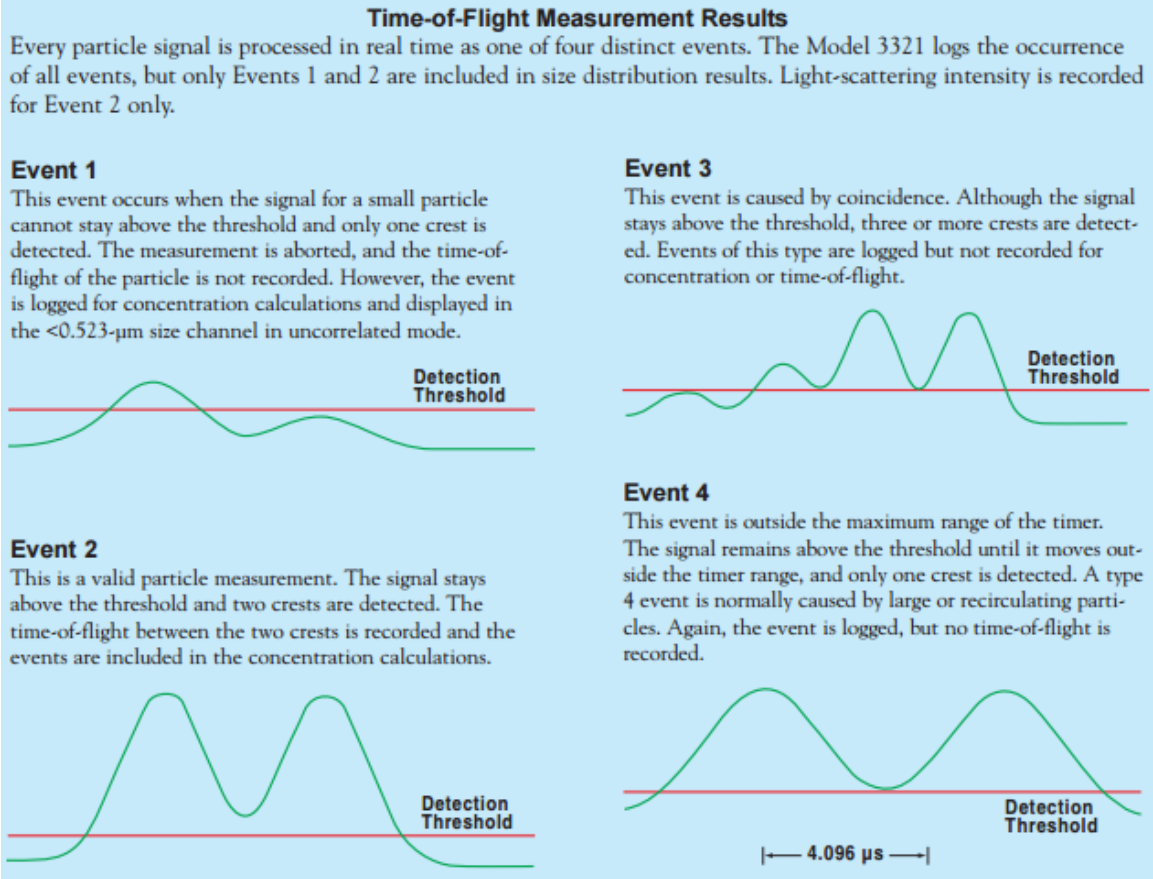

Figure 3.3 Time-of-Flight Events on the TSI APS Model 3321

Figure 3.3 shows the particle coincidence events that can be detected by the APS time of flight technique. The occurrence of these sampling events can be reduced by placing aerosol diluters before the APS. The TSI Model 3302A aerosol diluter can reduce the aerosol number concentration at 20:1 and/or 100:1 dilution ratios, and can be stacked for maximum dilution effects up to 10000:1. The filter loading tests at MSU ICET use a 20:1 and two separately assigned 100:1 diluters on the APS and SMPS, depending on the aerosol generated.

3.5.2 Scanning Mobility Particle Sizer

The TSI Model 3082 SMPS is used to verify the particle number concentration in the upstream and downstream duct sections in the RLSTS. The SMPS surpasses the APS in processing the particle number concentration because of the SMPS uses a differential mobility analyzer (DMA) and a condensation particle counter (CPC). The DMA is a custom 95 cm unit from TSI and operates by method of sorting particle sizes based on electric mobility diameter. The DMA uses high voltages to accurately sort the particle sizes ranging from 24 nm to 1 micron based on the electric mobility diameter before being sent to the CPC. The TSI Model 3775 CPC is used to determine the particle number concentration, where the operation is based on vaporized butanol to condensate the sampled airstream. The condensed airstream with particles larger than the threshold diameter is then passed through an optical detector to be measured accurately. The CPC can detect a number particle concentration ranging from 5E4 to 10E6 particles/cm^3. Figure 3.4 shows the setup for the SMPS on the RLSTS.

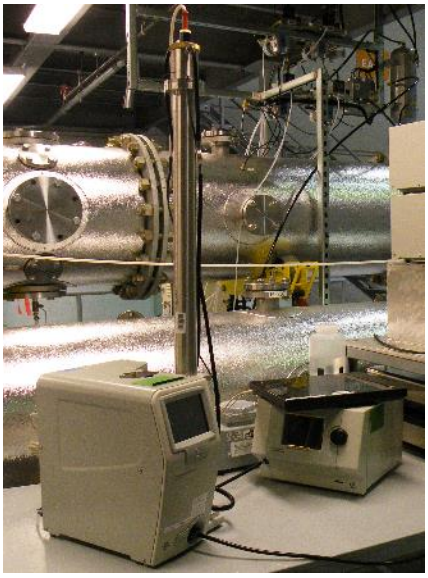

Figure 3.4 TSI Model 3082 SMPS and TSI Model 3775 CPC for the RLSTS.

The TSI SMPS and CPC are used in unison to detect the effective particle mobility diameter and number concentration, respectively. The SMPS lacks in mass determination because of the operation technique of sorting based on mobility diameter to determine the mass concentration, whereas the APS operates based on a time-of flight technique to estimate the mass based on aerodynamic diameter. The SMPS has a much smaller detectable size range at 24 nm and larger range of particle number concentration up to 10E+6 particles/cm^3. The SMPS is ideal for detecting particles of smaller diameter such as acetylene soot, whereas the APS is better suited for aerosols such as aluminum trihydroxide and ARD. The TSI 3302A aerosol diluters can also be used to reduce the sampled particle concentration prior reaching the instruments.

3.5.3 Mk. V Pilat Cascade Impactor

The Mk. V Pilat Cascade Impactor is a cascade impactor developed by Michael J. Pilat of University of Washington to collect differential masses of samples from 0.200 to 80 microns. Implementation of the cascade impactor determines the aerodynamic size distribution of the challenge aerosol, in addition to the electronic particle sizing instrumentation on the RLSTS. The Pilat impactor has an advantage of withstanding elevated condition testing within the RLSTS. The use of electronically monitored impactors may be sensitive to the elevated temperature and relative humidity during loading tests. The Pilat impactor relies solely on an isokinetic vacuum flow through the inlet nozzle through a series of jet stages to categorize particles based on aerodynamic diameter. A study conducted by Pilat et. al during elevated condition testing of emissions from a pressurized fluidized coal combustion test facility has been performed to study the particle size distribution on the life of gas turbine blades [29]. Temperatures and pressures for those tests ranged from 107 to 238^{o}C (~225 to 460.4^{o}F) and up to 506.6 kPa (~73.5 psi). The testing conditions at MSU ICET are well within range for the Pilat impactor operate and acquire data under elevated testing conditions.

The impactor consists of 11 jet stages, each featuring specific cut diameters for various inlet flowrate configurations. The jet stages operate by separating the particles entering the impactor assembly based on their aerodynamic diameters. Equation 3.1 is used to determine the jet stage aerodynamic diameter, da_{50}, is provided as seen in the Pilat impactor user's manual [30].

$$da_{50} = \frac{18*\mu*D_j*Y_{50}}{C*V_j} \quad (3.1)$$

Where:

da_{50} = aerodynamic cut diameter
μ = gas viscosity
D_j = diameter of the impactor stage jet holes
Y_{50} = inertial impaction parameter, 0.145 for cylindrical round jet stages
C = Cunningham slip correction factor for particle of diameter da_{50}
V_j = gas velocity at inlet prior entering the impactor jet on stage

Table 3.4 lists the jet stage parameters and cut diameters for each stage for the 0.3 to 0.5 scfm isokinetic sampling flow configuration. Included in Table 3.4 are the aerodynamic cut diameters for the elevated testing conditions as performed at ICET. The cut diameters listed below in Table 3.4 and are applicable to tests conducted during ambient and elevated conditions at 2000 cfm.

Table 3.4 Mk. V Pilat Impactor jet numbers and diameters for 0.3 to 0.5 scfm flow configuration.

Jet stage number	**Number of jets per stage**	**Jet diameter (inches)**	**Cut diameter, da_{50} (microns)**
1 (Nozzle jet stage)	1	0.5000	40.2
2	12	0.0960	3.50
3	90	0.0311	1.95
4	110	0.0200	1.40
5	110	0.0157	1.05
6	110	0.0135	0.800
7	105	0.0118	0.590
8	105	0.0102	0.480
9	78	0.0102	0.380
10	56	0.0102	0.280
11	40	0.0102	0.220

The challenge aerosol is impacted onto greased, 304 stainless steel collection plates placed under each jet stage, prepared in accordance to MSU ICET procedure, HEPA-MTE-008_Mark 5 Pilat Impactor Readiness and Operation. Please refer to the Appendix for the entire referenced document. Figures 3.5 and 3.6 show the jet stages

with collection plates from stage 1 to stage 11 and the assembled Pilat impactor, respectively.

Figure 3.5 Jet stages and collection plates of the Pilat impactor.

Figure 3.6 Assembled Pilat impactor with 5/16” sampling nozzle.

Design considerations for the addition of the Pilat impactor into the RLSTS have included a cradle for maintaining the cascade impactor parallel towards the direction of the oncoming free stream flow. Figure 3.7 shows the Pilat impactor cradle installed into the ductwork directly upstream of the isokinetic sampler duct section. A design schematic and dimensions of the cradle are available in the Appendix.

Figure 3.7 Pilat impactor cradle installed within the upstream ductwork.

A main concern when designing this cradle was the airstream turbulence affecting the sampler collection effectiveness. The inertial effects from the particulate matter vary depending on the challenge aerosol used. The combination with airstream vortices may produce uneven, non-representative particle loading on the sampler coupons. A cradle was designed and fabricated with slopes angled at 15 degrees on both sides of the

mounting arms that streamline the airflow passing around the structure to minimize airstream turbulence. Figure 3.8 shows the 15-degree double bevel knife edges designed on the Pilat impactor cradle legs.

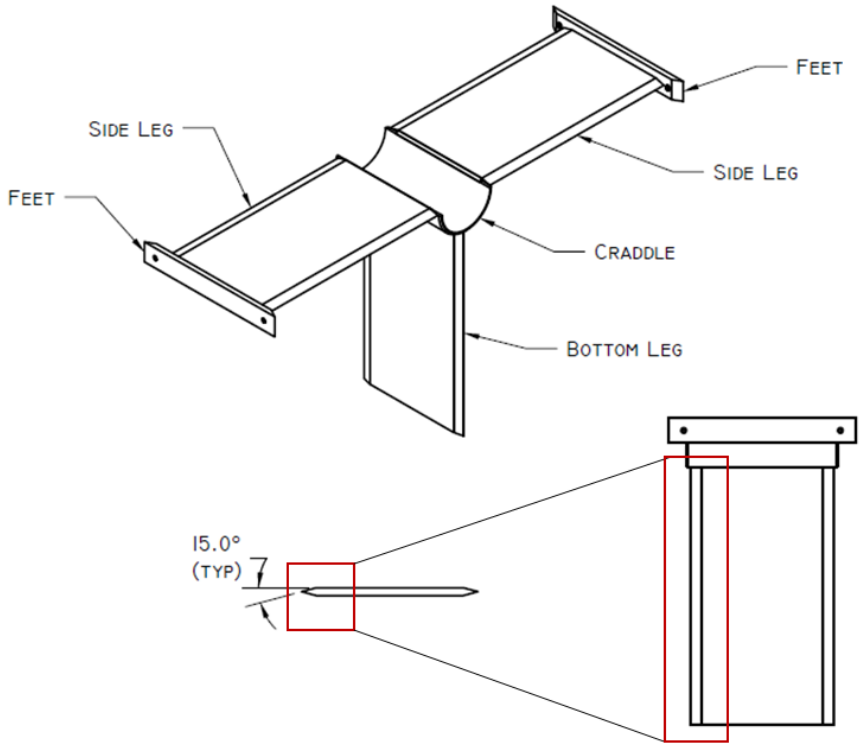

Figure 3.8 Pilat impactor cradle legs designed with two 15-degree double bevels.

The Pilat impactor cradle legs were designed with 15-degree bevels on each side of the legs to minimize the flow turbulence downstream of the cradle. The leading edge of the bevels create an aerodynamic profile for air flow after passing the impactor cradle. Additional design drawings of the Pilat impactor cradle can be found in Appendix A.

The previous setup for the Pilat impactor included a dry gas meter and fluid bed manometer contained within a large box attached to a sampling train with ice-bath cooled

impingers. This approach proved to be time costly and outdated when means to control and cool the incoming heated, moist air could be resolved with a MFC and the heat exchanger system, respectively. The construction of the heat exchanger system allowed for an alternate method for the impinger system. A MFC was installed specifically for the Pilat impactor and an additional vacuum line was attached to the air ballast tank. The flow settings for the Pilat impactor is primarily at the setpoint for optimal isokinetic sampling at 0.310 scfm to fall within a +/- 10% isokinetic sampling range at 2000 cfm test conditions. The controls may also be manually operated, but in all previous tests for ambient and elevated conditions, the automatic sampling function on the control panel has been activated for the optimal isokinetic sampling conditions. The SCADA maintains the flow readings at 0.310 scfm for the 5/16" inlet nozzle chosen. This flow automation was explained in Section 2.2.2.1 Consideration of Moist Air Sampled During Elevated Conditions.

CHAPTER IV

RESULTS AND DISCUSSION

4.1 Test System Characterization

The incoming airflow within the duct is required to be free of uneven airflow regions at the sampler locations to ensure that sampling is not affected by vortices. Uneven loading may occur on the samples if this requirement is not met. The mass loading results of the isokinetic samplers would not be representative of their intended loading percentages as reflected by the full-scale radial filter. There will be a discrepancy between the HEPA media coupons and full filter in regards to mass loaded. Methods for selecting traverse points free from cyclonic flow within square and round ductwork have been standardized by the U.S. Environmental Protection Agency (EPA).

Method 1 – Sample and Velocity Traverses for Stationary Sources, provides guidance for the selection of sampling ports and traverse points for sampling particulate matter. The method states that gas stacks with diameters equal to or less than 0.61 m (24 in.) will not have traverse point measurements located within 1.3 cm (0.50 in.) of the stack walls [20]. The method is based on the Equal-Area Method for round ducts that divides the cross-sectional area of the traverse plane into equal concentric circular area segments containing traverse points. The distance of each traverse point increases from the edge of the duct wall as the traverse points progresses towards the center. The Equal-Area Method states that no velocity readings are taken at the center of the duct, however,

a measurement was taken as an additional point of measurement. Airflow traverse measurements were made using a TSI Alnor Velometer Thermal Anemometer Model AVM440-A at varying depths within the RLSTS test stand duct. Six traverse points were each chosen for the horizontal and vertical orientation due to the requirement that the number of traverse points must be a multiple of four. The traverse points totaled to 13 traverse measurement locations including the location at the center of the duct. The following figure shows the schematic used to measure each horizontal and vertical traverse point location for the isokinetic samplers.

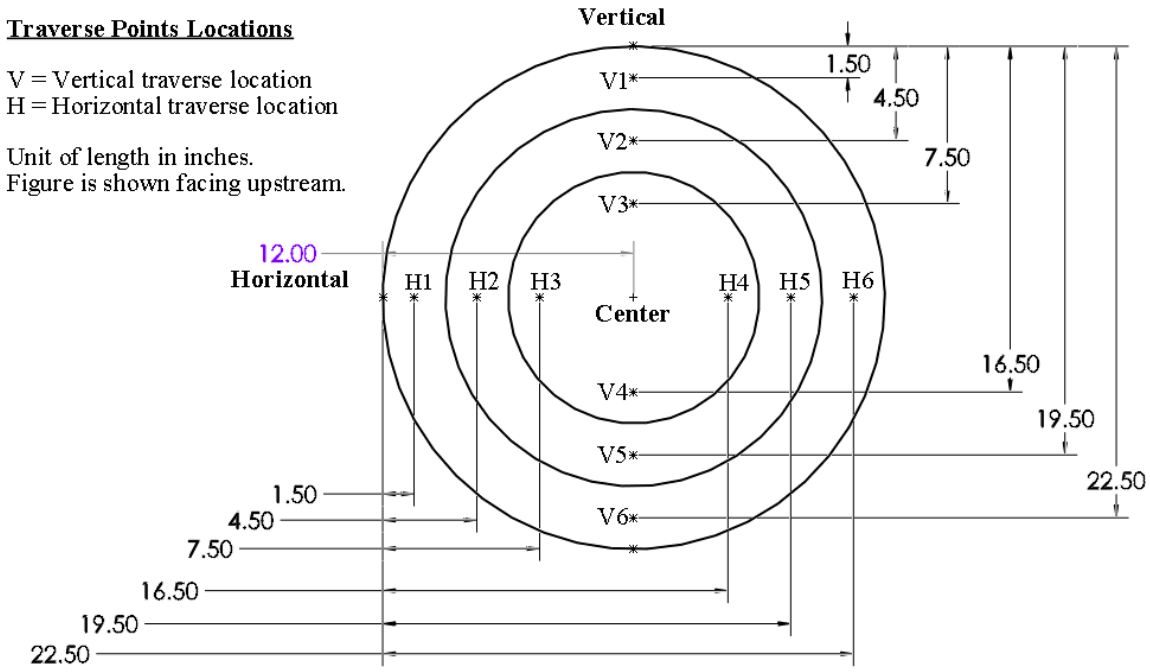

Figure 4.1 CAD schematic of traverse point locations using the Equal-Area Method.

Method 1 states that sites for sampling particulate matter must be performed at least eight stack or duct diameters downstream and two diameters upstream from any flow disturbance, such as visible flames, bends, expansions, contractions, and elbows

[20]. This criterion ensures that particulate matter sampled are not in locations where flow disturbances are present that may affect sampling accuracy. The results for the traverse measurements are shown in the following figures.

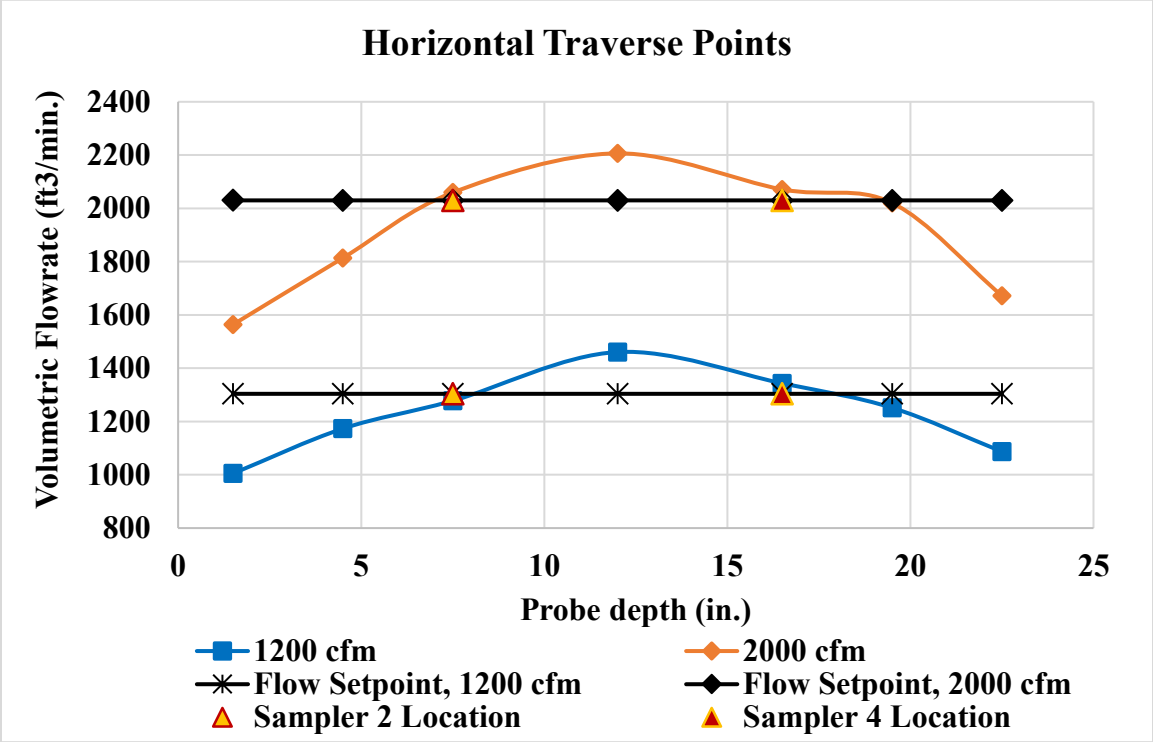

Figure 4.2 Horizontal traverse points for the isokinetic samplers.

Isokinetic sampler locations are 7.5 inches within the ductwork. The triangle symbols denote the sampler locations.

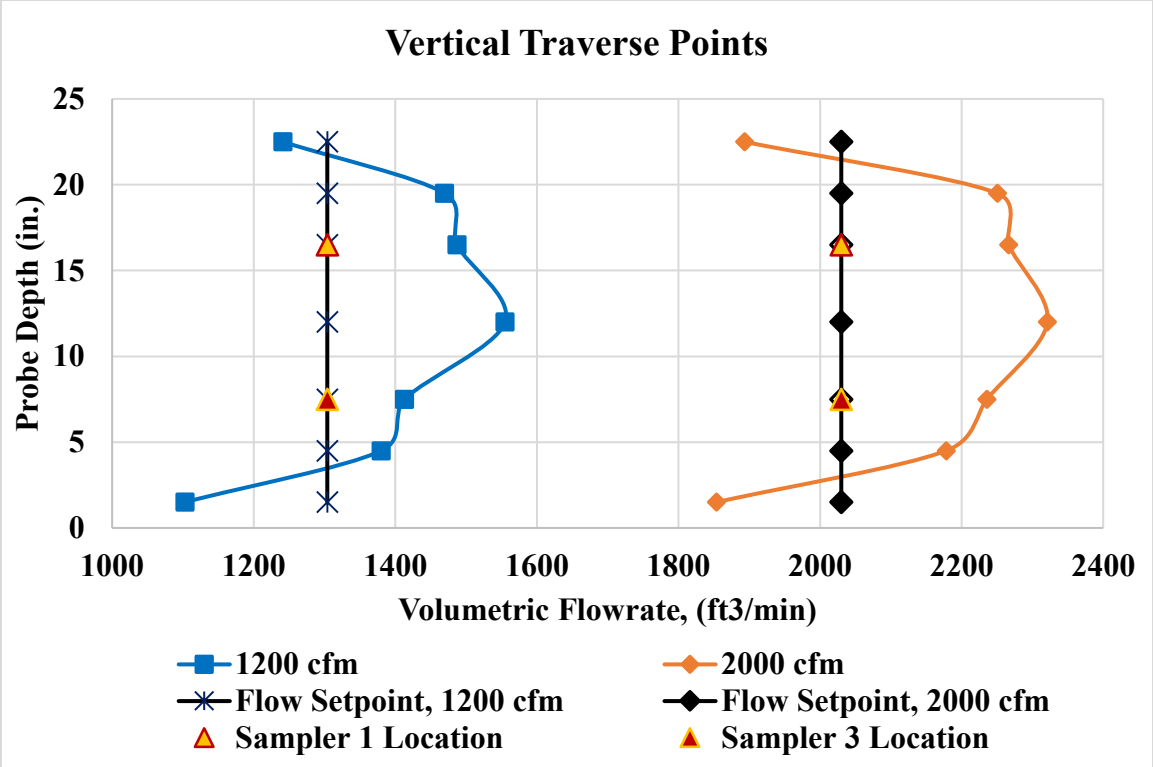

Figure 4.3 Vertical traverse points for the isokinetic samplers.

Isokinetic sampler locations are 7.5 inches within the ductwork. The triangle symbols denote the sampler locations.

The results shown in Figures 4.2 and 4.3 represent the horizontal and vertical airflow traverse points, respectively. The TSI AVM440-A allowed thorough measurements within the ductwork. Insertion points for the velocity probe were at Samplers 2 and 3. A traverse point was taken at each location shown on Figure 4.1. Each traverse point consisted of one measurement per second for a period of 10 seconds. Individual flow measurements were averaged for the two testing flowrates of 1200 cfm and 2000 cfm. The flow rates for the vertical and horizontal orientation were averaged to determine the mean flowrate for each respective axis of measurement. An averaged flow

of approximately 1300 cfm was calculated for the 1200 cfm traverse points, and an averaged flow of 2030 cfm was determined for the 2000 cfm traverse points. The flow measurements at the 1200 cfm setpoint measured higher at 1300 cfm. This is because at this flowrate the induced draft fan blower is not optimized to operate at the setpoint of 1200 cfm. The flow trajectories maintain a uniform flow pattern downstream of the Pilat impactor cradle with only minimal disturbance at the isokinetic samplers. The flow is uniform for the isokinetic sampling ductwork and the intended flowrates are within 10% error of their target setpoints of 1200 cfm and 2000 cfm.

The effect of cyclonic flow is minimized due to the aerodynamic designs from the Pilat impactor cradle and the isokinetic sampler nozzles. The 15 degree beveled knife-edges on the Pilat impactor cradle legs were designed for reducing cyclonic flow after the Pilat impactor sampling location. Any cyclonic flow disturbances within the duct or from the Pilat impactor sampling location would be minimized.

4.2 Isokinetic Sampler and APS Mass Data Comparison

This section presents the pressure drop and gravimetric mass loading data results for the HEPA media coupon samples. The initial and final pressure drop is shown for each isokinetic sampler coupon throughout the loading process from initial to 10 in. w.c. of aerosol loading. Particle number concentration from the APS and SMPS are compared to verify that the APS number concentration used in the APS mass calculations are justified. The gravimetric mass data obtained from HEPA-029-Gravimetric Analysis is entered and compared with the APS calculated masses. A correlation coefficient is determined to show the level of agreement between the gravimetric analysis masses and the APS calculated masses obtained. A total of 15 isokinetic sampler data sets are shown

to show the evaluation results for each test from initial to 10 in. w.c. of loading. The following table shows the matrix of test conditions and filter types tested.

Table 4.1 Isokinetic Sampler Test Matrix.

RunID	Challenge Aerosol	HEPA Media Tested	Radial Filter Type	Test Category	Temperature	Relative Humidity
12784-1	$Al(OH)_3$	3398 L2W	Safe Change	3	166° F	50%
12784-2	$Al(OH)_3$	3398 L2W	Safe Change	3	166° F	50%
12784-3	ARD	3398 L2W	Safe Change	2b	177°F	40%
12784-4	ARD	3398 L2W	Safe Change	2b	177°F	40%
12784-5	Acetylene Soot	3398 L2W	Safe Change	2b	177°F	40%
12784-6	Acetylene Soot	3398 L2W	Safe Change	2b	177°F	40%
13109-2	$Al(OH)_3$	3398 L2W	Safe Change	2b	177°F	40%
12719-3	$Al(OH)_3$	3398 L2W	Safe Change	2b	177°F	40%
13554-2	$Al(OH)_3$	3398 L2W	Remote change	2c	177°F	50%
13554-3	$Al(OH)_3$	3398 L2W	Remote change	2c	177°F	50%
13554-4	$Al(OH)_3$	3398 L2W	Remote change	2c	177°F	50%
13554-5	$Al(OH)_3$	3398 L2W	Remote change	2c	177°F	50%
13554-6	Acetylene Soot	3398 L2W	Remote change	2c	177°F	50%
13554-7	Acetylene Soot	3398 L2W	Remote change	2c	177°F	50%

The tests represented were performed with safe change and remote change orientation radial HEPA filters from initial clean differential pressure to 10 in. w.c., as specified in the test plan documentation.

The APS and SMPS use density factors of 1 g/ccm as their default particle density for calculation of mass concentration. A density correction factor was used for each challenge aerosol based on material. The bulk density of $Al(OH)_3$ and Arizona Road Dusts were referenced from manufacturer specification data sheets and from Lee et. al., where the study performed was conducted at room temperature and 55% relative humidity [31]. The bulk density of $Al(OH)_3$ was assumed to be 2.42 g/cm^3, and the bulk density of Arizona Road Dust was assumed to be 2.65 g/cm^3 for the APS mass estimations. The effects of hygroscopic growth can affect the particle size and tendencies for agglomeration and increased pressure drop if wetted. The bulk density of acetylene soot was assumed at 2.0 g/cm^3 based on studies of acetylene soot formation models from Fairweather et al., Woolderink et al., and Akridis et al. [32, 33, 34].

4.2.1 Isokinetic Sampler Evaluation Results

The test data for the isokinetic samplers collected simultaneously with a safe change orientation, full-scale radial flow filters are shown in this section. The removal of the isokinetic samplers throughout the test are scheduled according to differential pressure experienced across the full-scale filter. The changeout points based on pressure drop allows the isokinetic samples to be examined based on the equivalent loading between the full filter and HEPA media samples. The following table shows the scheduled changeout pressures on the full-filter for the tests conducted.

Table 4.2 Isokinetic Sampler Changeout dP and Loading percentages for safe change radial type filters.

Port Number	Isokinetic Sampler Number	Changeout dP (in. w. c.)	Loading Percentage
1	1 & 5	2.5 / 10.0	25% / 75%
2	2 & 6	4.0 / 10.0	50% / 50%
3	3	10.0	100%
4	4 & 7	6.0 / 10.0	75% / 25%

It should be pointed out that for Samplers 1 and 5 that a leak was not detected until the remote change tests were conducted. The sampler line for Samplers 1 and 5 are share the same condenser unit to prevent the humidified air from the test stand from entering the mass flow controller. The leak was a result of the lack of Teflon tape around the fitting located on the base of the condenser unit. The fitting where the leak occured is where the sampler line from the ductwork connects to the condenser unit. The issue was fixed once the remote change testing was conducted. The curves for Samplers 1 and 5 during all safe change radial type filter tests show that the leak caused decreased/erratic pressure drops and decreased mass collection results for the two samplers.

All plots have been set for the x-axis to represent data in logarithmic format with base 2 notation, with the exception of loading with acetylene soot evaluations. The mass accumulated for the acetylene soot tests are much less compared to the powder tests due to the particle size distribution of soot particles. Representation of plots with the x-axis in logarithmic format expresses the exponential increase in differential pressure as mass loading increases. This exponential increase is because the cumulative masses begin to affect filter loading more readily as pressure drop increases exponentially.

4.2.1.1 Aluminum Trihydroxide Evaluation

RunID tests 12784-1 and 12784-2 simulated Category 3 test conditions. Temperature and relative humidity conditions were maintained at 166 ^{o}F and 50%, respectively. The operating flowrate for the RLSTS was set at 1200 cfm for both tests that resulted in lesser media velocity for the flat sheet coupon samples. The following images for RunID tests 12784-1 and 12784-2 show data obtained from the APS and SMPS. The calculated APS mass is shown in comparison with the gravimetric analysis results. The correlation coefficients are shown highlighted in green. Data used in the determination of the correlation coefficient are the gravimetric analysis and APS calculated data.

Table 4.3 Isokinetic sampler mass collection and dP results for 12784-1.

Sample Number	HEPA Coupon Filter dP Initial	HEPA Coupon Filter dP Final	Cumulative Number Concentration (#/cc) APS # Conc.	Cumulative Number Concentration (#/cc) SMPS # Conc.	HEPA Coupon Accumulated Masses (mg) Grav. Analysis	HEPA Coupon Accumulated Masses (mg) APS Calc.	Accumulated Mass Correlation Coefficient
1	0.98	3.39	5.84E+04	4.16E+04	49.00	71.19	0.610
2	1.01	8.88	1.09E+05	1.16E+05	188.01	165.64	
3	1.06	14.40	2.36E+05	2.52E+05	358.58	361.85	
4	1.00	10.79	1.70E+05	1.59E+05	243.37	236.61	
5	1.16	12.65	1.77E+05	2.10E+05	59.08	307.12	
6	1.07	9.60	1.27E+05	1.36E+05	182.76	197.47	
7	1.05	7.76	6.56E+04	9.29E+04	111.15	126.79	

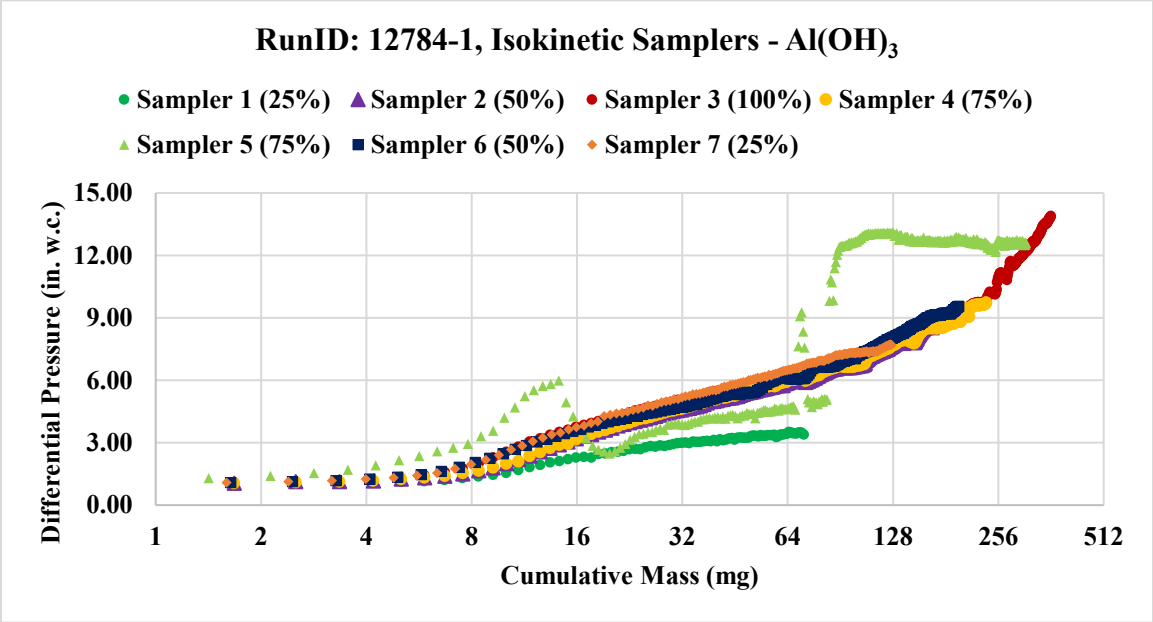

Figure 4.4 Cumulative mass vs. dP for RunID: 12784-1.

Sampler 1 and Sampler 5 show apparent signs of decreased/erratic pressure drop due to the leak located in the condenser unit.

Table 4.4 Isokinetic sampler mass collection and dP results for 12784-2.

Sample Number	HEPA Coupon Filter dP Initial	HEPA Coupon Filter dP Final	Cumulative Number Concentration (#/cc) APS # Conc.	Cumulative Number Concentration (#/cc) SMPS # Conc.	HEPA Coupon Accumulated Masses (mg) Grav. Analysis	HEPA Coupon Accumulated Masses (mg) APS Calc.	Accumulated Mass Correlation Coefficient
1	0.93	3.17	5.09E+04	5.01E+04	37.65	38.36	0.632
2	1.07	8.30	1.06E+05	1.04E+05	165.70	146.42	
3	1.10	12.81	2.03E+05	1.94E+05	356.73	341.48	
4	1.05	10.59	1.49E+05	1.44E+05	225.22	211.13	
5	0.99	12.20	1.52E+05	1.44E+05	72.68	303.10	
6	1.04	9.19	9.72E+04	9.07E+04	201.00	195.45	
7	1.08	6.61	5.39E+04	5.05E+04	118.85	130.27	

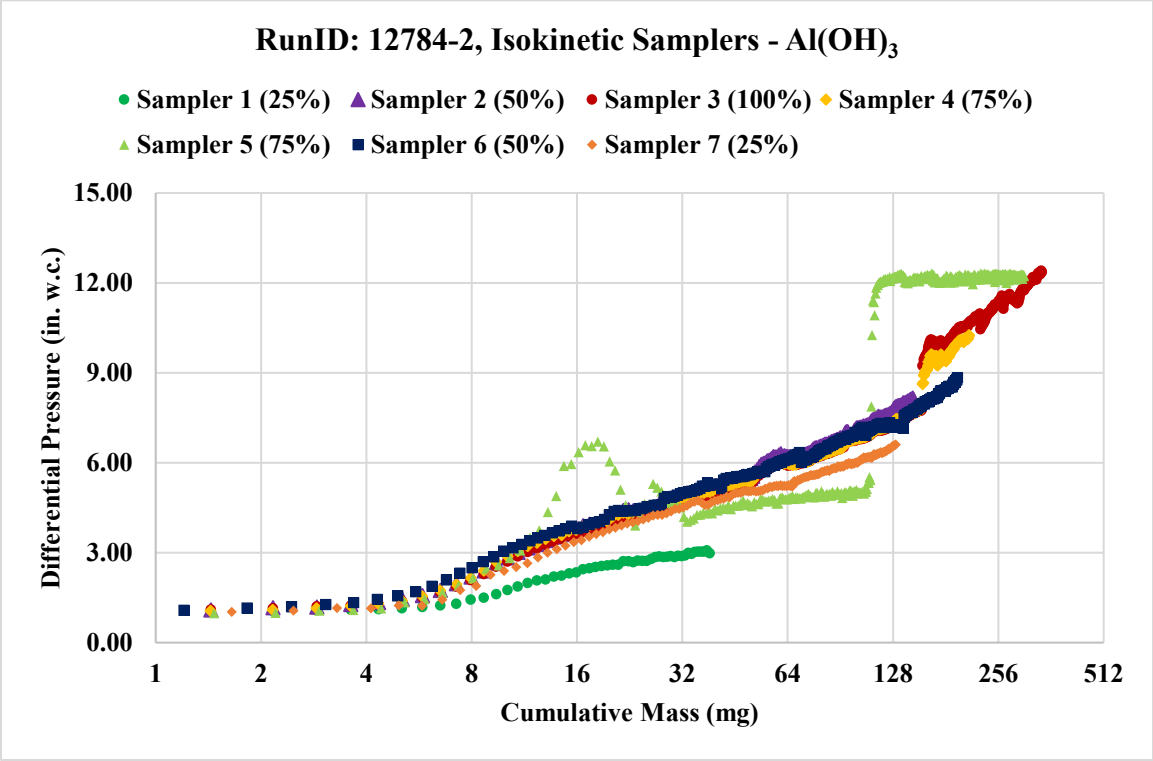

Figure 4.5 Cumulative mass vs. dP for RunID: 12784-2.

Sampler 1 and Sampler 5 show apparent signs of decreased/erratic pressure drop due to the leak located in the condenser unit.

Differential pressure is expected to increase throughout the loading process. The differential pressure during initial loading periods exhibit a linear increase due to depth loading into the thickness of the filter media. The differential pressure is expected to reach a transition regime that exhibits the change from linear to exponential differential pressure increase. When enough mass loading has deposited into the depth of the filter fibers, differential pressure begins to grow exponentially as mass loading progresses past depth loading phase towards surface loading. Once depth loading reaches a definitive state, the porosity of fibrous filters begins to rapidly clog with increasing challenge aerosol due to filtration mechanisms of impaction and interception.

The results for 12784-1 and 12784-2 show the 25% loading samples exhibit linear loading characteristics during depth loading. Pressure drop during this loading regime ranged from 3 to 3.5 in. w.c. for Sampler 1 on both tests, and from 6.5 to 7.5 in. w.c. for Sampler 7. It is assumed that differential pressure results for Sampler 1 are less than for Sampler 7 because of the leak in the sampling line. This affected the initial stage of loading, and the length of loading time required to reach the changeout pressure of 2.5 in. w.c. The full-filter has an initial tare differential pressure of approximately 1.0 in. w.c. The loading time for Sampler 1 to reach the changeout time of 2.5 in. w.c. is less than the time for Sampler 7 to load from 6 in. w.c. to 10 in. w.c. because of the initial differential pressure. The 50% loading from Samplers 2 and 6 showed pressure drops ranging from 8 to 9.5 in. w.c. The transitional regime from depth loading to surface loading occurs where the linear loading curve demonstrates an exponential rate of pressure drop. The maximum differential pressure ranged from 10.5 to 11 in. w.c. for the 75% loading coupon on Sampler 4. Sampler 5 experienced erratic pressure drop from the sampling line leak

which resulted in a much lesser gravimetric analysis result. Exponential pressure drop is more apparent after the 50% loading sample as the depth of the filter media has become increasingly saturated in particulate matter. Maximum pressure drops ranged from 12 to 14 in. w.c. for 100% loading coupons. The exponential pressure drop and filter clogging for the 100% loading coupon are apparent due to restricted flow resulting from pore size reduction.

The gravimetric analysis masses and APS calculated masses for RunID tests 12784-1 and 12784-2 correlated well for the samplers without leaks. The leaks are shown on the plots where spikes occurred after reaching 8 mg of loading at around 3 in. w.c., and after 64 mg of loading. The leak issue caused a discrepancy in the calculation of the correlation coefficient for Samplers 1 and 5, rendering the gravimetric and calculated masses at a poor level of correlation at coefficients of 0.610 and 0.632, respectively.

For RunID tests 13109-2 and 12719-3, test categories 2b and 2c were simulated. Both test category temperatures were maintained at 177 ^{o}F, but the relative humidity setpoint differed by 10%, with category 2b maintaining at 40% RH and category 2c maintaining at 50% RH. Both tests had the RLSTS flow setpoint maintained at 2000 cfm. The media velocity experienced by the isokinetic sampler coupons are higher because the SCADA programming maintains a volumetric flow setpoint for the mass flow controllers based on the effective filter area. The leak issue is still apparent with erratic pressure drop and decreased mass collection.

Table 4.5 Isokinetic sampler mass collection and dP results for 13109-2.

Sample Number	HEPA Coupon Filter dP Initial	HEPA Coupon Filter dP Final	Cumulative Number Concentration (#/cc) APS # Conc.	Cumulative Number Concentration (#/cc) SMPS # Conc.	HEPA Coupon Accumulated Masses (mg) Grav. Analysis	HEPA Coupon Accumulated Masses (mg) APS Calc.	Accumulated Mass Correlation Coefficient
1	1.58	5.78	3.67E+04	3.51E+04	21.95	38.26	0.944
2	2.10	10.80	7.03E+04	7.61E+04	42.85	55.91	
3	1.83	25.89	1.67E+05	1.39E+05	284.04	279.17	
4	1.86	15.73	1.04E+05	1.10E+05	102.20	102.47	
5	1.87	11.39	1.30E+05	1.04E+05	160.08	240.21	
6	1.77	24.03	9.66E+04	6.29E+04	246.39	223.40	
7	1.82	20.12	6.32E+04	2.94E+04	170.73	176.74	

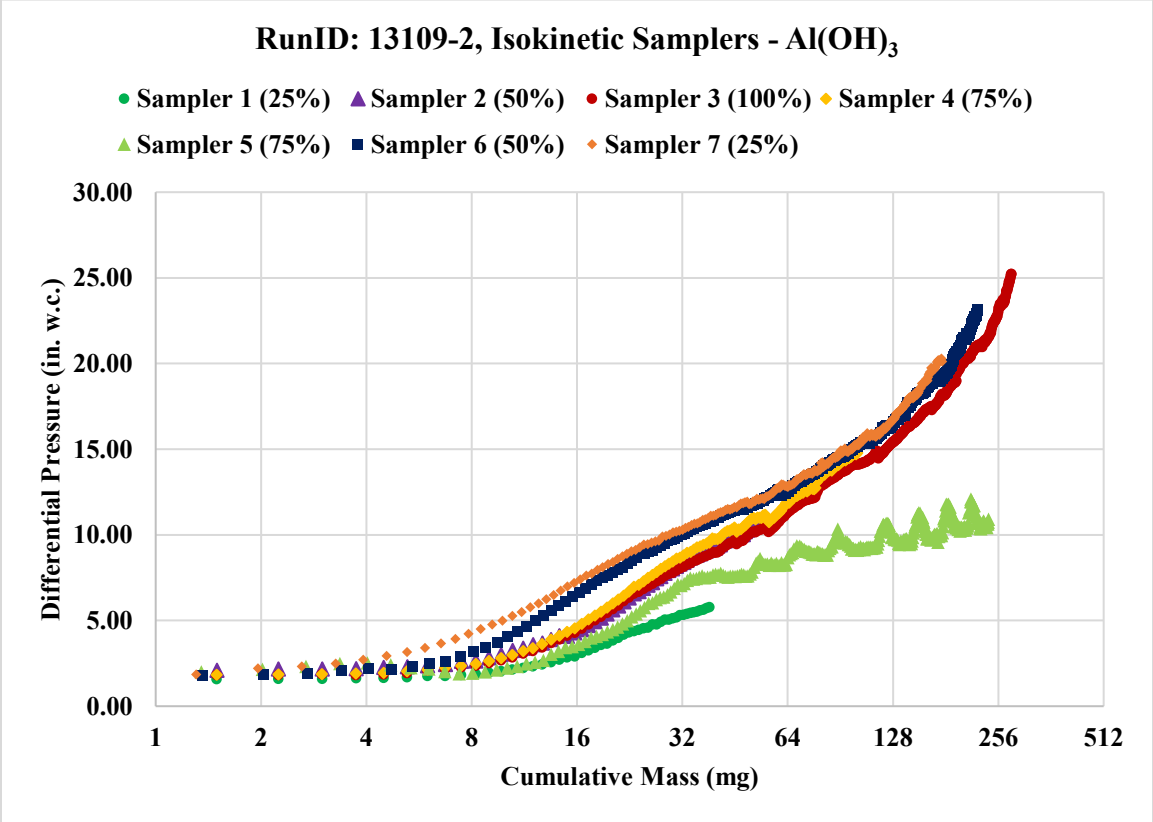

Figure 4.6 Cumulative mass vs. dP for RunID: 13109-2.

Table 4.6 Isokinetic sampler mass collection and dP results for 12719-3.

Sample Number	HEPA Coupon Filter dP Initial	HEPA Coupon Filter dP Final	Cumulative Number Concentration (#/cc) APS # Conc.	Cumulative Number Concentration (#/cc) SMPS # Conc.	HEPA Coupon Accumulated Masses (mg) Grav. Analysis	HEPA Coupon Accumulated Masses (mg) APS Calc.	Accumulated Mass Correlation Coefficient
1	1.69	5.99	3.75E+04	3.54E+04	25.29	23.76	0.924
2	2.62	12.16	6.90E+04	7.07E+04	51.01	41.07	
3	1.99	21.10	1.48E+05	1.89E+05	221.69	211.55	
4	1.97	14.95	1.10E+05	1.35E+05	89.87	71.36	
5	2.08	10.99	1.11E+05	1.54E+05	123.36	187.79	
6	1.87	18.68	7.90E+04	1.19E+05	174.84	170.70	
7	2.07	17.59	3.76E+04	5.43E+04	140.12	127.39	

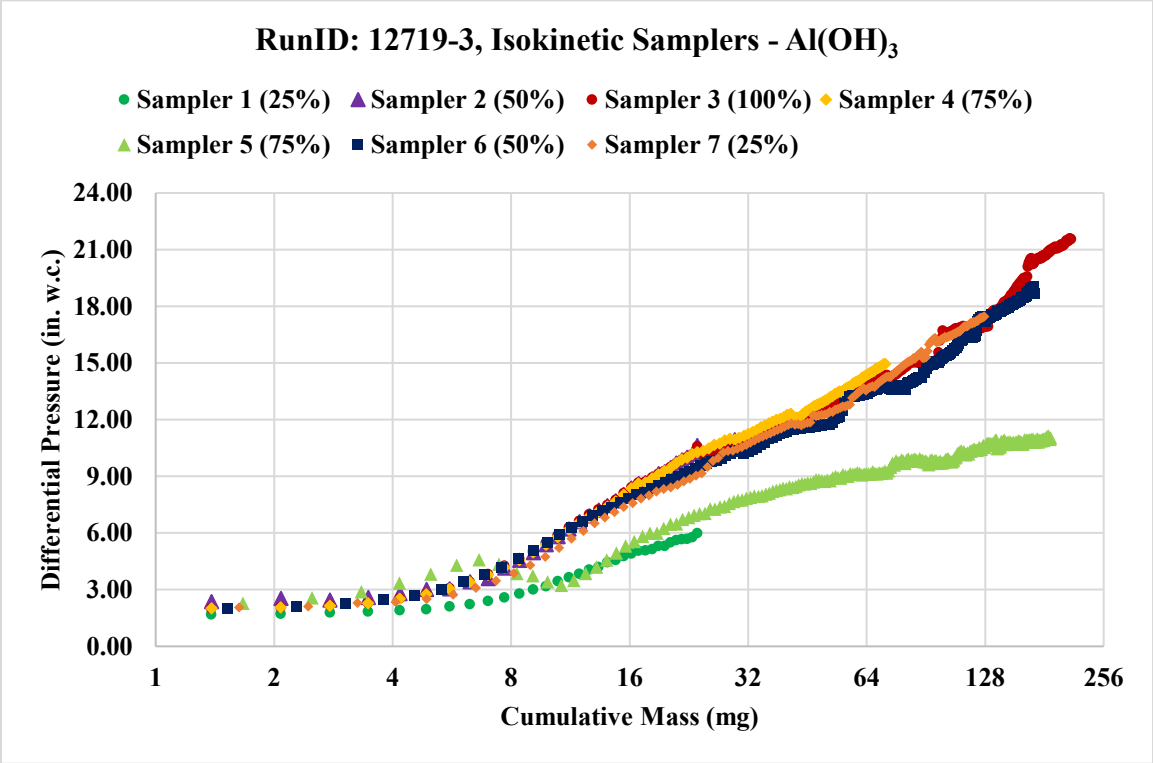

Figure 4.7 Cumulative mass vs. dP for RunID: 12719-3.

Results for the 13109-2 and 12719-3 show similarities in loading patterns, can be seen in the Figures 4.6 and 4.7 above. The initial differential pressure for RunID test

12719-3 showed a slightly higher initial dP. This increase may have been due to the increase of moisture content and the increased flow setpoint to compensate for the increase in RLSTS flowrate within the test duct for category 2c testing. The final differential pressures are nearly doubled when testing at 2000 cfm compared to the results obtained for testing at 1200 cfm. The accumulated masses for Sampler 3 (100% loading) are less for RunID tests 13109-2 and 12719-3 when compared to 12784-1 and 12784-2. The increase in final differential pressure shows that filtration mechanisms of impaction and interception with this challenge aerosol at lower media velocities accumulate mass during stages of depth loading at a slower rate than at 2000 cfm evaluations. This would show that increased pressure drop experienced by the full filter would be dominated by the increase of media velocity at the full-scale filter, rather than the actual mass accumulated. At higher media velocities, aerosols penetration into the depth of the fibrous filter media would exhibit faster pore clogging due to the filtration mechanisms stated.

The safe change filter housing was interchanged for a remote change orientation filter housing to evaluate remote change filters. All other test stand components remained the same for remote change filter evaluations. The remote change filters resulted in a higher clean initial pressure drop at rated flow, which surpassed the first sampler changeout pressure of 2.5 in. w.c. The higher clean initial pressure drop resulted in Sampler 1 and Sampler 5 to be representative of of 50% loading. The increase in initial clean pressure drop was seen for all remote change filters.

RunID tests 13554-2 through 13554-5 were performed under category 2c test conditions. The leak issue from previous tests was not addressed until RunID 13554-3.

Troubleshooting procedures were performed, and Teflon tape was placed on the condenser unit fitting to seal the vacuum leak.

Table 4.7 Isokinetic sampler mass collection and dP results for 13554-2.

Sample Number	HEPA Coupon Filter dP Initial	HEPA Coupon Filter dP Final	Cumulative Number Concentration (#/cc) APS # Conc.	Cumulative Number Concentration (#/cc) SMPS # Conc.	HEPA Coupon Accumulated Masses (mg) Grav. Analysis	HEPA Coupon Accumulated Masses (mg) APS Calc.	Accumulated Mass Correlation Coefficient
1	2.04	7.77	3.92E+04	2.53E+04	40.14	38.51	0.962
2	1.93	10.59	3.92E+04	2.53E+04	42.25	38.55	
3	1.98	15.13	1.21E+05	1.12E+05	78.89	73.17	
4	1.94	13.30	8.17E+04	6.58E+04	59.24	51.83	
5	1.36	4.62	8.19E+04	8.71E+04	25.70	35.53	
6	1.62	5.44	8.19E+04	8.71E+04	28.45	35.56	
7	1.87	7.59	3.94E+04	4.66E+04	22.10	21.33	

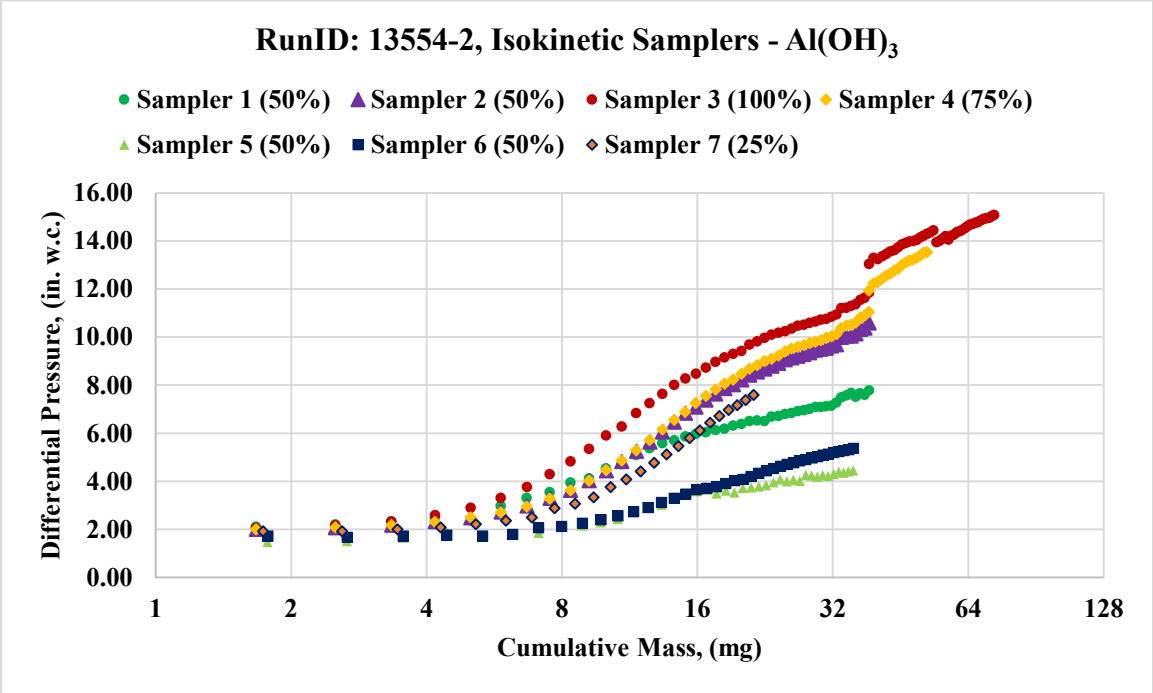

Figure 4.8 Cumulative mass vs. dP for RunID: 13554-2.

Table 4.8 Isokinetic sampler mass collection and dP results for 13554-3.

Sample Number	HEPA Coupon Filter dP Initial	HEPA Coupon Filter dP Final	Cumulative Number Concentration (#/cc) APS # Conc.	Cumulative Number Concentration (#/cc) SMPS # Conc.	HEPA Coupon Accumulated Masses (mg) Grav. Analysis	HEPA Coupon Accumulated Masses (mg) APS Calc.	Accumulated Mass Correlation Coefficient
1	2.16	10.50	6.50E+05	6.20E+05	41.79	39.80	0.998
2	2.06	10.99	6.50E+05	6.20E+05	41.70	39.83	
3	2.03	11.24	7.10E+05	6.99E+05	56.57	53.45	
4	2.09	12.23	6.79E+05	5.86E+05	48.87	46.05	
5	1.78	4.84	6.01E+04	7.93E+04	12.68	14.74	
6	1.69	4.53	6.01E+04	7.93E+04	11.90	14.75	
7	1.84	3.51	3.10E+04	3.97E+04	8.28	7.38	

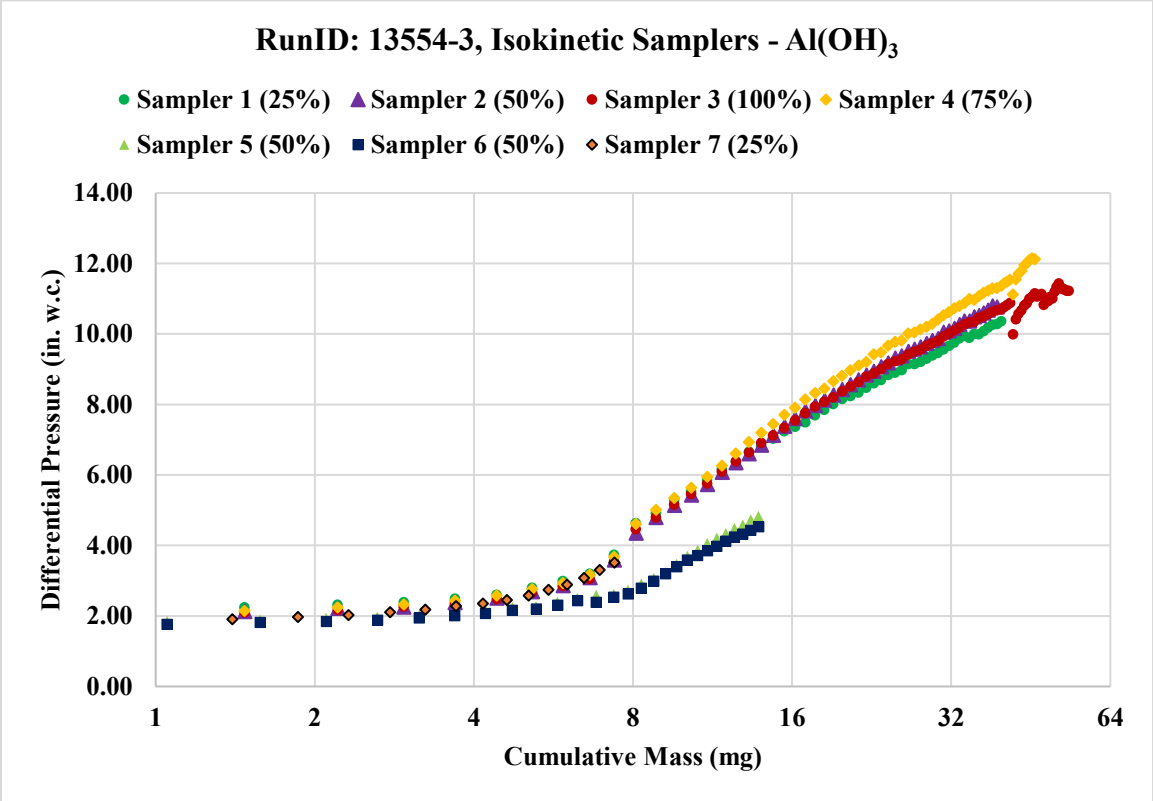

Figure 4.9 Cumulative mass vs. dP for RunID: 13554-3.

Table 4.9 Isokinetic sampler mass collection and dP results for 13554-4.

Sample Number	HEPA Coupon Filter dP Initial	HEPA Coupon Filter dP Final	Cumulative Number Concentration (#/cc) APS # Conc.	Cumulative Number Concentration (#/cc) SMPS # Conc.	HEPA Coupon Accumulated Masses (mg) Grav. Analysis	HEPA Coupon Accumulated Masses (mg) APS Calc.	Accumulated Mass Correlation Coefficient
1	2.06	9.90	3.20E+04	4.49E+04	38.96	29.71	0.947
2	1.94	10.13	3.20E+04	4.49E+04	37.82	29.73	
3	1.96	14.02	1.04E+05	1.07E+05	70.94	81.51	
4	1.95	11.66	6.63E+04	7.12E+04	54.86	43.59	
5	1.97	14.30	7.19E+04	6.20E+04	34.87	27.51	
6	1.58	6.48	7.19E+04	6.20E+04	26.10	27.54	
7	1.91	6.29	3.76E+04	3.57E+04	18.65	13.62	

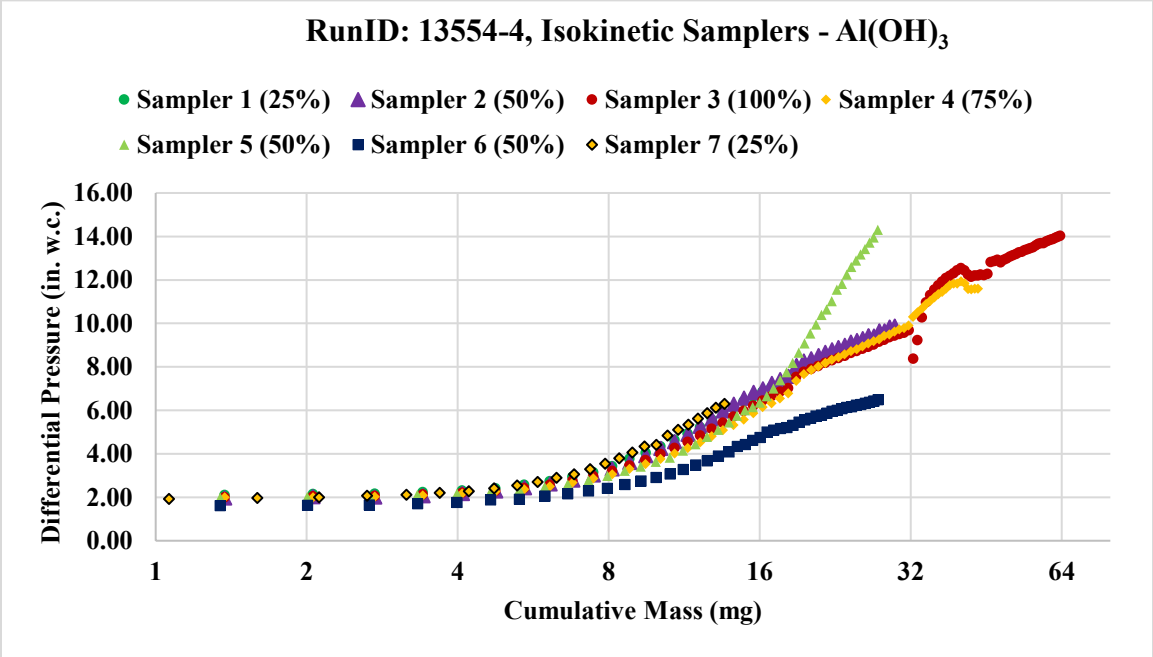

Figure 4.10 Cumulative mass vs. dP for RunID: 13554-4.

Table 4.10 Isokinetic sampler mass collection and dP results for 13554-5.

Sample Number	HEPA Coupon Filter dP Initial	HEPA Coupon Filter dP Final	Cumulative Number Concentration (#/cc) APS # Conc.	Cumulative Number Concentration (#/cc) SMPS # Conc.	HEPA Coupon Accumulated Masses (mg) Grav. Analysis	HEPA Coupon Accumulated Masses (mg) APS Calc.	Accumulated Mass Correlation Coefficient
1	1.30	11.40	4.98E+04	2.19E+04	52.64	57.30	0.982
2	1.28	11.40	4.98E+04	2.19E+04	51.83	56.46	
3	1.38	15.00	1.21E+05	1.01E+05	92.12	91.42	
4	1.35	13.60	8.59E+04	6.84E+04	73.53	73.25	
5	1.97	11.20	7.15E+04	7.88E+04	42.50	34.16	
6	1.63	6.90	7.15E+04	7.88E+04	30.79	34.17	
7	1.98	12.00	3.54E+04	3.24E+04	22.56	18.19	

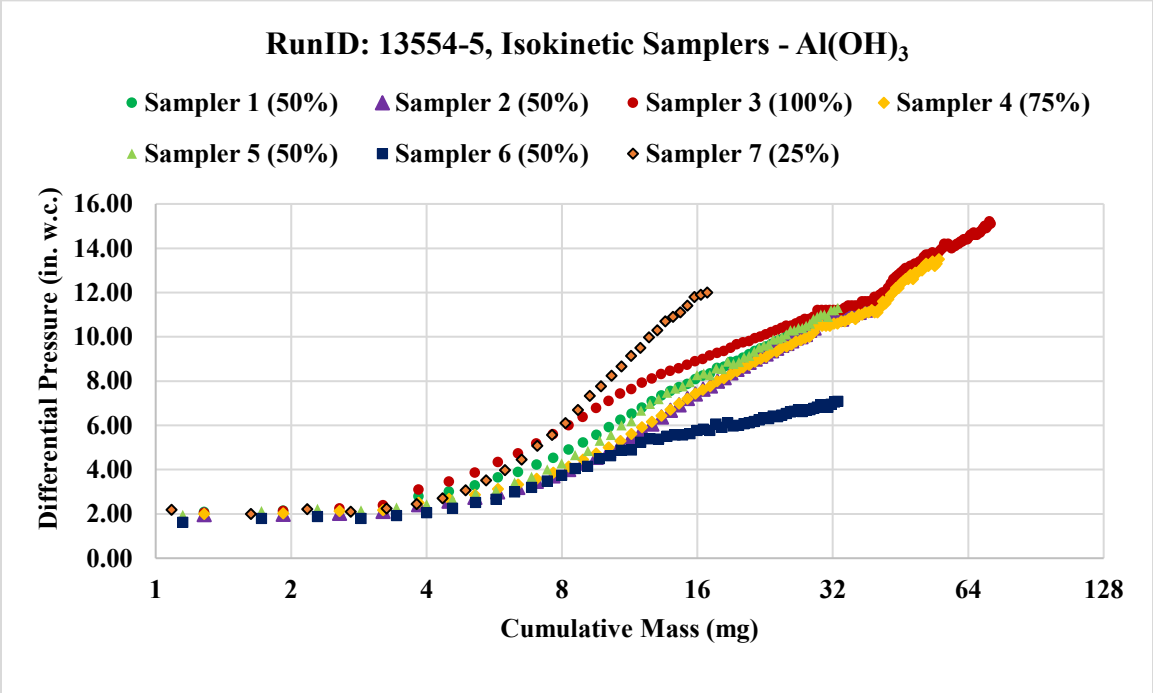

Figure 4.11 Cumulative mass vs. dP for RunID: 13554-5.

The results for RunID tests 13554-2 through 13554-5 differed from the safe change radial filter evaluations. A noticeable difference is the amount of mass sampled and maximum final pressure drop achieved for Sampler 3. The changeout time for

Sampler 1 is performed at 4.0 in w.c., since each test begins at a higher initial clean differential pressure. This effectively reduced the sampling time for the isokinetic sampler coupons. All 100% loading samples resulted in less than 100 mg accumulated mass on the samples. This was less than half of the mass obtained when comparing to the safe change tests for RunID 12719-3 and 13109-2. Pressure drops ranging from 11 in. w.c. to 15 in. w.c, occurred for these tests, which was attributed to the decreased sampling time and mass accumulated during testing.

The data acquisition (DAQ) unit was found to be set at 15 second intervals for RunID test 13554-5. The correlation coefficients for the proceeding tests were well into agreement above 0.90 once the leak issues were addressed after RunID test 13554-2. Mass estimation results using the APS came to about 10 mg of accuracy for each gravimetric sample, with longer loading tests decreasing in accuracy.

4.2.1.2 Arizona Road Dust Evaluation

The isokinetic samplers were evaluated under test category 2b for RunID tests 12784-3 and 12784-4 with temperature and relative humidity maintained at 177 ^{o}F and 40%, respectively. The challenge aerosol of fine Arizona Road Dust was used in the evaluations due to their coarse morphology and larger particle size. The testing flowrate for the radial full-filter was set at the rated flow of 2000 cfm, resulting in a higher volumetric flowrate and media velocity experienced by the isokinetic sampler coupons.

Table 4.11 Isokinetic sampler mass collection and dP results for 12784-3.

Sample Number	HEPA Coupon Filter dP Initial	HEPA Coupon Filter dP Final	Cumulative Number Concentration (#/cc) APS # Conc.	Cumulative Number Concentration (#/cc) SMPS # Conc.	HEPA Coupon Accumulated Masses (mg) Grav. Analysis	HEPA Coupon Accumulated Masses (mg) APS Calc.	Accumulated Mass Correlation Coefficient
1	1.55	5.20	2.77E+04	6.80E+04	61.79	35.30	0.921
2	1.84	12.66	5.29E+04	1.35E+05	144.43	46.31	
3	1.85	35.52	1.03E+05	2.60E+05	982.26	239.12	
4	1.90	18.57	7.86E+04	1.95E+05	288.82	80.36	
5	1.43	8.95	7.49E+04	1.92E+05	501.36	203.94	
6	1.90	35.63	4.98E+04	1.25E+05	877.95	193.09	
7	1.76	31.24	2.41E+04	6.57E+04	722.20	158.18	

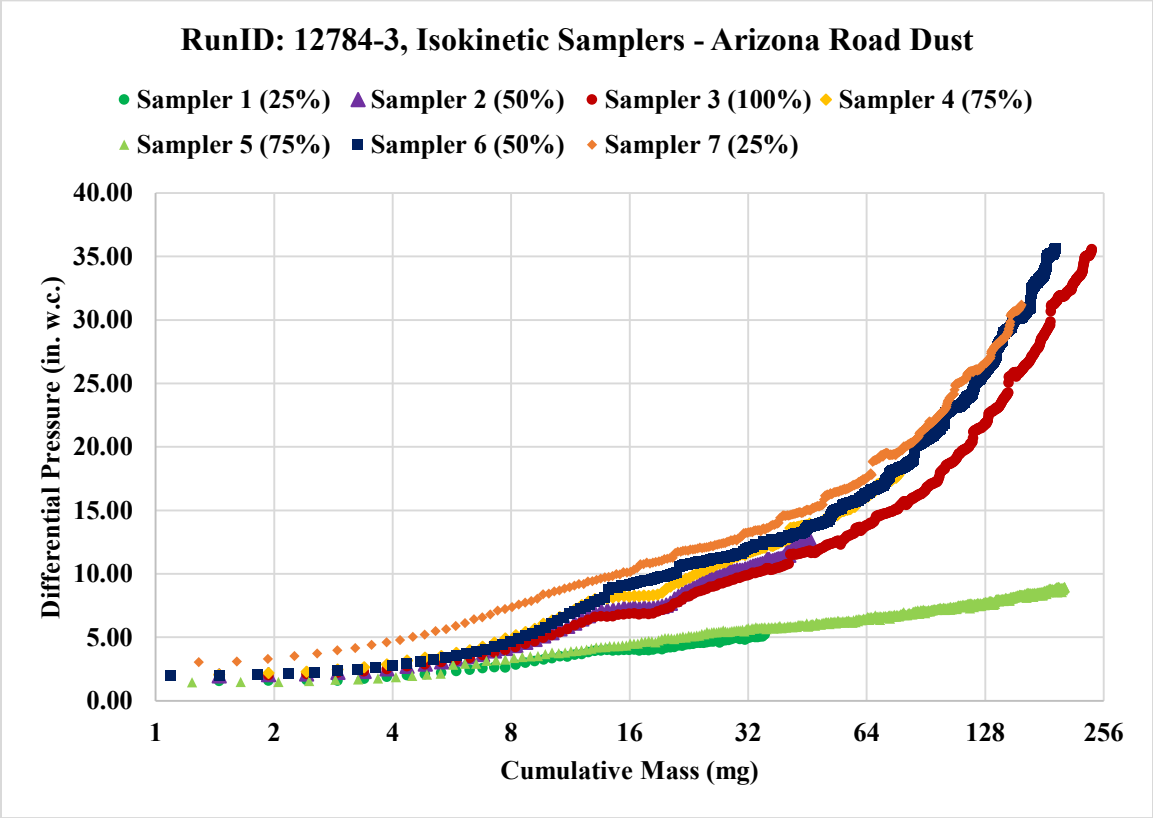

Figure 4.12 Cumulative mass vs. dP for RunID: 12784-3.

Table 4.12 Isokinetic sampler mass collection and dP results for 12784-4.

Sample Number	HEPA Coupon Filter dP Initial	HEPA Coupon Filter dP Final	Cumulative Number Concentration (#/cc) APS # Conc.	Cumulative Number Concentration (#/cc) SMPS # Conc.	HEPA Coupon Accumulated Masses (mg) Grav. Analysis	HEPA Coupon Accumulated Masses (mg) APS Calc.	Accumulated Mass Correlation Coefficient
1	0.97	4.51	1.34E+04	1.46E+04	48.81	36.15	0.929
2	1.12	11.67	2.70E+04	3.25E+04	123.38	51.60	
3	0.67	30.76	6.45E+04	6.98E+04	787.55	251.87	
4	1.14	18.18	4.54E+04	5.18E+04	331.37	94.30	
5	1.47	8.49	5.11E+04	5.51E+04	440.93	214.89	
6	1.90	32.82	3.75E+04	3.72E+04	724.54	203.26	
7	1.78	23.47	1.91E+04	1.80E+04	469.81	142.73	

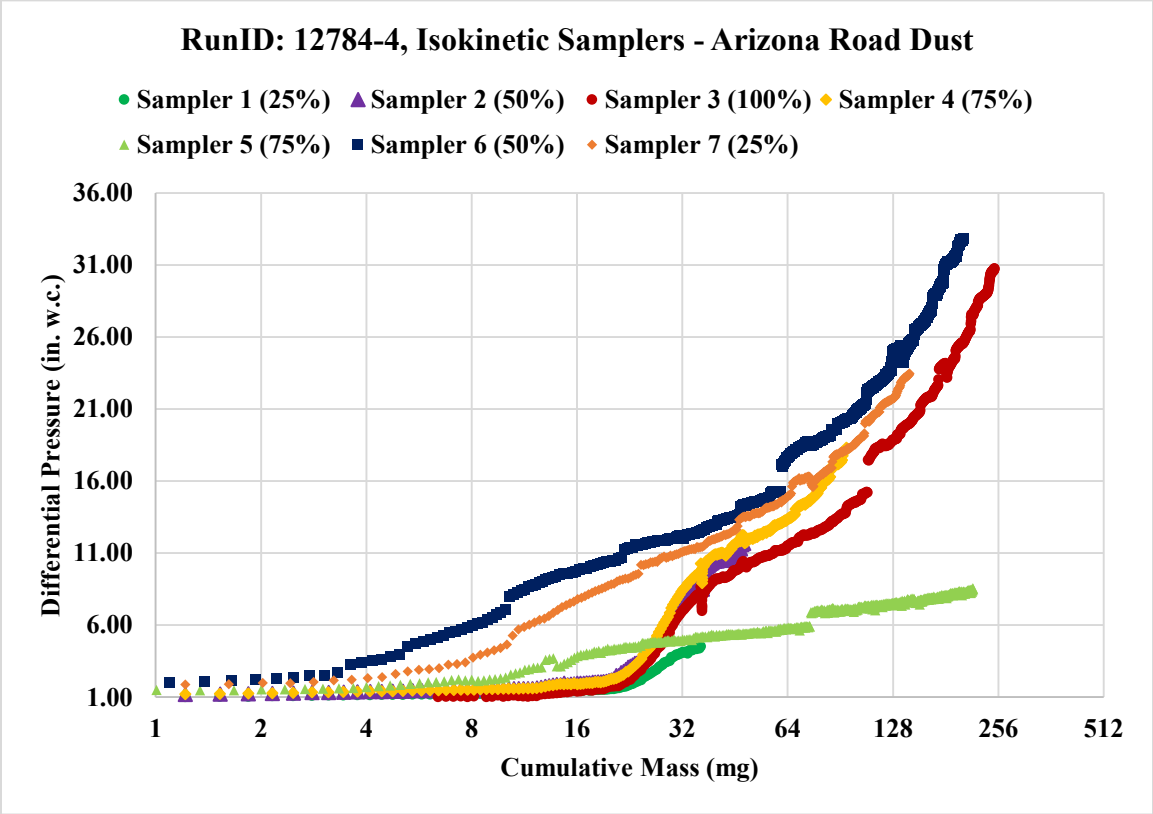

Figure 4.13 Cumulative mass vs. dP for RunID: 12784-4.

Evaluations using Arizona Road Dust proved to be difficult in estimating the mass using the APS. The sampled mass concentration was much less for each sampling interval ranging from 0.2 to 0.4 mg/ccm in contrast to $Al(OH)_3$ aerosols which have provided mass concentrations up to 1.2 mg/ccm. This reduction of sampled mass concentration reduced the estimated masses substantially. This is seen in the above tables for Arizona Road Dust.

The possible cause of this reduction of sampled mass in the APS is due to the aerosol passing through the diffusion dryer before reaching the diluter module. Both instruments used diffusion dryers and a 100:1 diluter during sampling intervals. The measured number concentrations obtained from the APS and SMPS showed agreement between the two instruments. The number concentrations for both tests using the APS and SMPS ranged from 1E+4 to 1E+5 #/cc.

The lack of particle mass concentration is attributed to the loss of particles during transport through the diffusion dryers during sampling. Another factor would be the aerodynamic diameters and particle masses are also larger, therefore resulting in impaction losses on sampling tubing walls, through the diffusion dryers, and when passing through the diluter capillary tube inner walls.

The gravimetric analysis shows that the accumulated masses for Arizona Road Dust are approximately three times the amount sampled for $Al(OH)_3$ for RunID tests 13109-2 and 12719-3. Pressure drops ranging from 30 to 35.5 in. w.c. were achieved for the 100% loading samples. This shows that the full-filter and the loaded filter coupons experienced greater mass accumulation and pressure drop before reaching the pressure changeout times. The fibrous filter clogging and filter caking characteristics occur much

deeper within the depth of the HEPA filter media. This would mean that the morphological structures accumulated within the HEPA fibers are dominated by impaction and interception mechanics, highly influenced by the large aerodynamic size.

4.2.1.3 Acetylene Soot Evaluation

Evaluations for the acetylene soot aerosols were performed at test categories 2b and 2c. The four burner ports were installed at the aerosol injection location, where the torches were lit at approximately seven inches of flame height to generate a suitable particle number concentration range from 10E5 to 10E6. Flame heights were measured with a retractable steel rule every time the burners were lit. Temperatures were maintained and monitored at 177 ^{o}F and 40% RH (Category 2b) and 50% RH (Category 2c) for fluctuations due to the additional heat from the burner ports and indoor air from the open ports.

The use of acetylene soot showed that the process of aerosol loading was not completely dependent upon the particle mass for the monodisperse aerosol. Factors such as the tendency to form agglomerates in mid-flight and the rapid clogging of pores in less time as compared with powder aerosols were observed. The soot proved to be the quickest evaluation tests because of the tendency for particles to produce chains upon contact with intercepted particles. Particle sizes ranging from 40 nm to 600 nm in size were prevalent during loading. Filtration mechanisms of diffusion and interception occurred at these size ranges due to aliphatic particle characteristics of soot particles. The combination with submicron particle sizes allowed depth loading to occur at a much higher rate. This resulted in a drastic increase in pressure drop with substantially less mass loading.

Table 4.13 Isokinetic sampler mass collection and dP results for 12784-5.

Sample Number	HEPA Coupon Filter dP Initial	HEPA Coupon Filter dP Final	Cumulative Number Concentration (#/cc) APS # Conc.	Cumulative Number Concentration (#/cc) SMPS # Conc.	HEPA Coupon Accumulated Masses (mg) Grav. Analysis	HEPA Coupon Accumulated Masses (mg) APS Calc.	Accumulated Mass Correlation Coefficient
1	1.69	8.76	3.30E+05	2.71E+06	2.71	5.01	0.928
2	1.89	12.54	5.09E+05	2.93E+06	3.51	8.44	
3	1.93	25.13	7.74E+05	3.08E+06	10.44	16.80	
4	1.98	24.91	6.38E+05	3.01E+06	7.95	13.08	
5	1.66	10.33	4.45E+05	3.74E+05	4.47	11.80	
6	1.92	17.39	2.66E+05	1.52E+05	5.09	8.38	
7	1.76	13.66	1.36E+05	7.58E+04	2.31	3.72	

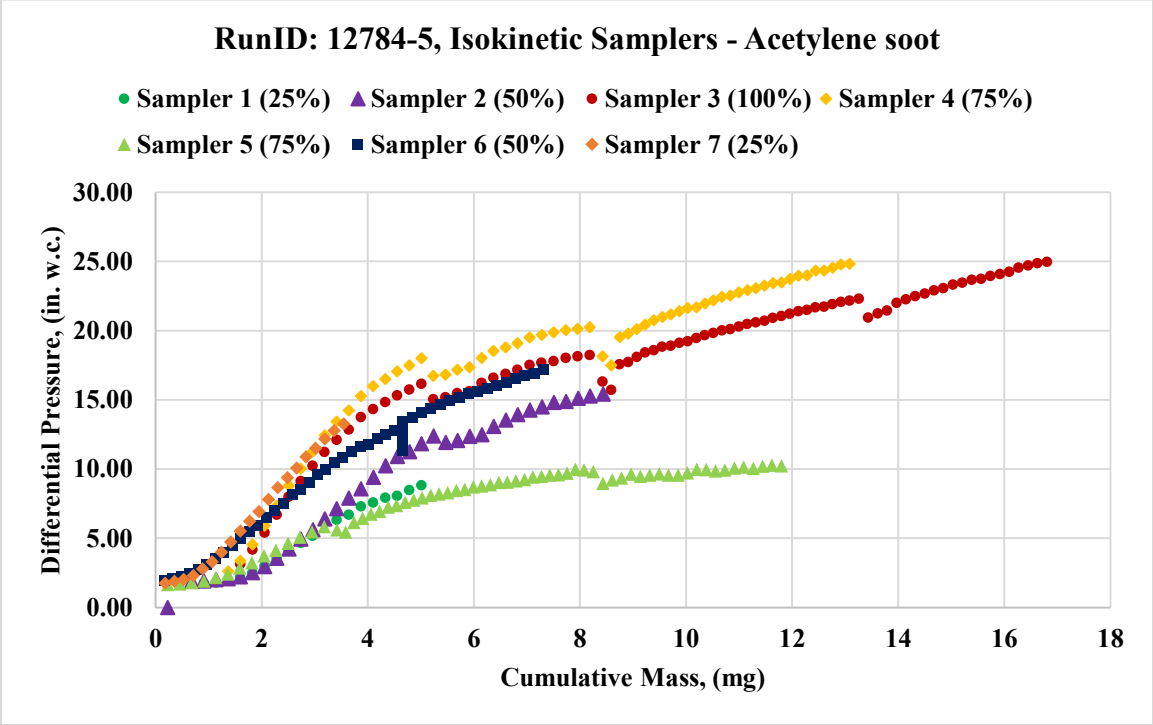

Figure 4.14 Cumulative mass vs. dP for RunID: 12784-5.

Table 4.14 Isokinetic sampler mass collection and dP results for 12784-6.

Sample Number	HEPA Coupon Filter dP Initial	HEPA Coupon Filter dP Final	Cumulative Number Concentration (#/cc) APS # Conc.	Cumulative Number Concentration (#/cc) SMPS # Conc.	HEPA Coupon Accumulated Masses (mg) Grav. Analysis	HEPA Coupon Accumulated Masses (mg) APS Calc.	Accumulated Mass Correlation Coefficient
1	1.59	6.45	1.28E+05	1.04E+06	1.94	1.99	0.870
2	1.87	14.12	2.56E+05	2.07E+06	2.50	2.81	
3	1.88	20.34	6.00E+05	3.78E+06	6.88	7.38	
4	1.97	16.76	4.28E+05	2.93E+06	5.33	5.63	
5	2.55	9.64	4.72E+05	2.74E+06	2.44	5.38	
6	1.92	13.87	3.43E+05	1.70E+06	2.75	4.57	
7	1.70	4.37	1.72E+05	8.52E+05	1.15	1.71	

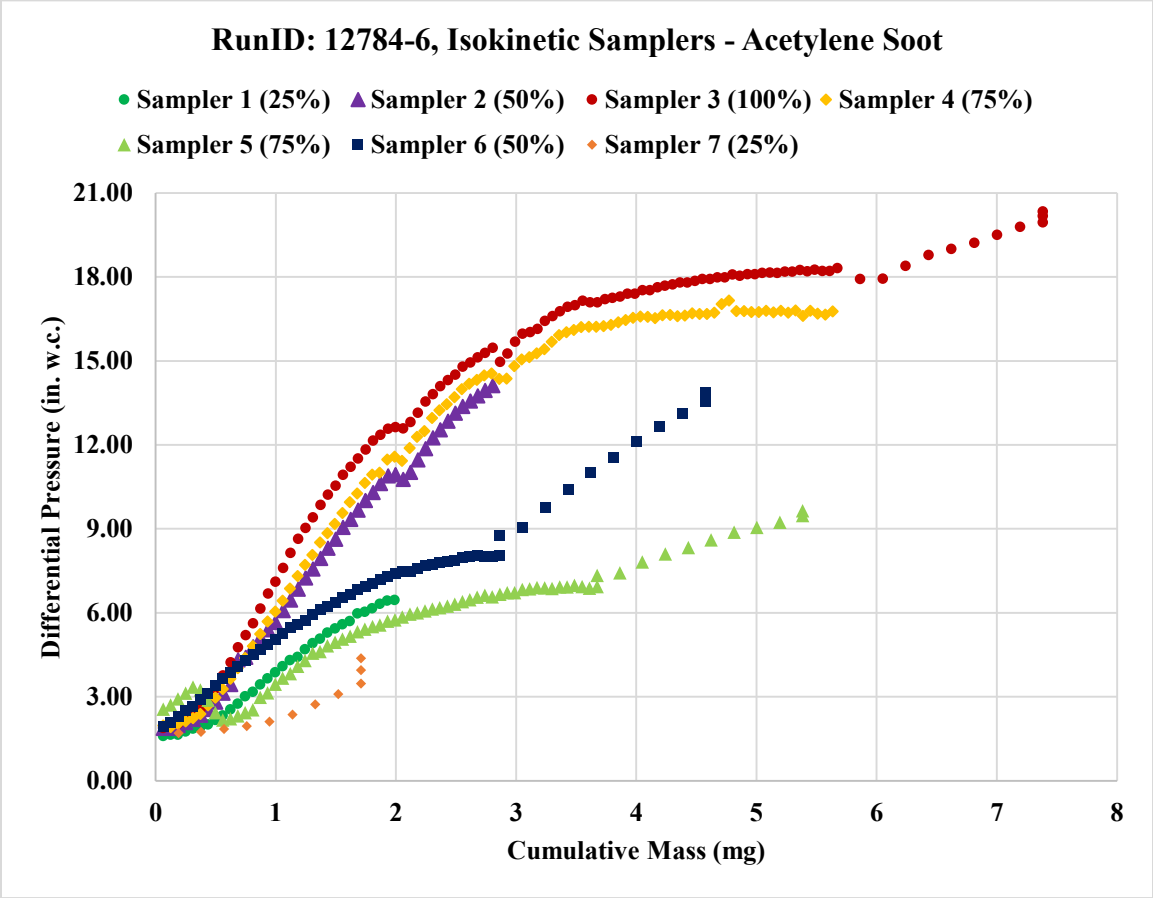

Figure 4.15 Cumulative mass vs. dP for RunID: 12784-6.

Table 4.15 Isokinetic sampler mass collection and dP results for 13554-6.

Sample Number	HEPA Coupon Filter dP Initial	HEPA Coupon Filter dP Final	Cumulative Number Concentration (#/cc) APS # Conc.	Cumulative Number Concentration (#/cc) SMPS # Conc.	HEPA Coupon Accumulated Masses (mg) Grav. Analysis	HEPA Coupon Accumulated Masses (mg) APS Calc.	Accumulated Mass Correlation Coefficient
1	2.03	22.65	1.82E+05	2.41E+06	8.30	7.27	0.962
2	1.95	20.56	1.82E+05	2.41E+06	8.18	7.28	
3	2.03	34.99	3.20E+05	3.96E+06	16.22	11.51	
4	1.97	29.45	2.68E+05	3.06E+06	12.84	9.44	
5	2.08	19.79	1.38E+05	1.56E+06	6.75	4.24	
6	1.98	20.86	1.38E+05	1.56E+06	6.90	4.25	
7	2.03	15.12	5.16E+04	5.40E+05	3.83	1.99	

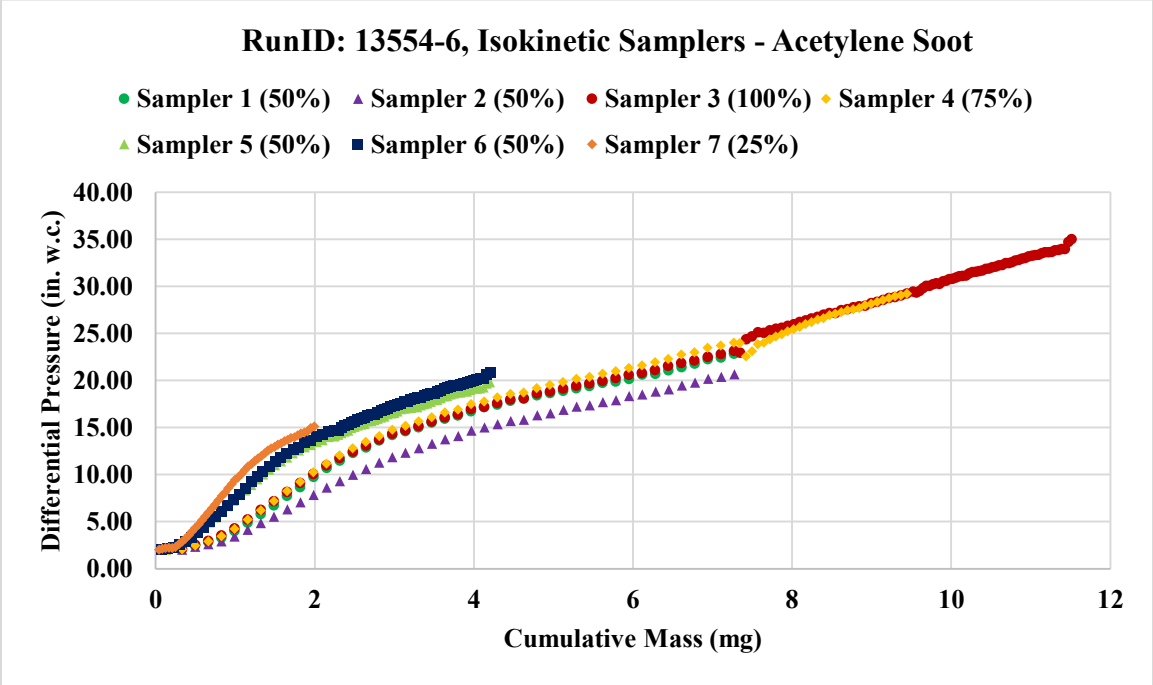

Figure 4.16 Cumulative mass vs. dP for RunID: 13554-6.

Table 4.16 Isokinetic sampler mass collection and dP results for 13554-7.

Sample Number	HEPA Coupon Filter dP Initial	HEPA Coupon Filter dP Final	Cumulative Number Concentration (#/cc) APS # Conc.	Cumulative Number Concentration (#/cc) SMPS # Conc.	HEPA Coupon Accumulated Masses (mg) Grav. Analysis	HEPA Coupon Accumulated Masses (mg) APS Calc.	Accumulated Mass Correlation Coefficient
1	1.40	19.49	8.55E+04	9.12E+05	13.75	13.72	0.998
2	1.56	20.64	8.55E+04	9.12E+05	12.41	11.81	
3	1.62	31.73	3.12E+05	2.38E+06	20.05	19.96	
4	1.60	27.84	2.17E+05	1.63E+06	17.29	17.64	
5	2.09	18.57	2.26E+05	1.47E+06	7.12	6.24	
6	2.05	21.37	2.26E+05	1.47E+06	7.00	6.25	
7	1.89	16.28	9.48E+04	8.26E+05	4.12	2.14	

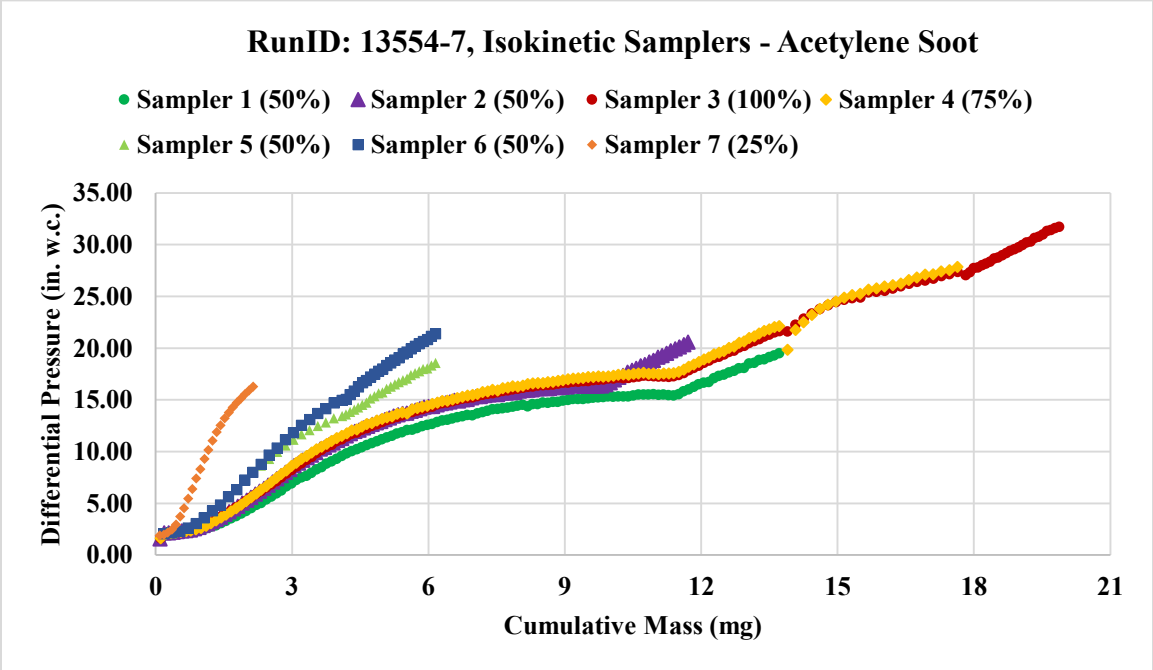

Figure 4.17 Cumulative mass vs. dP for RunID: 13554-7.

RunID tests for 12784-5 and 12784-6 show that the pressure drops achieved for Sampler 3 are comparable to the pressure drops observed for $Al(OH)_3$ under the same testing conditions, with substantially less mass accumulation. In RunID 12784-6 the

DAQ was unavailable throughout the loading test up to 10 in. w.c.. The SCADA recorded data was used in place for the test stand data to accommodate for the lack of test data for RunID test 12784-6. The shape of the loading curves for both tests is less defined in relation to depth loading and surface loading because of the amount of loading time per interval. The short sampling times resulted in less opportunity for the personnel to collect samples with the APS and SMPS due to the quick pressure drop with acetylene soot. APS samples were difficult to obtain and for the mass estimation to compare with the gravimetric analysis results due to the lack of sampling intervals during soot testing. Therefore, APS estimated masses may be overestimated or under estimated due to the lack of mass concentration data available for calculations. The resulting accumulated mass correlation coefficients were found to be 0.928 and 0.870, respectively, for RunID tests 12784-5 and 12784-6. The sampler line leak associated with Samplers 1 and 5, decreased correlation coefficients in RunID tests 12784-5 and 12784-6.

Differential pressures reached for Sampler 3 on RunID tests 13554-6 and 13554-7 were greater for the remote change tests as compared to safe change evaluation tests. The accumulated masses for the remote change filter tests show that the remote change filters can withstand a longer duration of filter loading. The longer filter loading time shows that higher differential pressure can be achieved as well as mass loading The HEPA media coupons show a higher gravimetric mass loading for the remote change tests. The increased pressure drop and mass loading would mean that the remote change radial filter has a greater capacity for loaded aerosols before reaching a sampler changeout point. The accumulated mass correlation coefficients show very good agreement with the

gravimetric analysis data set. The difference of having the sampler lines fixed make a substantial difference in the correlation coefficient.

4.2.2 Pilat Cascade Impactor Evaluation

The Pilat impactor is used to verify the aerodynamic particle size range for each aerosol type used. The jet stage showing the greatest amount of mass collected shows that the mass mean diameter for the monodisperse aerosol would be equivalent to the d50 cutoff diameter that the stage was designed for. In comparing the MMD obtained from the APS, to the jet stage cutoff diameter with the greatest mass loading, this would effectively verify the mass mean diameter of the challenge aerosol. The jet stage d50 parameter changes with air viscosity during elevated conditions. The jet stage d50 diameters were approximated according to the Pilat impactor manual and are shown in the Table 4.17 below.

Table 4.17 Jet Stage d50 cutoff diameters for ambient and elevated conditions.

Jet Stage	**1**	**2**	**3**	**4**	**5**	**6**	**7**	**8**	**9**	**10**	**11**
Ambient Condition d50 (µm)	40.00	3.37	1.75	1.25	1.00	0.75	0.575	0.465	0.370	0.280	0.215
Elevated Condition d50 (µm)	40.20	3.50	1.90	1.35	1.10	0.80	0.600	0.480	0.380	0.285	0.215

The d50 cutoff diameter size decreases as the jet stages progresses to stage 11 due to the change in air viscosity as a function of temperature increase. The Pilat impactor was set at to automatically sample at 0.310 cfm for optimized isokinetic flow at test

conditions 3, 2b, and 2c. The results of each evaluation are shown in each subheading representing each aerosol type tested.

The particle number concentration data for the SMPS and APS were combined to show the number concentration and particle diameter of $Al(OH)_3$. DeCarlo et al. used Equation 4.1 to convert the SMPS electric mobility diameter to the aerodynamic diameter equivalent [35].

$$d_a = d_e\sqrt{\frac{\rho_p}{\rho_0 * X}} \tag{4.1}$$

Where:

d_a = Aerodynamic diameter
d_e = Electric mobility diameter
ρ_p = Particle density
ρ_p = Unit density
X_c = Particle shape factor

The SMPS electric mobility diameter is converted to the aerodynamic diameter equivalent using the shape factor, particle density, and unit density parameters. The process of determining the shape factor through method of scanning electron microscopy was used in the conversion process.

4.2.2.1 Pilat Impactor – Aluminum Trihydroxide

The Pilat impactor was used during the filter loading tests along with the isokinetic samplers. The following data show the mass accumulated in the jet stage collection plates of the Pilat impactor. RunID tests 12784-1 and 12784-2 were sampled

for 1 hour each, and the remainder of $Al(OH)_3$ tests afterwards were sampled at 30 minutes. The tests that were tested for 1 hour showed an abundance of particles collected on jet stages 3 through 5 due to sampling for too long. The Pilat impactor for RunID tests 13109-2, 12719-3, and 13554-2 through 13554-5 were sampled for 30 minutes. The following figures show data collected from the tests.

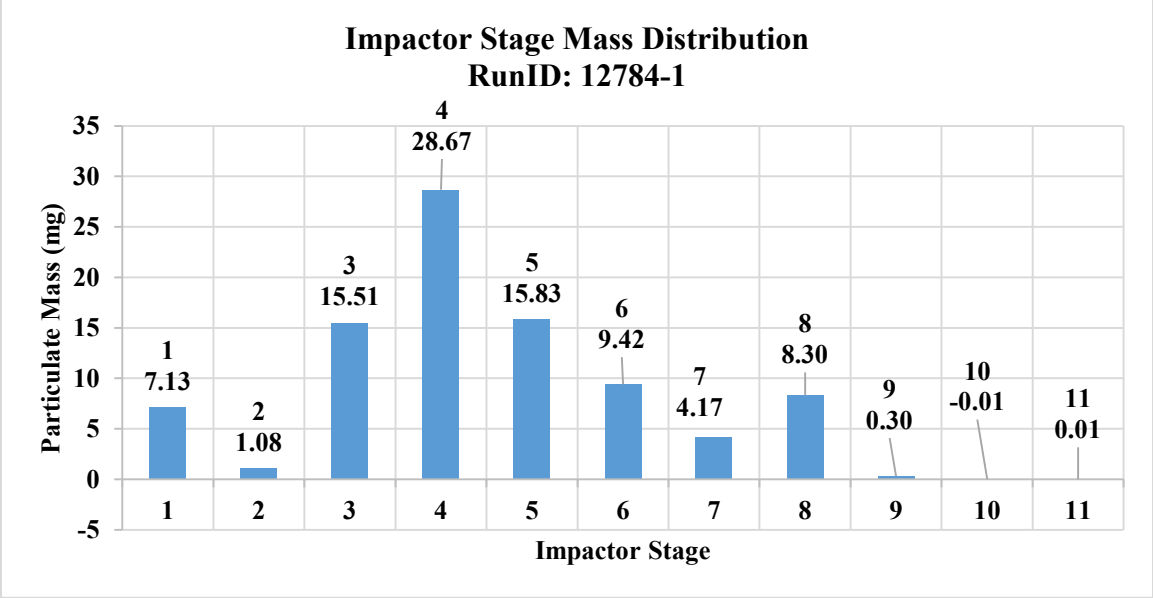

Figure 4.18 Pilat Impactor data for RunID 12784-1.

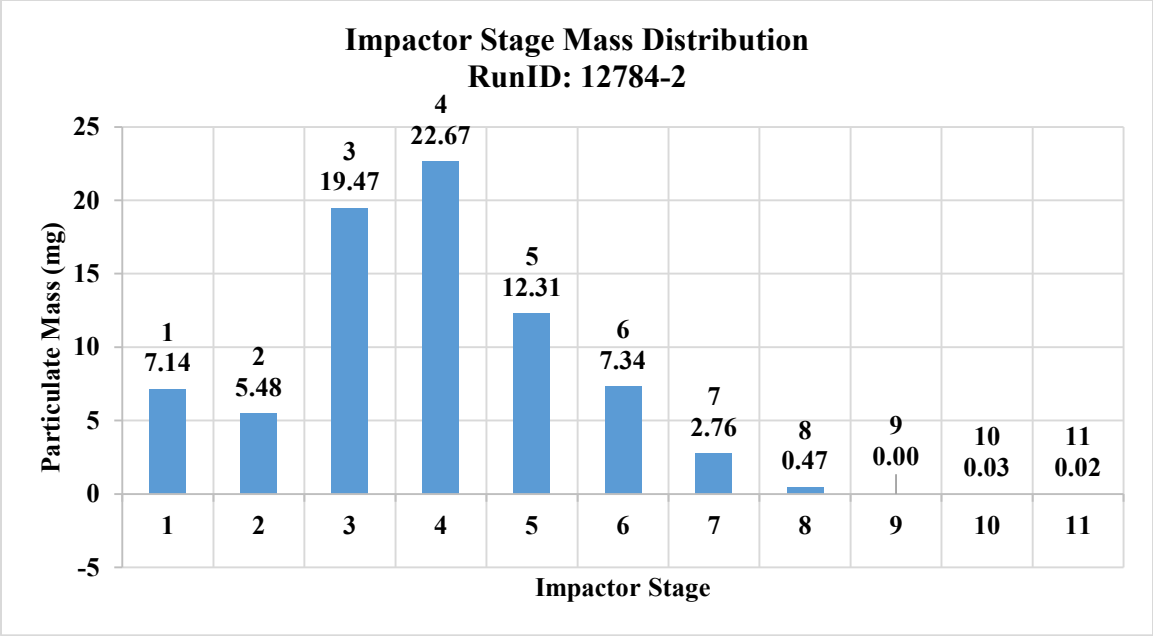

Figure 4.19 Pilat Impactor data for RunID 12784-2.

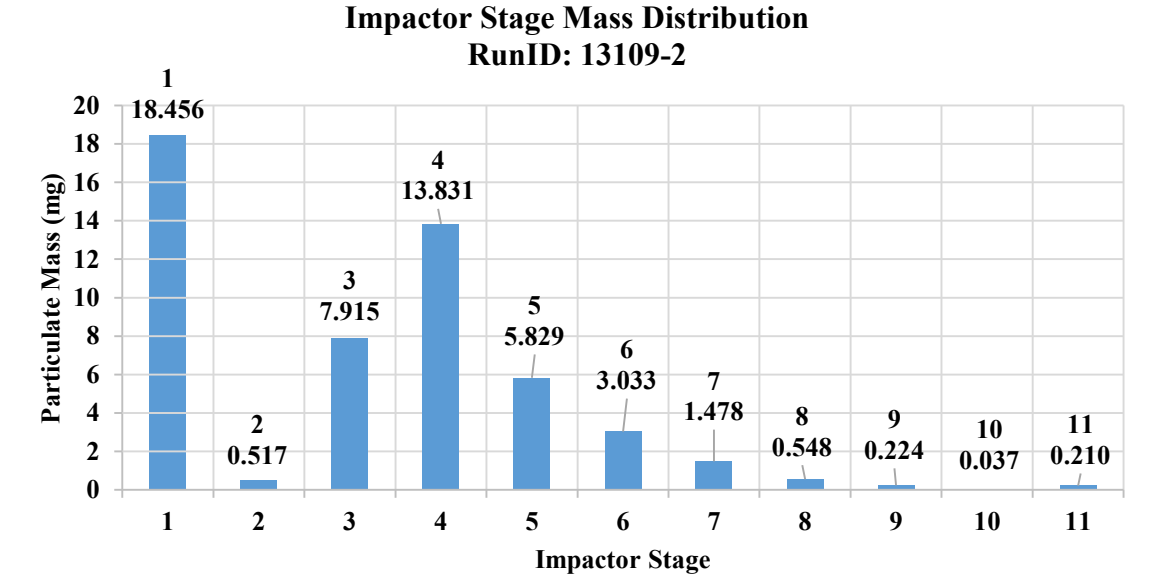

Figure 4.20 Pilat Impactor data for RunID 13109-2.

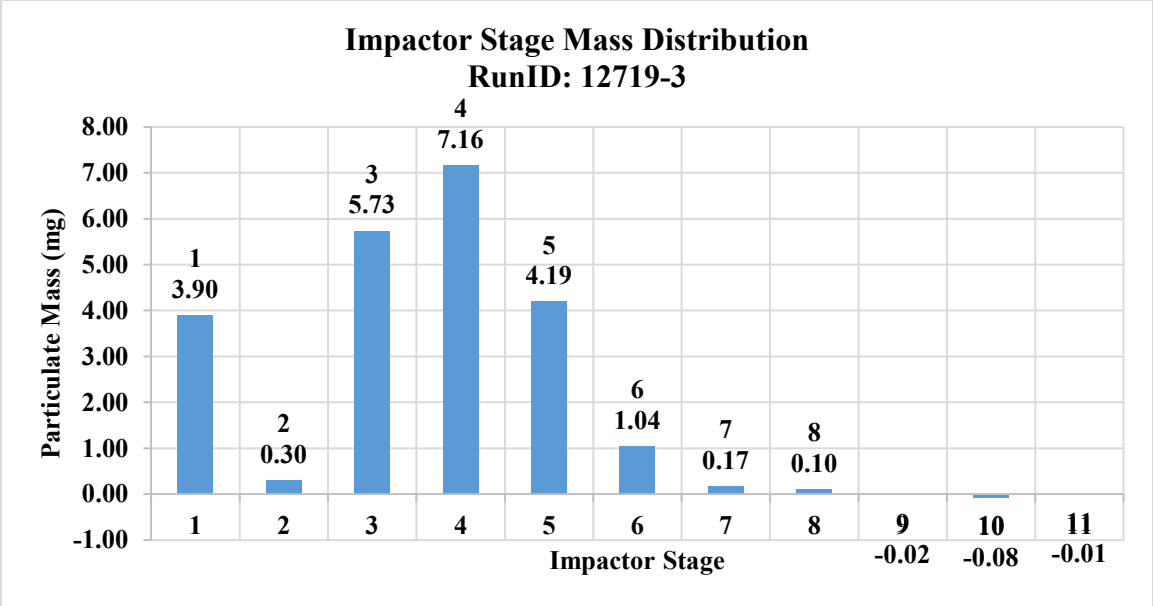

Figure 4.21 Pilat Impactor data for RunID 12719-3.

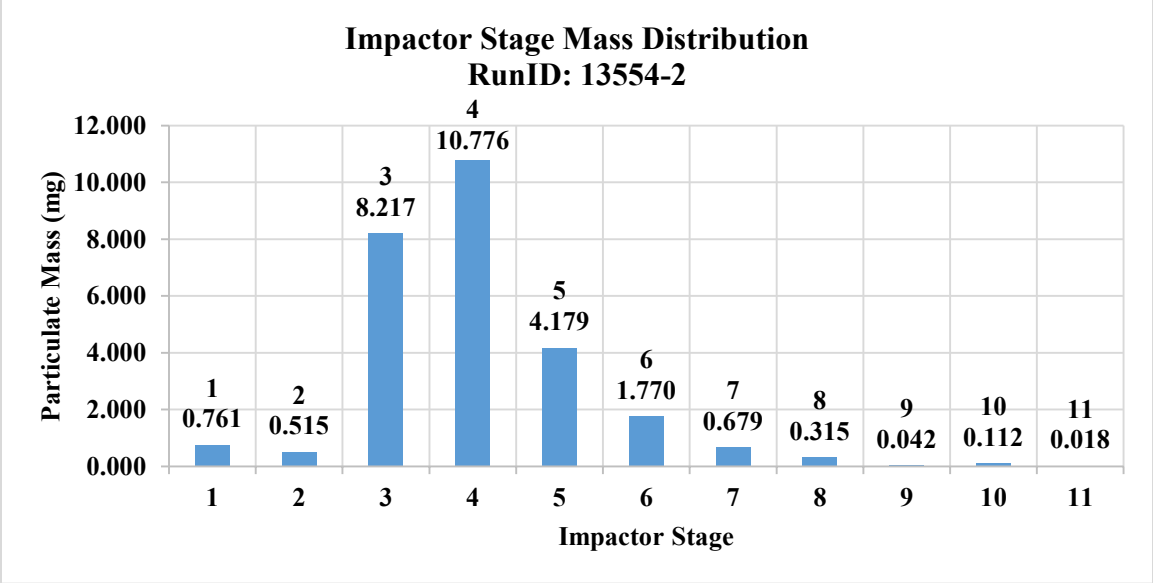

Figure 4.22 Pilat Impactor data for RunID 13554-2.

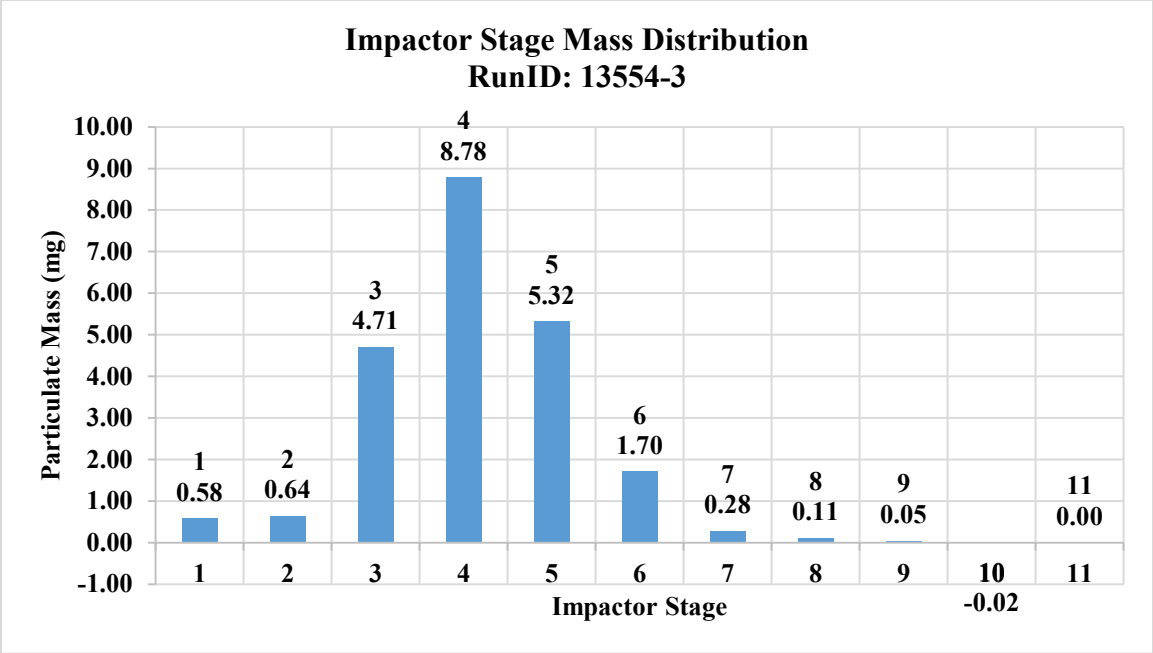

Figure 4.23 Pilat Impactor data for RunID 13554-3.

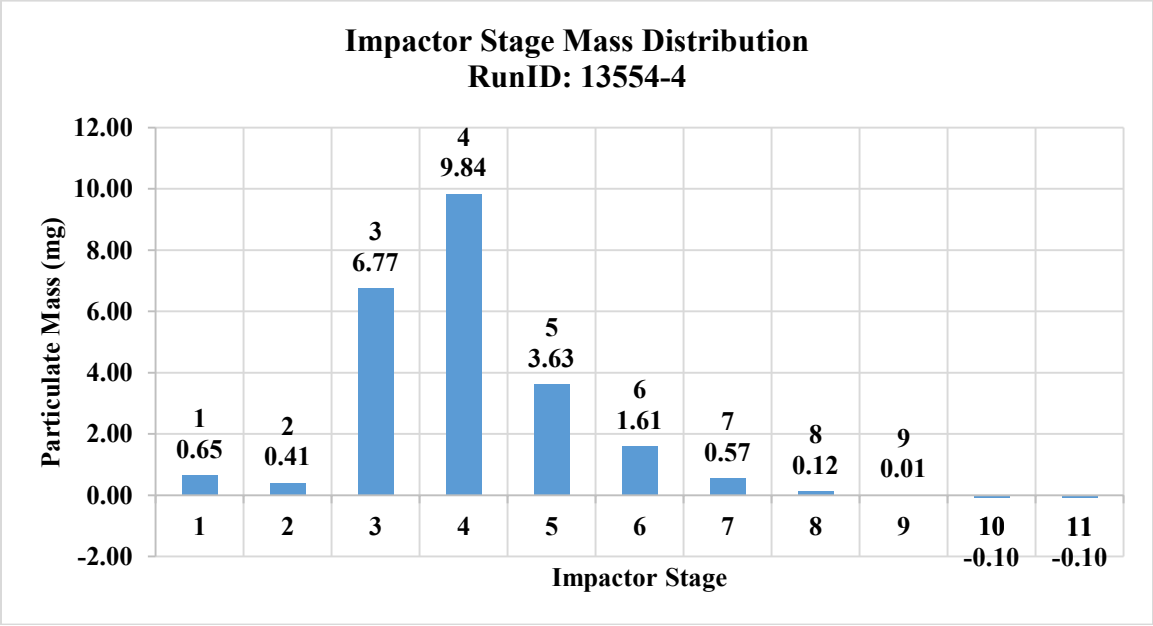

Figure 4.24 Pilat Impactor data for RunID 13554-4.

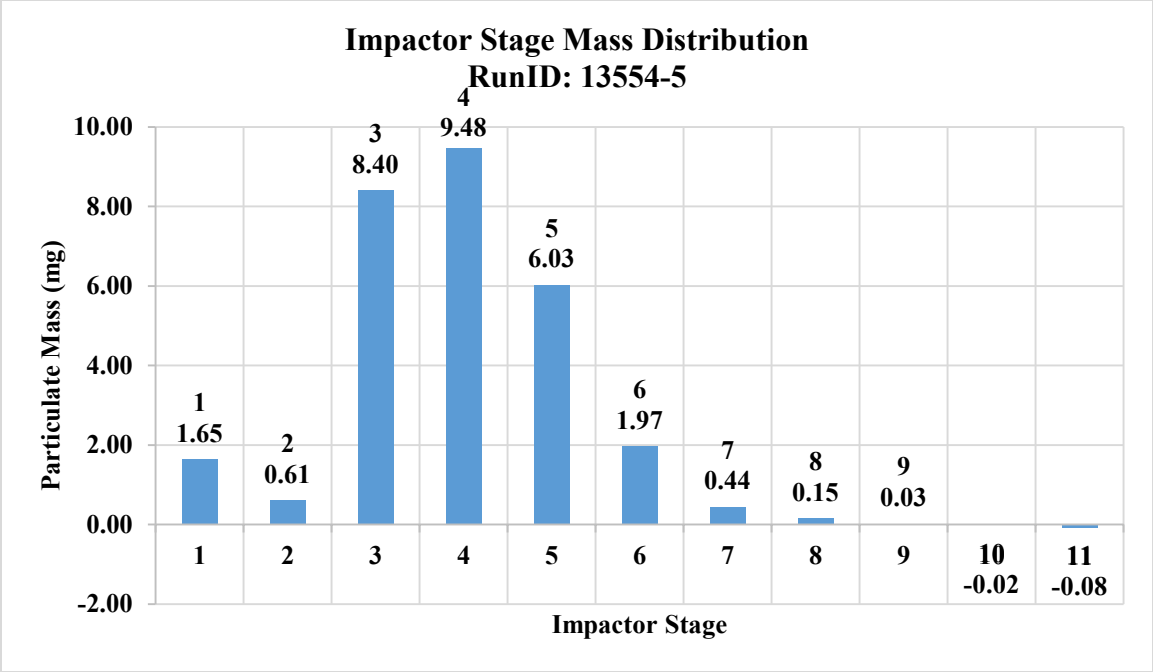

Figure 4.25 Pilat Impactor data for RunID 13554-5.

Impactor stages 3 through 5 obtained the most mass ranging from the d50 aerodynamic cutoff diameters of 1.9 microns to 1.10 microns for all evaluations using $Al(OH)_3$. This particle size data obtained by the Pilat impactor shows that collected particles were larger than what is stated in the manufacturer data sheet for $Al(OH)_3$. The d50 stated on the manufacturer data sheet for $Al(OH)_3$ is listed as 1.0 micron in size. This finding agrees with the APS determined MMD for the $Al(OH)_3$ tests shown above, where the averaged MMD for all tests are approximately 1.92 micron in size. The increase in particle size observed is most likely a result of aerosol agglomeration during flight, resulting a larger particle size and mass. RunID 13109-2 experienced high amounts of loading on impactor jet stage 1. This stage collects all large particles above 40 microns in size. This excessive loading may have originated from the removal of the impactor.

Residual $Al(OH)_3$ collected around the nozzle entrance may have fallen through the nozzle and onto the jet nozzle stage causing an increase in particle mass on stage 1.

The SMPS and APS data were used in validating the mass obtained by the Pilat impactor. The SMPS and APS data were combined and plotted to show a single trend spanning the combined size ranges of both instruments. The shape factor of 1.30 was obtained from scanning electron microscopy (SEM), and the assumed bulk density of 2.42 g/cm^3 was used in the conversion from SMPS electric mobility diameter to SMPS aerodynamic diameter. The SEM imaging of the three aerosols types will be further explained in Section 4.4 SEM Particle Sizing. Figure 4.26 shows the combined SMPS and APS data for $Al(OH)_3$.

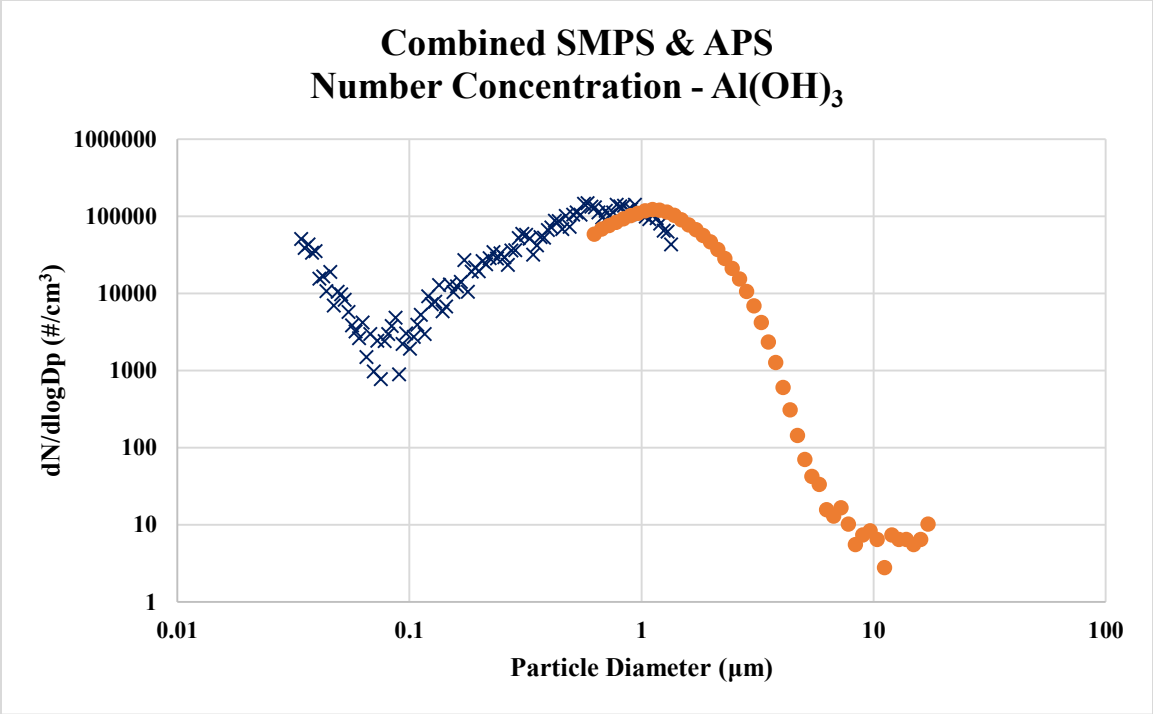

Figure 4.26 Combined SMPS and APS number concentration for $Al(OH)_3$.

The overlapping region occurs from 0.63 micron of the APS to 1.31 micron of the SMPS, respectively. The first three or four points of the APS size range were removed because of the unreliability due to aerosol refractive index in that size range. The decrease in shape factor parameter increases the aerodynamic particle size conversion. The increase in the bulk density parameter is directly proportional to the increase in SMPS aerodynamic particle size. The MMD obtained from the SMPS is approximately 0.99 micron, and the CMD is 0.578 micron. The APS MMD obtained is 1.92 micron, and the CMD is 1.12 micron.

4.2.2.2 Pilat Impactor – Arizona Road Dust

RunID tests 12784-3 and 12784-4 were sampled for one hour each. It was discovered after these two tests that one hour of loading was deemed excessive for the sampling time. The disassembly of the jet stages showed noticeable amounts of piling on the collection plates where “pillars” had formed due to piling of particles. Most particles collected on jet stage 2 where the d50 cutoff diameter is 3.5 micron in size. This had an impact on the jet stages because the pillars disrupt the aerodynamics of the particles entering from the preceding jet stage. The large amount of particulate matter piled on the collection plates introduced particle bounce for oncoming particles. This eventually caused additional error in the sampling process for smaller particles as loading continued. The following figures show data collected from the tests.

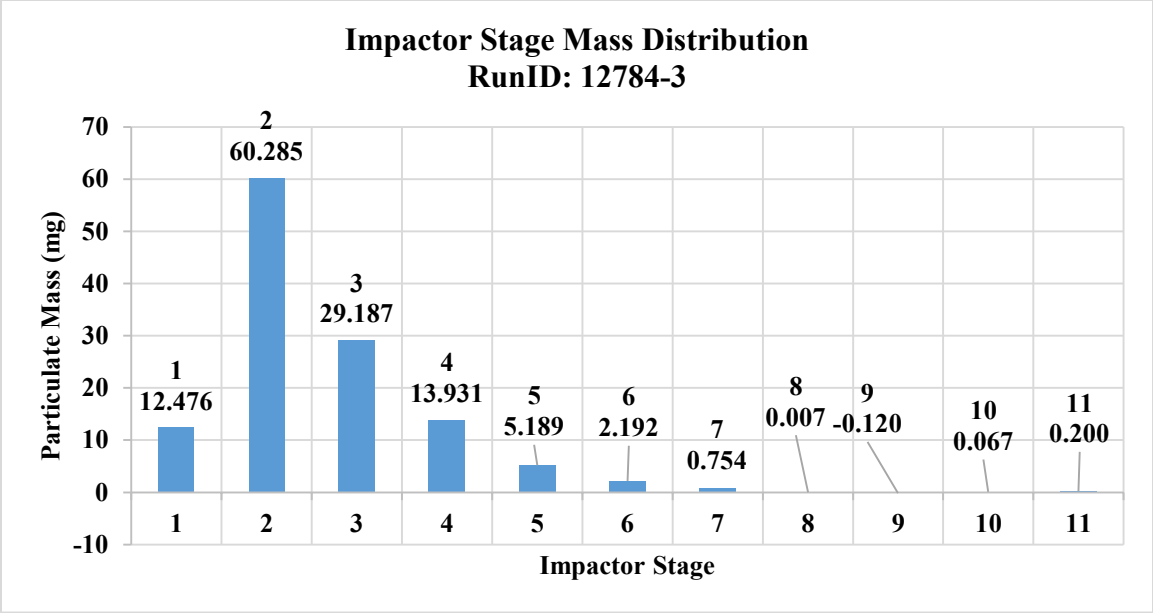

Figure 4.27 Pilat Impactor data for RunID 12784-3.

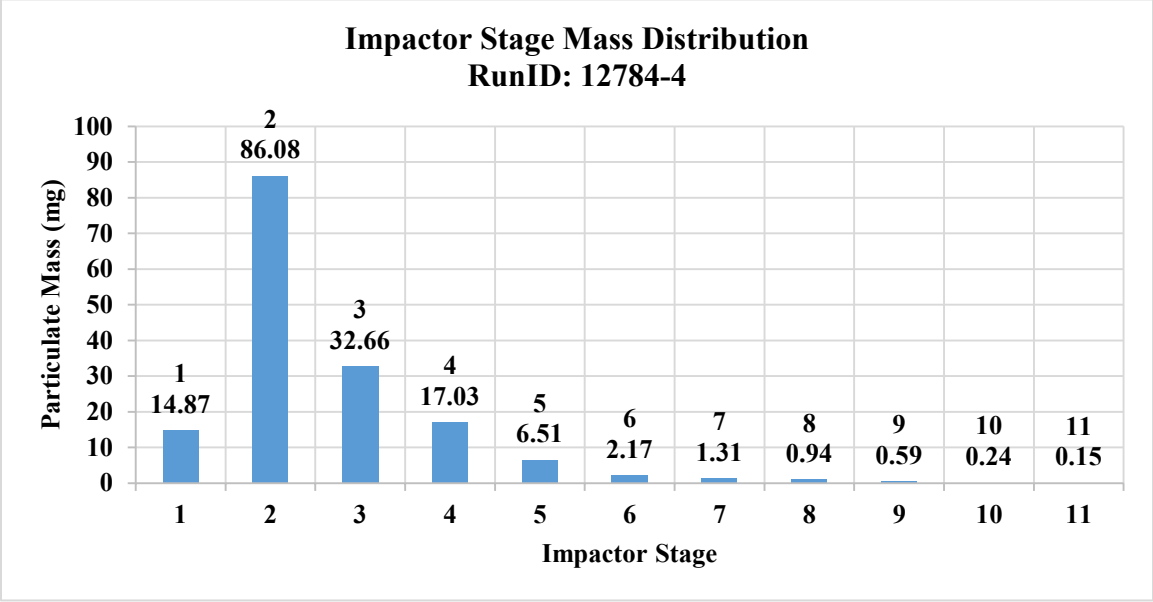

Figure 4.28 Pilat Impactor data for RunID 12784-4.

The evaluations with ARD showed larger MMD sizes due to the greater particle mass found in ARD. The impactor stages with the highest differential mass collected were on jet stages 2 and 3, which corresponds to the d50s of 3.63 and 2.00 microns, respectively. This data agrees with the APS collected data, where the MMD for all sampling intervals for both tests averaged at 2.87 microns in size. Negative values may appear for stages with low mass loading because the gravimetric analysis procedure uses a correction factor. This correction factor considers user error handling during assembly and disassembly. Samples resulting in low differential masses collected may be dominated by the correction factor and result in negative differential masses sampled.

The combined SMPS and APS data are used to show a single size range spanning across the minimum and maximum size ranges of both instruments. A select number of samples were taken with the SMPS during the elevated condition tests. The ambient condition data was therefore used in place of the SMPS elevated condition data. This was because the elevated condition tests lacked sufficient number of samples for averaging and plotting the SMPS particle number concentration. The shape factor of 1.41 was determined from using SEM particle sizing procedures. The assumed bulk density of 2.65 g/cm^3 was used for the SMPS size range conversion to aerodynamic diameter. The following figure shows the combined SMPS and APS data for ARD.

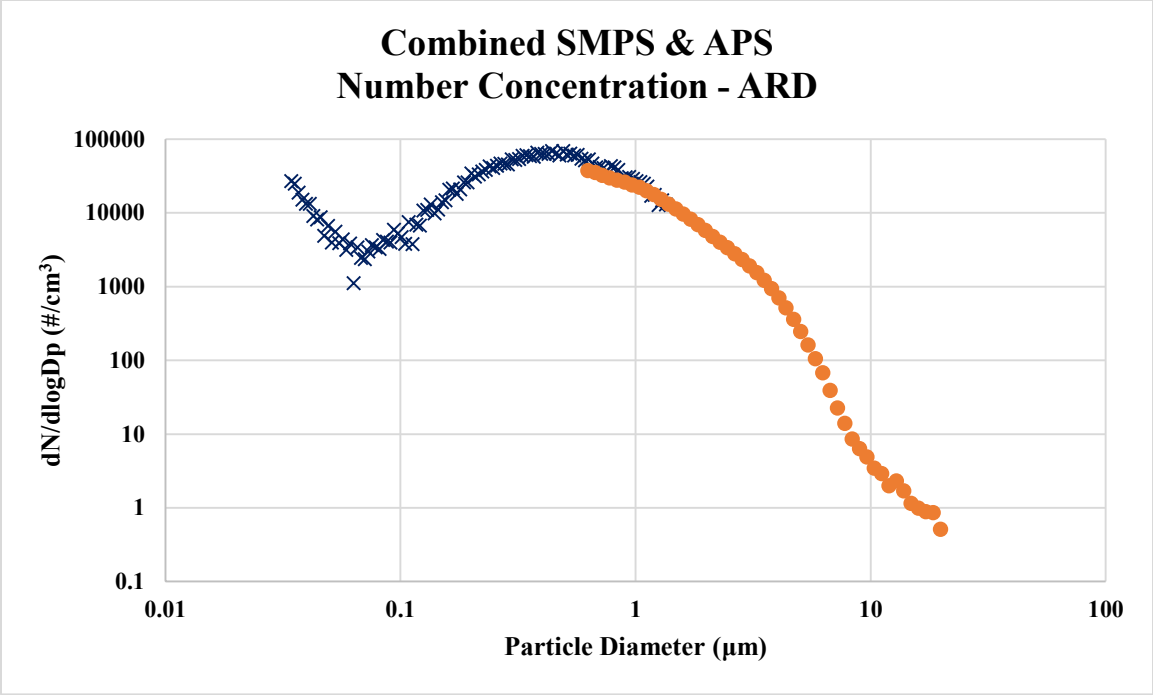

Figure 4.29 Combined SMPS and APS number concentration for ARD.

The first three points were omitted from the APS data because the unreliability due to the aerosol refractive index at those three size range points. The overlapping SMPS and APS regions begin from 0.60 micron to 1.5 micron. The CMD obtained from the SMPS is approximately 0.94 micron, and the MMD is 1.93 micron after converting the values to aerodynamic diameters. The APS MMD obtained is 2.87 micron, and the APS CMD is 0.87 micron. The Pilat impactor data for RunID tests 12784-3 and 12784-4 show that stage 2 of the impactor with a d50 cutoff diameter of 3.30 micron shows the greatest amount of mass loading. This would mean that most of the mass accumulated would have a MMD larger than 3.30 micron instead of between 0.935 micron and 1.93 micron as observed by the SMPS and APS. The discrepancy in the jet stage creating

"pillars" due to excessive sampling time may have influenced the Pilat impactor jet stages.

4.2.2.3 Pilat Impactor – Acetylene Soot

RunID tests 12784-5 and 12784-6 were evaluated for safe change radial type full filters. These tests sampled for 30 minutes each with the Pilat impactor after realizing that the previous tests had sampled excessive amounts of particles at one hour sampling time. The previous tests for all acetylene soot tests were powder particles. The test stand upstream duct was not cleaned of residual powder particles for both safe and remote change full filter tests. The isokinetic samplers and the Pilat impactor jet stages showed trace amounts of alumina powders and ARD loaded with the soot particles. Trace amounts of ARD was found on the isokinetic HEPA media coupons and Pilat impactor jet stages for RunID tests 12784-5 and 12784-6. Trace amounts of alumina powders were also found on RunID tests 13554-6 and 13554-7. The accumulated particle masses on the jet stages covered a large size range as seen in the images below. Keep in mind that due to the lightweight characteristic of acetylene soot accumulated masses are more sensitive to mass change on the collection plates.

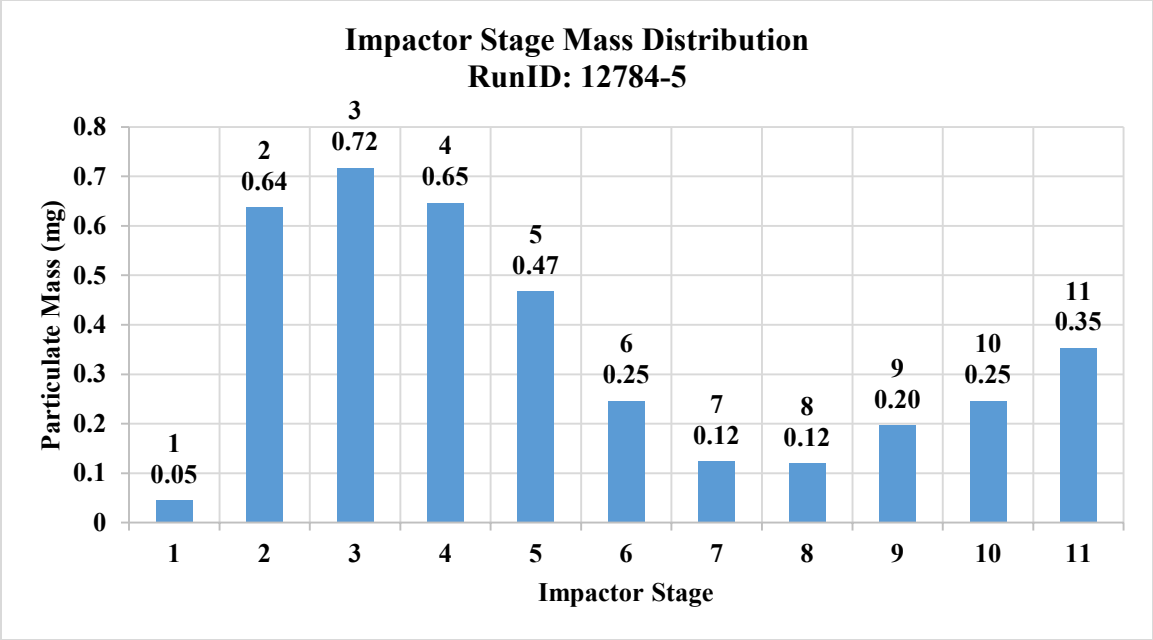

Figure 4.30 Pilat Impactor data for RunID 12784-5.

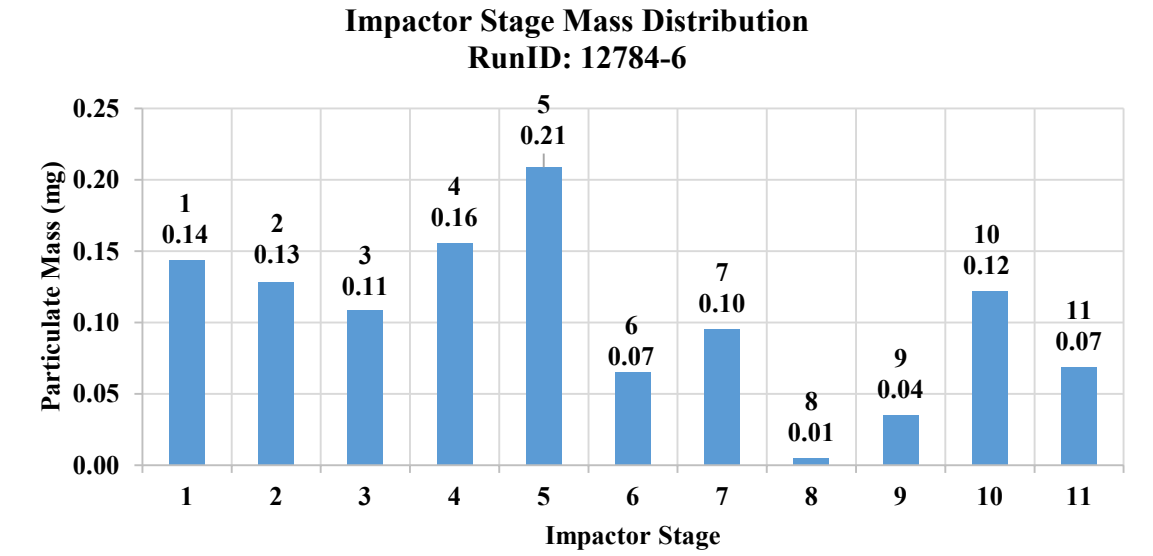

Figure 4.31 Pilat Impactor data for RunID 12784-6.

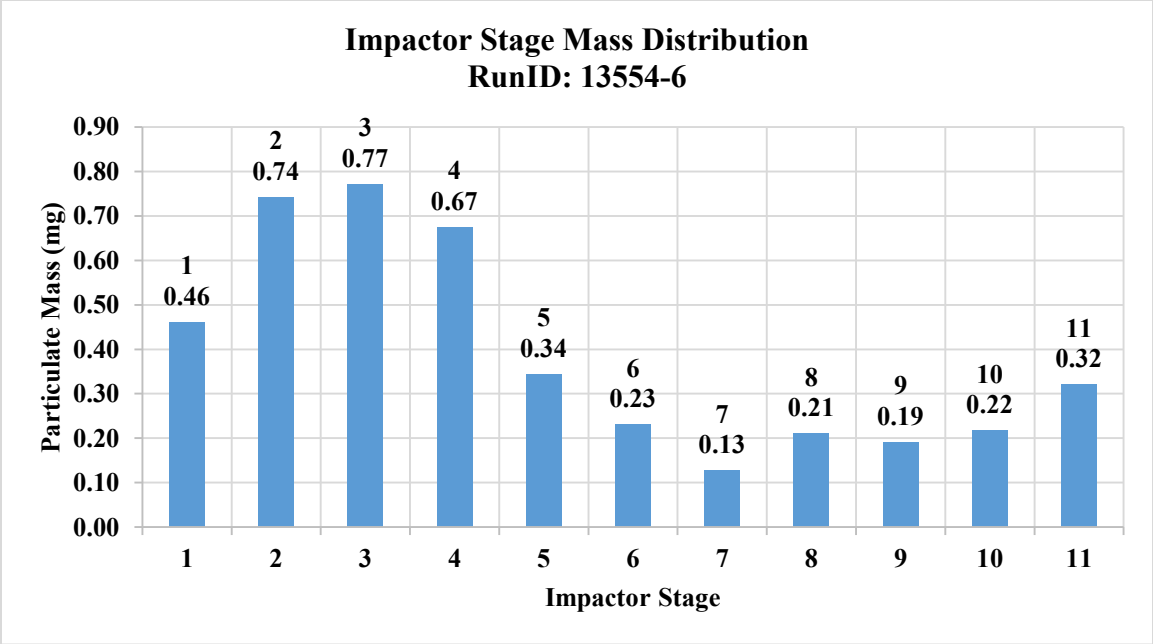

Figure 4.32 Pilat Impactor data for RunID 13554-6.

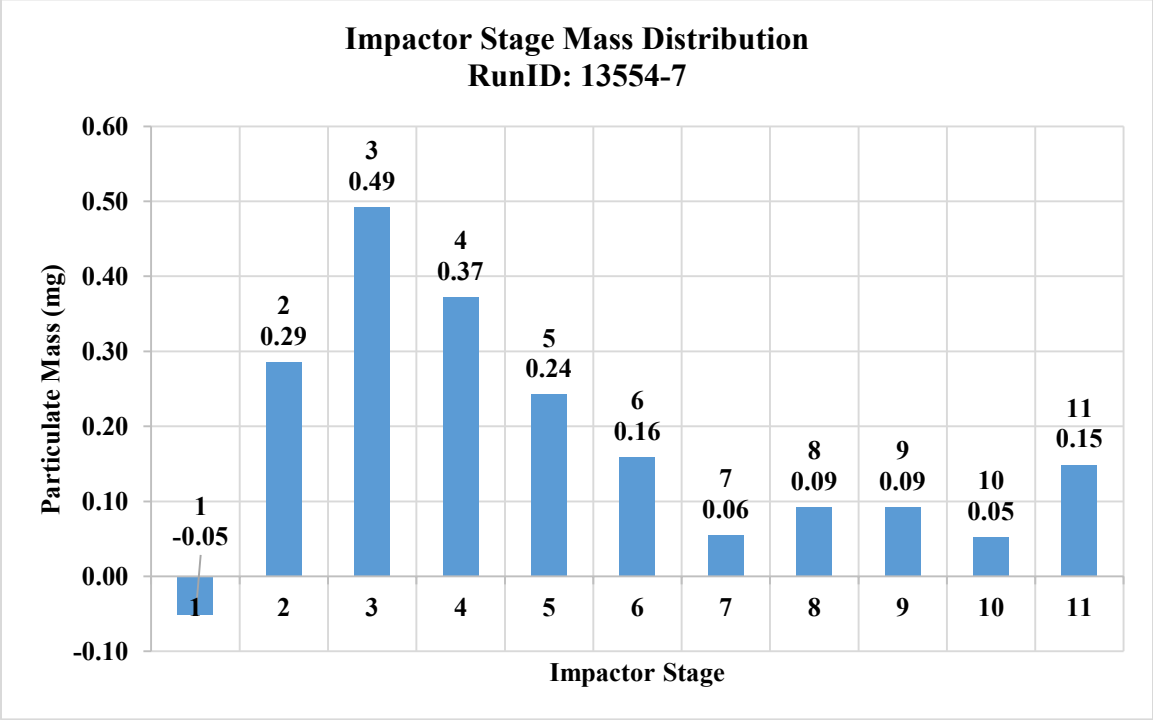

Figure 4.33 Pilat Impactor data for RunID 13554-7.

Evaluations for acetylene soot have shown that the MMD is difficult to obtain. All the Pilat impactor evaluations above have shown variability for stages 1 through 11. A pattern of loading can be seen for stages 2 through 5 (3.5 to 1.10 microns), and stage 10 (0.285 micron) onwards, where repeated differential mass results occurs for nearly all cases. The APS measured MMD values ranging from 1.33 to 17.81 microns in size for larger agglomerates. This size distribution can be attributed to the aliphatic nature of acetylene soot particles during mid-flight through the ductwork. The jet stages progressing through stage 10 show the particle sizes become increasingly smaller as they get smaller to individual particle sizes. Upon disassembling the Pilat impactor, the backup filter stage that was placed on the level proceeding stage 11 appeared to be depth loaded with soot particles. This is possible because individual acetylene soot particles have been sized using scanning electron microscopy methods can as small as 40 nm in size. The particulate size of individual soot particles is so small and are classified in the nucleation size mode. Filtration mechanisms of diffusion are dominant for these smaller, non-agglomerated particles, whereas for larger, agglomerates are prone to impaction and interception mechanisms.

The combined SMPS and APS data show the ambient condition SMPS and elevated condition APS data. The APS data points are less defined because during elevated testing there were limited number of samples taken for the APS. The differential pressure of the full filter would reach the next changeout point before an APS and SMPS sample could be made during the elevated test. The figure bellow shows the plot for the combined SMPS and APS data for acetylene soot.

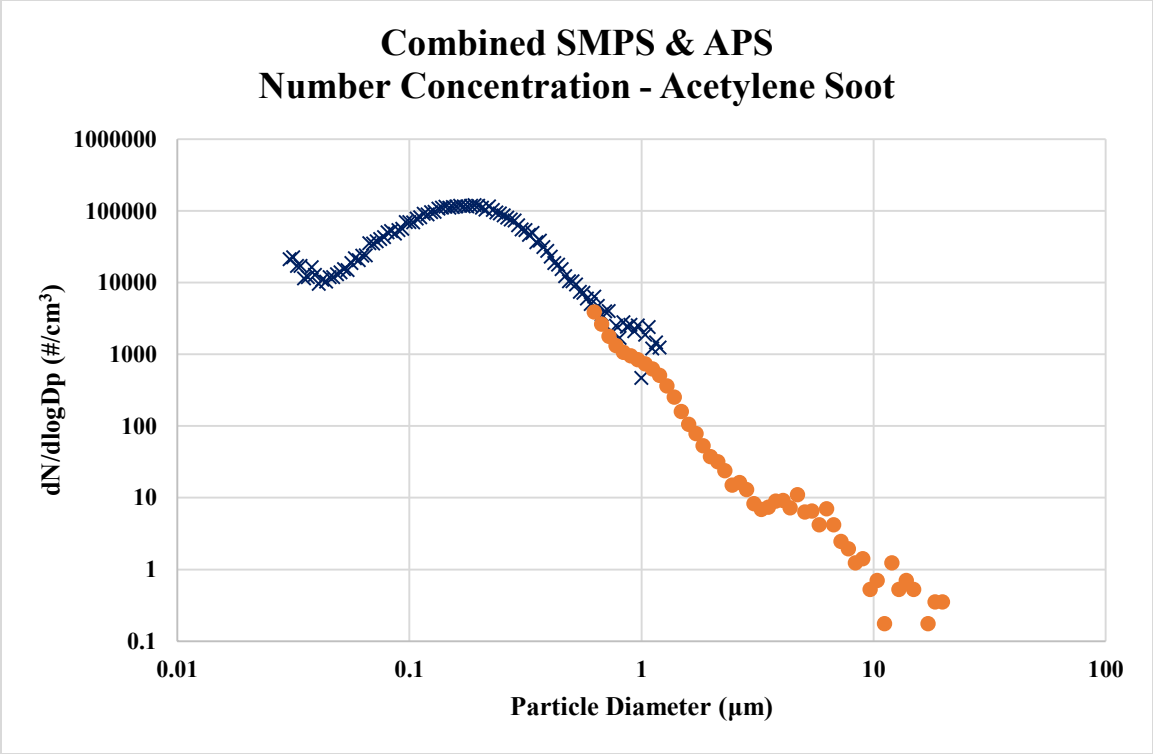

Figure 4.34 Combined SMPS and APS number concentration for acetylene soot.

An AR shape factor of approximately 1.35 was averaged from the individual particles and agglomerates using the SEM imaging. The assumed bulk density of 2.0 g/cm^3 was used. The MMD obtained from the SMPS is approximately 440 nm in size, and the CMD is found to be 169 nm. The APS MMD was found to be 5.67 microns, and the CMD is 630 nm. The large variation in the SMPS and APS MMD and CMD can be attributed to the level of agglomeration occurring. Data collected during the ambient and elevated condition test show that the level of agglomeration is dependent on the aliphatic chains forming before reaching the instruments. The combustion of acetylene fuel at the burner ports may vary depending on the fuel to air mixture during combustion.

The larger particle sizes have been shown to have residual amounts of alumina powder in the Pilat impactor jet stages from stage 1 through 5. Impaction of these larger particles onto surfaces such as fibers have shown the formation of dendritic bodies of soot particles. These residual alumina powder particles may increase in aerodynamic size during flight depending on the soot particles agglomerated during mid-flight. The agglomeration of larger residual powder particles and acetylene soot particles are the cause of the wide range of aerodynamic diameters sampled in the Pilat impactor. More studies should be performed to observe this phenomenon.

4.3 SEM Filter Fiber Diameter Sizing

Scanning electron microscopy (SEM) filter fiber diameter sizing was performed at the MSU Institute for Imaging & Analytical Technologies (I2AT). A control specimen each for Lydall 3398 L1W and L2W were brought for fiber diameter sizing images. Images for a control specimen were taken at five locations of the HEPA media coupon. The locations consisted of the center, and near the edges in each cardinal direction (West, North, East, South). This imaging method was performed to ensure that particle sizing was not biased at one location, and that the particle size and fiber diameter sizing covered locations across the surface of the filter coupons.

The images were processed using an open-source Java based image processing program developed at the National Institutes of Health by Wayne Rasband [36]. DiameterJ was used to post process the images for fiber sizing. This downloaded plugin for ImageJ utilized an image processing algorithm on binary format SEM images at x1000 and x2300 magnification. The images were processed under automatic and/or user controlled image thresholding, called segmentation, to regulate the amount of black and

white pixels on the image. The process of segmentation is used to show the suitable number of white pixels of fibers on black background. The white pixels were counted and summed for the total area of the fibers in each image once the SEM images were segmented. The parameter “Super pixel” was determined based on the algorithm to process the white pixels. A summarized output file is created listing the imaged fiber parameters. The resulting range of fiber diameter sizes ranged from 0.5 to 3.0 microns in diameter. The following picture is a L1W control specimen taken under SEM at x1000 and x2300 magnification near the Eastern and Northern edges, respective of the HEPA media coupon.

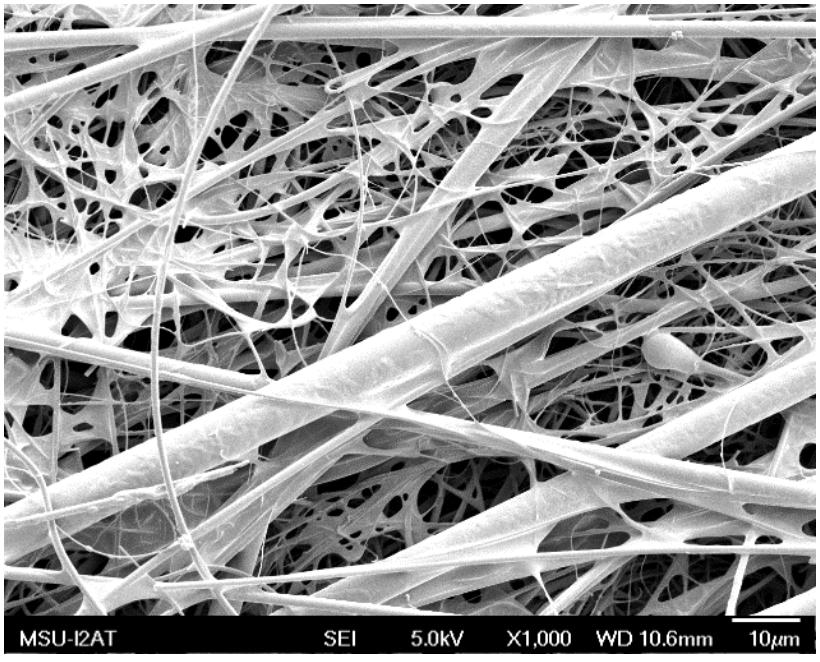

Figure 4.35 SEM image of fiber sizing at x1000 magnification.

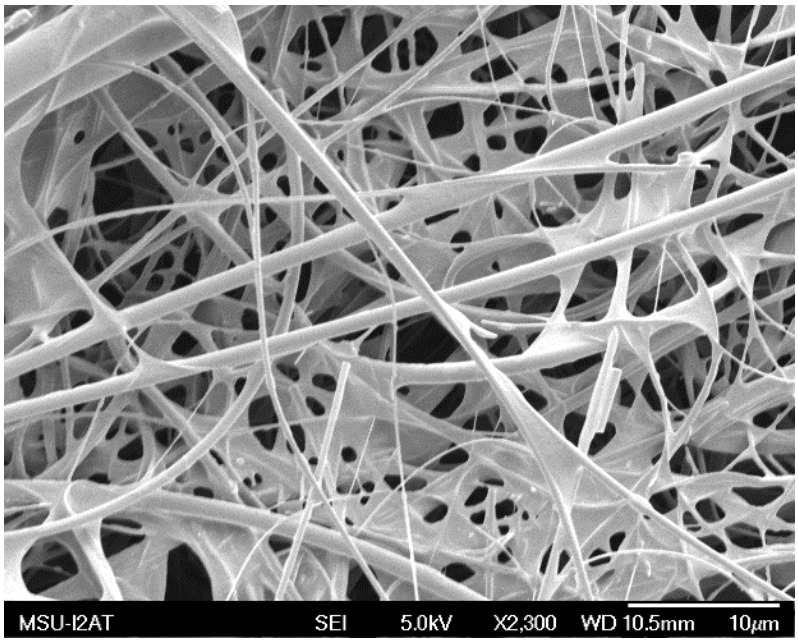

Figure 4.36 SEM image of fiber sizing at x2300 magnification.

The images show large white regions spanning between the fibers. These spanning regions are the acrylate binding glue that is used to hold the fibers together. This has an effect of overestimating the fiber sizes during post processing using the algorithm. Individual fiber sizes are also seen to have the acrylate binding coating the fibers as well. The algorithm performs surprisingly well in estimating the effective fiber diameters regardless of other inhomogeneous factors during fiber imaging. Using the algorithm simplifies the process of post-processing the fibers individually. Fiber diameters were measured using the built-in sizing tool on the SEM to assist in the verification of the fiber diameters.

4.4 SEM Particle Sizing

The sizing of particles was performed at the MSU I2AT for each challenge aerosol under ambient condition loading. Samples loaded in ambient conditions with

alumina powder, ARD, and acetylene soot were examined under the SEM. The examination of samples under elevated full-scale testing could not be performed due to the amount of static charging associated with the high content of loaded particles that could not be sputter coated during the SEM preparation process. Ambient condition tests with 10-minute loading intervals for each challenge aerosol were used for imaging. The 10-minute loading intervals provided sufficient loading on the HEPA media coupons to show depth and surface loading. This could provide enough loading for particle size to be determined without encountering extreme amounts of static charging during SEM analysis. ASTM F1877 Standard Practice for Characterization of Particles was used as reference for determining the particle diameters and shape factors [37].

The equivalent circle diameter (ECD) is the diameter of a circle with an equivalent area of the particle under study. The particle sizing was obtained with the ImageJ base application by using the circle measurement tool to measure the ECD of the particles and agglomerates to verify the particle sizes for each aerosol. The circle tool is used to place a circle around the particle and measure area. Each particle is measured and tabulated up to at least 10 particles for all five locations imaged on the HEPA media coupon before calculating for the average ECD. Equation 4.2 shows the definition of the ECD.

$$ECD = \left(4 * \frac{A}{\pi}\right)^{\frac{1}{2}} \tag{4.2}$$

Where:

ECD = Equivalent circle diameter
A = Area of a circle

The line tool is used to measure the minimum and maximum cross-sectional lengths of particles and agglomerates for determining the aspect ratio (AR). The AR is the most commonly used shape factor when determining the shape of particles. Equation 4.3 shows the definition of an aspect ratio.

$$AR = \frac{d_{max}}{d_{min}} \tag{4.3}$$

Where:

AR = Aspect ratio shape factor
d_{max} = Maximum particle cross-sectional diameter
d_{min} = Minimum particle cross-sectional diameter

The ellipse tool is used to draw an oval around each particle to mark the boundaries of the particle under study. The line tool is then used to measure the maximum and minimum diameters of each particle. Equation 4.3 is used to calculate the tabulated minimum and maximum diameters to determine the AR shape factor on all particles. All AR measured are then averaged to determine the overall mean AR shape factor.

The ellipse tool is useful in determining the roundness shape factor of the particles because it acts as an additional method to compare the AR shape factor. The roundness shape factor is another method of measuring the shape factor of a particle. The roundness shape factor measures how well the particle is similar to a circle. The ImageJ software automatically includes the roundness value when measuring the elliptic shapes. The shape factors used in this study will use the AR shape factor while using the roundness shape factor as an additional method of validation. The following images show

samples of images processed for the challenge aerosols under 25%, 50%, 75%, and 100% loading in various locations of the HEPA media coupon.

4.4.1 SEM Imaging of Aluminum Trihydroxide

Sizing for aluminum trihydroxide powders were performed for the ambient condition tests with 10-minute loading intervals under ambient conditions. The particle sizes examined showed ECD averaging at 1.1 micron in size. The average ECD size agrees with the information provided in the manufacturer data sheet where the size is 1.0 micron. The ECD value is also in agreement with the Pilat impactor jet stages 3 through 5 spanning from 1.9 micron to 1.1 micron. The SMPS MMD of 1.01 micron shows agreement with SEM imaging results of 1.1 micron. The APS MMD of 1.92 shows agreement with the Pilat impactor. Imaged particle agglomerates and larger alumina particles were in agreement with the APS MMD. The AR shape factor calculated from the minimum and maximum diameters is found to be approximately 1.30. The roundness shape factor calculated from the ImageJ ellipse tool measured to be approximately 1.37.

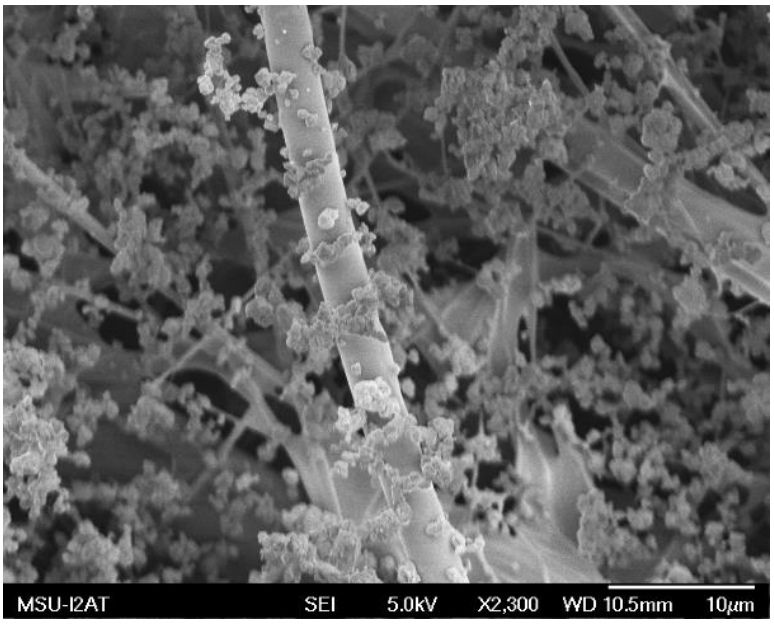

Figure 4.37 25% loading for $Al(OH)_3$ at the center location.

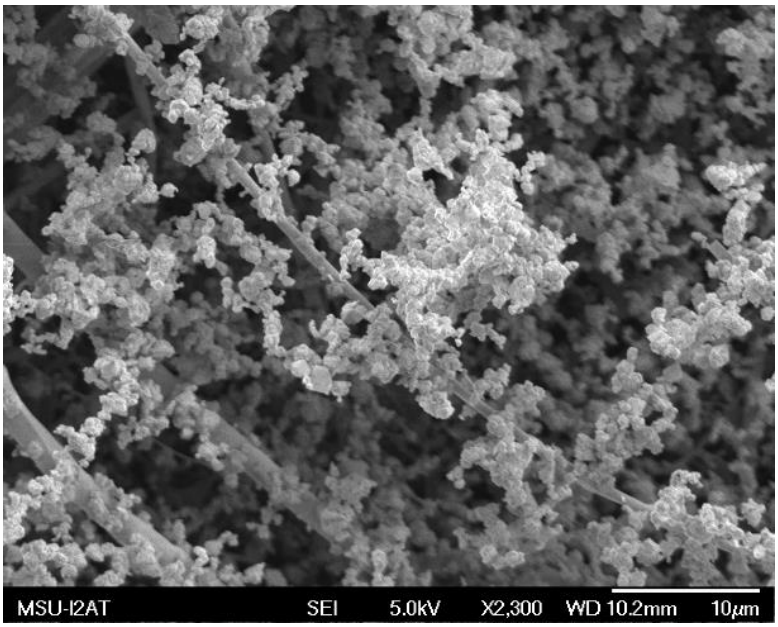

Figure 4.38 50% loading for $Al(OH)_3$ at left edge location.

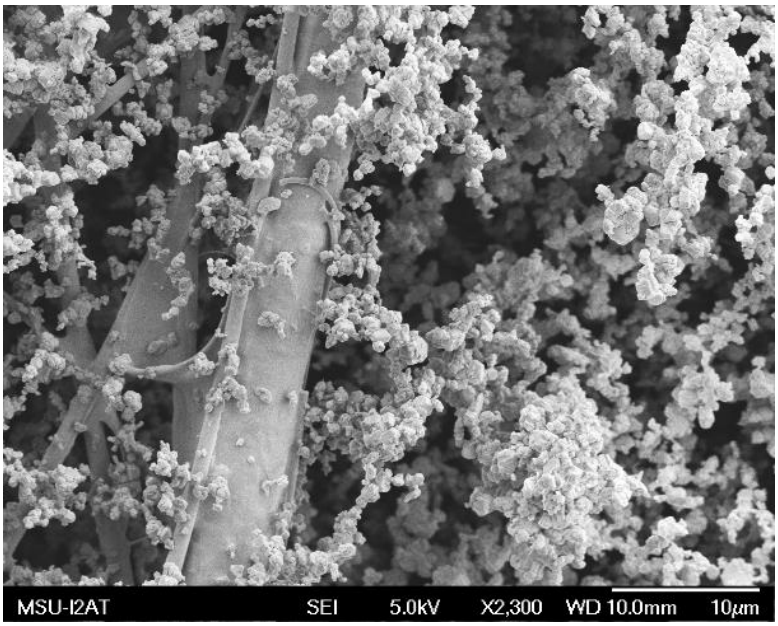

Figure 4.39 75% loading for $Al(OH)_3$ at right edge location.

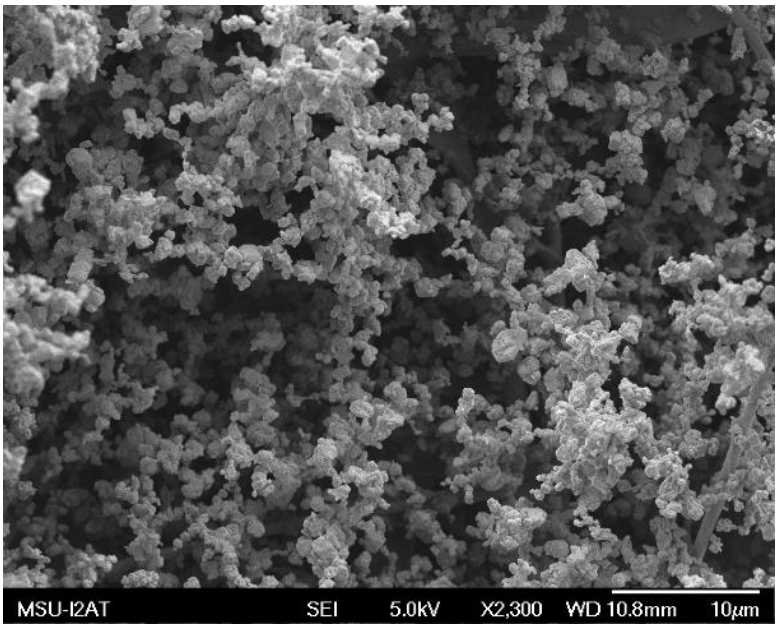

Figure 4.40 100% loading for $Al(OH)_3$ at the bottom edge location.

The loading regimes with $Al(OH)_3$ are shown in the above images. These images show the progressive increase in particulate matter impaction and interception as depth loading occurs. At 25% loading, impaction on filter fibers were apparent, with the formation of dendritic bodies beginning due to interception of oncoming particles. Many of the particles had developed dendritic bodies once 50% loading had occurred within the depth of the fibrous media. From 75% to 100%, the pore sizes between dendritic bodies had closed and surface loading is becoming apparent. Particle agglomerate sizes that were measured averaged at approximately 1.1 micron in size, with finer particle chains as small as 0.5 micron and larger particle chains up to 2.0 microns in size.

4.4.2 SEM Imaging of Arizona Road Dust

Sizing for ARD powders were performed with the 10-minute loading interval samples under ambient condition. The particle sizes examined showed the ECD sizes ranging from 2.40 to 6.50 micron in size. The average diameter was calculated from the manufacturer data sheet to determine the d50 diameter of the ARD. The average diameter was calculated to be 4.38 micron in size. The averaged ECD from the imaging analysis agrees with the manufacturer data sheet. The averaged ECD was calculated to be approximately 4.45 micron in size. The SMPS and APS MMD values are in slight disagreement with the SEM imaged particle sizes. The SMPS MMD is found to be approximately 1.93 micron, and the APS MMD is 2.87 micron. The SMPS CMD is 0.94 micron, and the APS CMD is 1.12 micron. The effects of isokinetic sampling suffer when encounter particles in the coarse particle size mode from 1 micron to 10 microns. A decrease in sampling efficiency is expected. For the smaller size ranged particles smaller particles tend to be sampled with isokinetic flow. The particles in size greater than 1

micron have the tendency undersample as their particle size increases. The larger particle sizes and greater inertia cause the sampling efficiency to drop as particle size increases. The AR shape factor and roundness shape factor of 1.4 is calculated from the processed images. The shape factors of approximately 1.4 are common for coarse powders such as ARD.

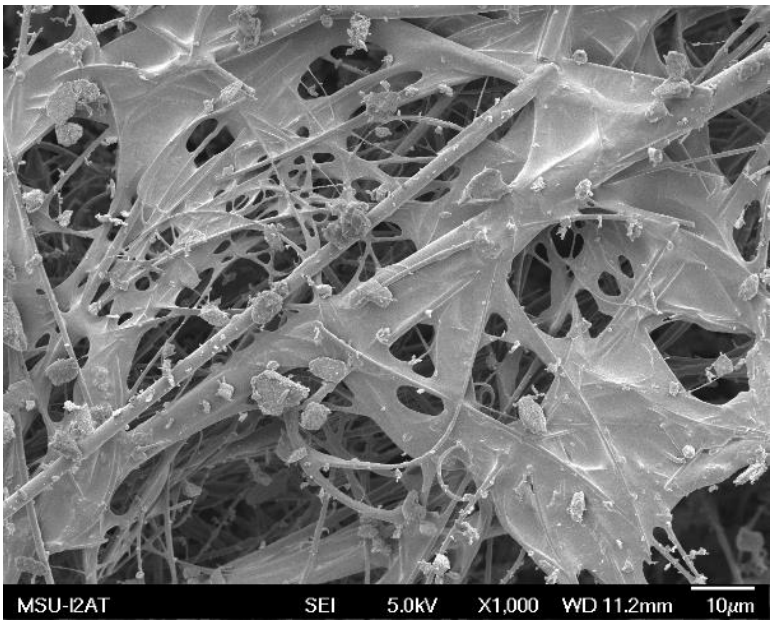

Figure 4.41 25% loading for ARD at the top edge location.

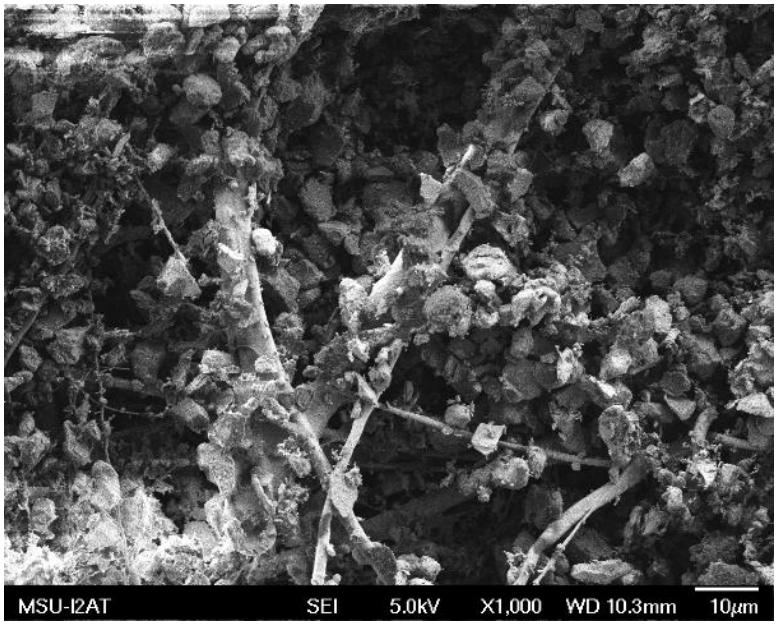

Figure 4.42 50% loading for ARD at the center location.

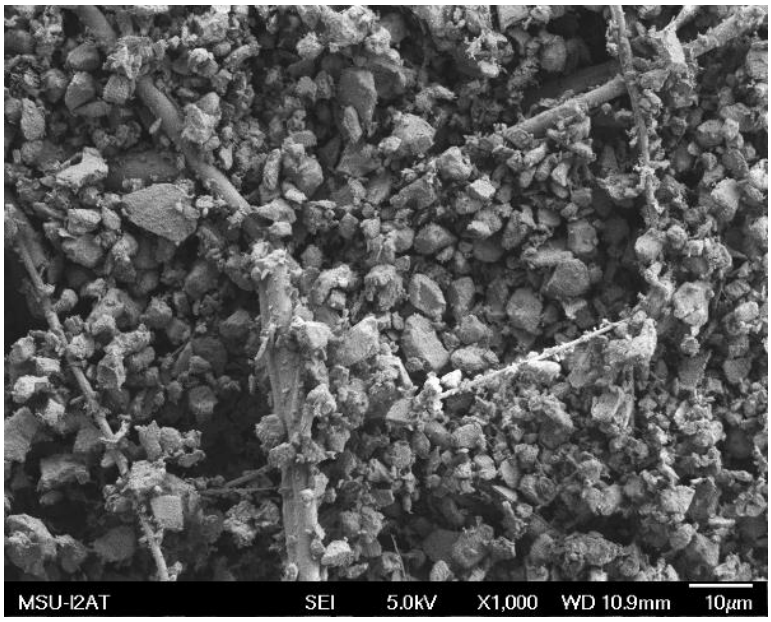

Figure 4.43 75% loading for ARD at the right edge location.

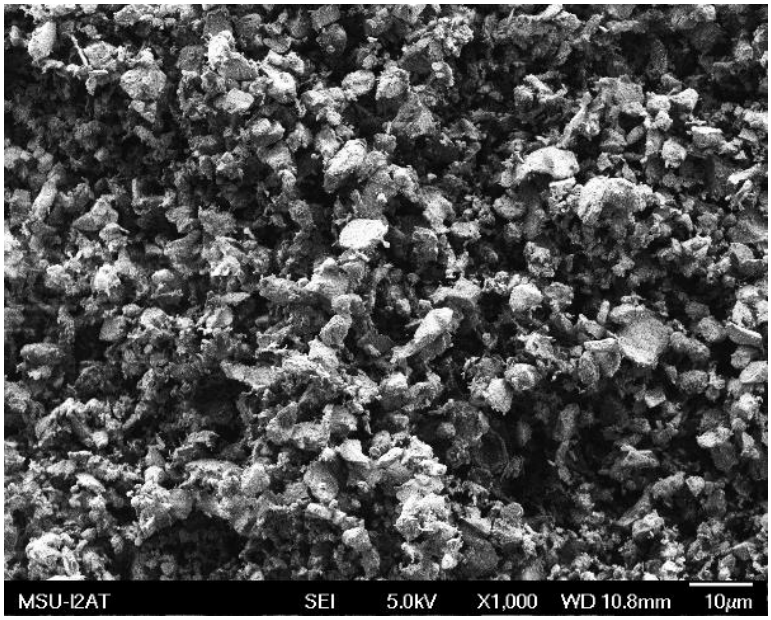

Figure 4.44 100% loading for ARD at the left edge location.

The loading regimes for ARD are shown in the images above. Slight static charging was encountered on loading stages progressing further than 25% loading. Impaction mechanisms were similar to that found with $Al(OH)_3$ loading where similar patterns are apparent as seen in the 25% loading regime. Progressing to 50% loading shows that dendritic bodies had formed and depth loading had occurred much quicker than on $Al(OH)_3$. Fibrous filter clogging is apparent in the 75% loading regime, progressing to a fully surface-loaded regime in the 100% image. The particles measured at an average of approximately 5.0 microns in size, which agrees with the estimated d50 value on the manufacturer data sheet. Particles as low as 1 micron were measured, up to large particles of 10 microns in size.

4.4.3 SEM Imaging of Acetylene Soot

The sizing for acetylene soot was performed on the 10-minute loading interval samples under ambient conditions. The particle sizes examined showed the ECD sizes for individual and smaller agglomerates ranged from 70 nm to 1.5 microns. The ECD determined from the larger agglomerates ranged from 0.9 to 12 microns. Residual powder particles impacted on the fiber filters were determined to be fine alumina powder particles ranging from 0.9 to 2 microns in size. Shape factor values of 1.35 were determined for both AR shape factor and roundness shape factors. The size range obtained from the imaging analysis shows that the acetylene soot particles can vary depending on agglomeration characteristics. Many of the individual particles were found impacted onto the surface of the HEPA fibers showing dendritic growth as loading percentage increased. A key aspect of the acetylene soot was forming dendritic growth on the impacted residual alumina powder particles. Chain-like growths formed off the neighboring soot particles without requiring as much depth loading as seen with powder aerosols. The surface growth of acetylene soot particles is a major factor in sharp pressure drops in HEPA filters during soot loading tests.

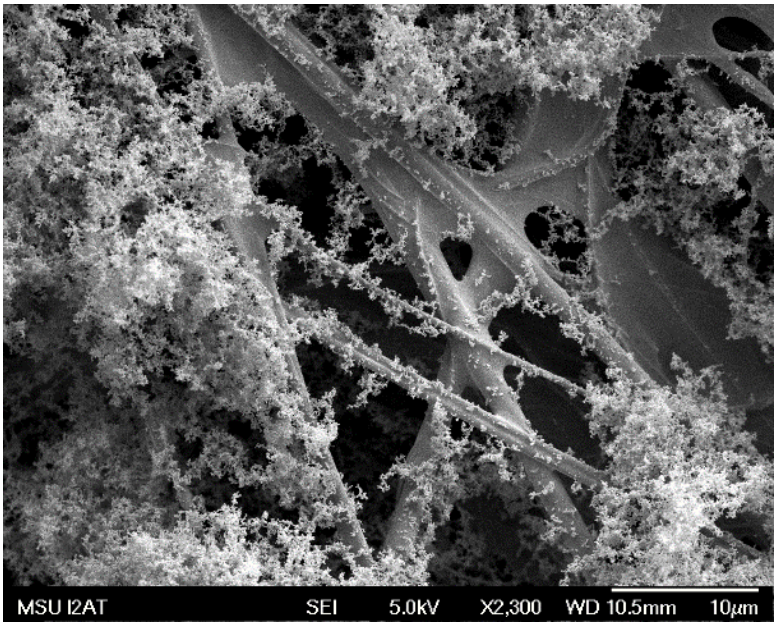

Figure 4.45 25% loading for acetylene soot at the center location.

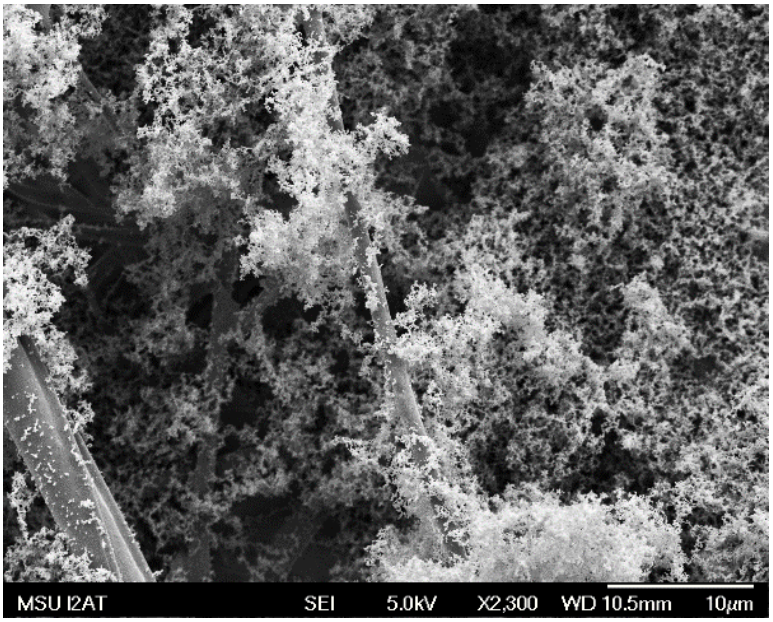

Figure 4.46 50% loading for acetylene soot at top edge location.

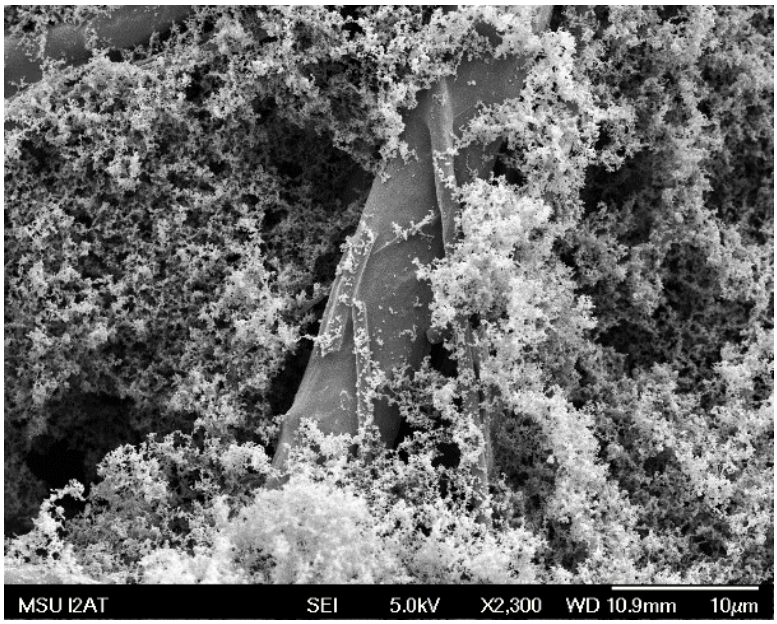

Figure 4.47 75% loading for acetylene soot at bottom edge location.

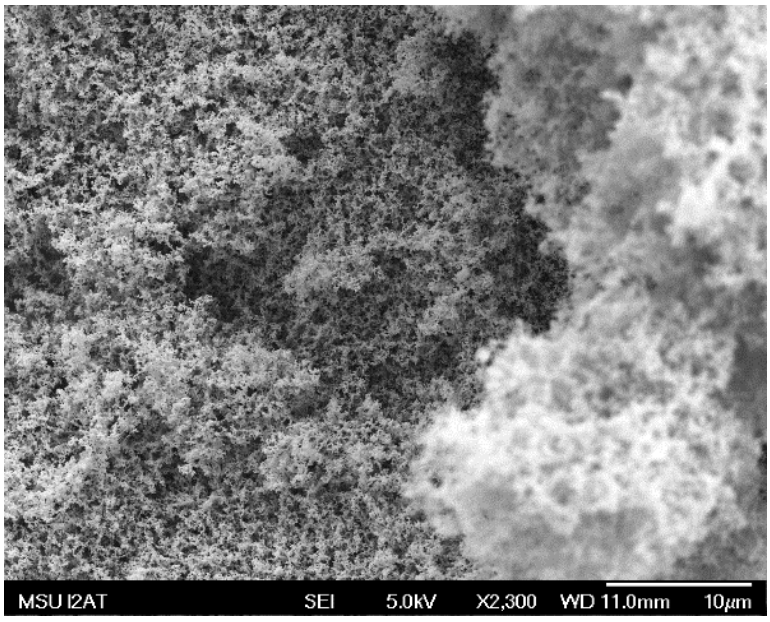

Figure 4.48 100% loading for acetylene soot at the right edge location.

ASTM F1877 states that for particle size ranges from 0.1 to 1.0 micron a magnification of x10000 is recommended for particle imaging [37]. Images at

magnifications of x20000 and x35000 were used to image the individual particles and smaller agglomerates on the surfaces of fiber media. Particles evaluated under the SEM for acetylene soot showed excellent mechanisms of impaction, interception, and diffusion. The formation of dendritic bodies is apparent along neighboring acetylene soot particles and fibrous filters. Residual particles from previous $Al(OH)_3$ tests were still existing within the ductwork when these samples were loaded. Purging the upstream ductwork of the RLSTS to clear residual particles from powder tests did not suffice in removing all the residual particles from the inner duct walls. Trace amounts of $Al(OH)_3$ from the duct walls were found loaded onto the HEPA media coupons. The residual $Al(OH)_3$ particles had impacted onto the fibrous media. These particles then formed dendritic bodies with the acetylene soot. Figure 4.49 represents the $Al(OH)_3$ and acetylene soot particles agglomerated onto a filter fiber.

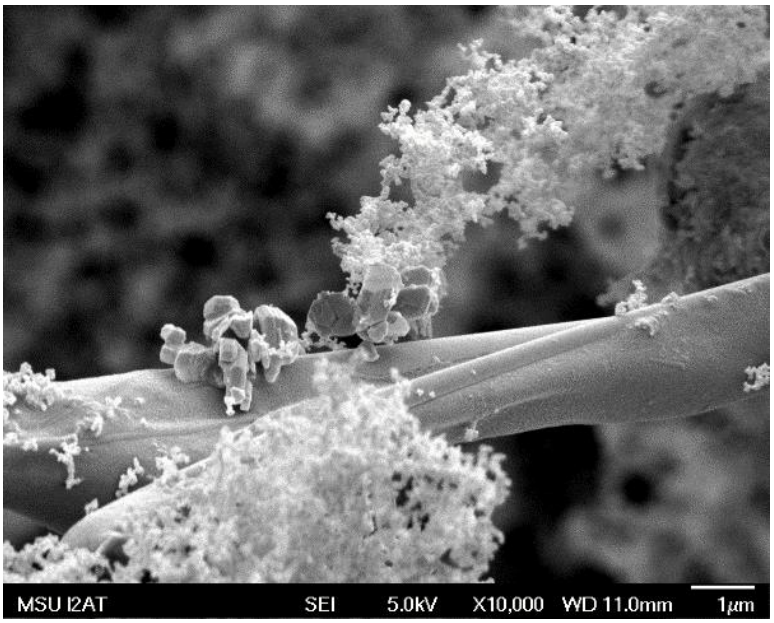

Figure 4.49 $Al(OH)_3$ impacted onto the surface of a HEPA filter, with acetylene soot chains attached.

Figure 4.49 shows the growth of dendritic bodies of soot particles from residual $Al(OH)_3$ particles impacted onto the surface of the HEPA fibers. The gravimetric analysis masses obtained in the Pilat impactors during elevated conditions ranged from stages 1 through 6 (40.42 to 0.82 microns). Trace amounts $Al(OH)_3$ could be seen in the stages upon disassembly of the Pilat impactor jet collection stages. The sizing became more difficult for individual particles due to the aliphatic nature of acetylene soot. The difficulty of determining the edges of the soot particles in dendritic formation made it difficult to properly size the individual particles. The viewing angle from which the SEM was viewing from was difficult to obtain where the edges of the particles existed.

The progression of depth loading increased steadily as the dendritic growths accumulated. The light, aliphatic chaining of acetylene soot is capable of restricting airflow much faster because of faster surface area growth and formation of dendritic bodies. The smaller individual particle sizing of acetylene soot particles and the tendency to form dendritic bodies resulted in filter pores clogged by the acetylene soot particles at early stages of loading. Acetylene soot particles are more effective in increasing pressure drop than by effects due to mass loading. The combination of another solid aerosol in the same test should substantially increase the pressure drop more than by using monodisperse acetylene soot. The observations shown in Figure 4.49 prove that the formation of dendritic bodies with bimodal nuclei mode soot particles and coarse mode powder aerosols may have combined effects in increasing pressure drop across a filter.

CHAPTER V

CONCLUSION

5.1 Conclusions

The goal of this project has been to establish a testing system capable of isokinetic sampling of polydisperse challenge aerosols simultaneously with a radial full-scale HEPA filter test stand. Performance data from evaluated HEPA media coupons can be helpful in optimizing full-scale filter designs in terms of pressure drop and mass loading capacity. The baseline characteristics of the pleated media of full-scale filters can be established for a filter design by using the in-place isokinetic sampling system simultaneously with the full-scale filter. Gravimetric analysis procedures performed in accordance to industry testing standards were used to obtain the differential mass accumulated on the filter coupons. The utilization of mass-weighted and number-weighted particle instrumentation data from the TSI APS and SMPS was used to verify the experimental data obtained for all aerosol types specified in this project.

The correlation of mass estimation with the APS agreed for all tests with exception of the Arizona Road Dust tests. Mass estimation for the APS samples using Arizona Road Dust were underestimated compared to the gravimetric analysis. The underestimation is due to the loss in particles through the diffusion dryer and at the APS upstream sampler inlet. The tests evaluating filters with $Al(OH)_3$ and acetylene soot showed good agreement between their gravimetric analysis and APS calculated masses.

The correlation coefficients for all tests were in good agreement for all aerosol evaluation tests. The safe change filter tests lowered the correlation coefficient because of under sampling due to the sampling line leak in Samplers 1 and 5. For RunID tests 12784-1 and 12784-2 the correlation coefficients were in poor agreement because of the leak in Samplers 1 and 5. Once the sampler line was repaired the gravimetric analysis mass loading values were in better agreement with the APS estimated masses.

The particle size distributions collected by the Pilat impactor agreed with the aerosol instrumentation size distributions from the APS and SMPS. The particle size distribution for $Al(OH)_3$ and Arizona Road Dusts agreed with the APS and SMPS combined particle size ranges. The CMD and MMD of the $Al(OH)_3$ and Arizona Road Dusts agreed with the APS and SMPS values. The Pilat impactor collected masses of acetylene soot were more sporadic due to agglomeration and aliphatic chaining of acetylene soot particles. For smaller particles and agglomerates the Pilat impactor agreed with the impactor aerodynamic cutoff diameters smaller than 0.3 micron. The larger agglomerates accumulated on stages larger than 1 micron.

The examination of particles under methods of SEM imaging and post processing is used to further verification of particle sizing and morphology. The size of the HEPA media samples to be sputter coated and imaged for SEM analysis without disrupting the caking structure of the loaded mass. The study of the HEPA media samples provide images for the samples under 25%, 50%, 75%, and 100% up to 10 in. w.c. for the full filter. The images taken from the SEM entail a visual understanding of the phenomena of depth loading. Images under 50% loading showed increasing mass loading and filter pore blockage within the depth of the filter. Images after 50% loading showed a transition

from depth loading to surface loading. The 100% loaded HEPA media exhibited exponential differential pressure increase, whereas the 25% loading showed linear loading curves.

5.2 Recommendations

The following modifications are recommended for this test system to accomplish further testing with greater effect and refined results.

- Ensure that all applicable fittings installed onto the test system have Teflon tape. This will prevent leaks and provide a higher assurance of differential pressure data obtained. The application of Teflon tape can be tested by placing HEPA media coupons into the isokinetic samplers and installing them onto the ductwork. The isokinetic samplers will be activated for test stand flow rates of 1200 cfm and 2000 cfm for 15 minutes to allow the SCADA to collect the clean differential pressure for each sampler. If differential pressure varies more than 0.5 in. w.c. after 15 minutes then the sampler lines will be checked for leaks from the sampler stem to the mass flow controllers.
- The addition of flat Teflon O-rings between the HEPA media coupon and sampling nozzle will ensure additional sealing around the edges of the sample. This can prevent unnecessary leaks from occurring due to lack of tightening of the brass retaining collar.
- The impulse lines on the dP gauges should be the same length to prevent pressure bias when sampling. The impulse line lengths and diameters for this application should be designed in accordance to ISO 2186:2007.

- The use of lengthened sampling nozzles should be used to ensure uniform particle deposition is across the depth and surface of the HEPA media coupon. This will allow distributed loading throughout the sample, reducing the amount of loose caking structures from being lost when removing the samples for gravimetric analysis.
- The addition of sensors humidity sensors prior the mass flow controllers. This will allow monitoring of humidity levels of air leaving the condenser units before reaching the mass flow controllers. This will ensure that mass flow controllers will not contain condensed air after leaving the condenser units.
- The redesign of moisture collection units in the condenser system should be done to ensure that all moisture collected from the condensing process is collected in containers large enough for each test. Containers with quick-release fittings that provide sufficient sealing under vacuum should be used. Current design uses threaded containers that are difficult to remove and result in the loss of collected water. The mass of collected water is to be weighed and compared to the moist air sampled through each isokinetic nozzle. The collected moisture will be used to determine the moisture collected by the full filter during the 4 in. w.c. and 10 in. w.c. loading tests.

REFERENCES

[1] U.S. Department of Energy (DOE): Nuclear Air Cleaning Handbook (DOE-HDBK-1169-2003), DOE Handbook, 2003, Chap. 1.

[2] Gilbert, H., 1961, *High-Efficiency Particulate Air Filter Units, Inspection, Handling, Installation*, AEC Report TID-7023, National Technical Information Service, Springfield, VA.

[3] ASME AG-1-2012, Code on Nuclear Air and Gas Treatment, American Society of Mechanical Engineers.

[4] U.S. Department of Energy (DOE): Nuclear Air Cleaning Handbook (DOE-HDBK-1169-2003), DOE Handbook, 2003, Chap. 3 pp. 13.

[5] Giffin, P., Parsons, M., Unz, R., and Waggoner, C. A., 2012, "Large-scale generic test stand for testing of multiple configurations of air filters utilizing a range of particle size distributions," Review of Scientific Instruments **83** 055105.

[6] Giffin, P. Parsons, M., Wilson, J. and Waggoner, C. A., 2012, "Performance Comparison of Dimple Pleat and Ribbon Separated Radial Flow HEPA Filters," *32nd Nuclear Air Cleaning Conference*, International Society for Nuclear Air Treatment Technologies, Denver, CO.

[7] Waggoner, C. A., 2012, "Is a Filter Loading Qualification Test Needed?," *32nd Nuclear Air Cleaning Conference*, International Society for Nuclear Air Treatment Technologies, Denver, CO.

[8] Stenhouse, J. and Trottier, R., 1991, "The Loading of Fibrous Filters With Submicron Particles," J. Aerosol Sci., **22**(1), pp. S777-S780.

[9] Japuntich, D. A., 1991, "Clogging of Fibrous Filters with Monodisperse Aerosols," Ph.D. thesis, Loughborough University of Technology.

[10] Endo, Y., Chen, D. and Pui, D. Y. H., 1998, "Bimodal Aerosol Loading and Dust Cake Formation on Air Filters," Filtration and Separation, **35**(2), pp. 191-195.

[11] Lee, J., Kim, S. and Liu, B. Y. H., 2001, "Effect of Bi-Modal Aerosol Mass Loading on the Pressure Drop for Gas Cleaning Industrial Filters," Aerosol Science and Technology, **35**, pp. 805-814.

[12] Carter, J., Taylor, D., and Baron, P. A., 1984, "Method 7400 Revision #3: 5/15/89," NIOSH Manual of Analytical Methods, NIOSH, Cincinatti, OH.

[13] Baron, P. A., Chen, C., Hemenway, D. R., and O Shaughnessy, P., 1994, "Nonuniform air flow in inlets: The effect on filter deposits in the fiber sampling cassette," American Industrial Hygiene Association Journal, **55**, pp. 722.

[14] Belyaev, S. P. and Levin, L. M., 1974, "Techniques for collection of representative aerosol samples," J. Aerosol Sci., **5**, pp. 325-338.

[15] Pena, J. A., Norman, J. M., and Thomson, D. W., 2012, "Isokinetic Sampler for Continuous Airborne Aerosol Measurements," Journal of the Air Pollution Control Association, **27**(4)**,** pp. 337-341.

[16] Thomas, D., Penicot, P., Contal, P., Leclerc, D., and Vendel, J., 2001, "Clogging of fibrous filters by solid aerosol particles Experimental and modelling study," Chemical Engineering Science, **56**, pp. 3549-3561.

[17] Borrous, S., Bouilloux, L., Ouf, F.-X., Appert-Collin, J.-C., Thomas, D., Tampère, L., and Morele, Y., 2014, "Measurement of the Nanoparticles Distribution in Flat and Pleated Filters During Clogging," Aerosol Science and Technology, **48**(4), pp. 392-400.

[18] Hines, W., 1999, *Aerosol Technology*, John Wiley & Sons, Inc., Hoboken, NJ, Chap. 10.

[19] Sparrow, E. M., Abraham, J. P., and Minkowycz, W. J., 2009, "Flow separation in a diverging conical duct: Effect of Reynolds number and divergence angle," International Journal of Heat and Mass Transfer, **52**, pp. 3079-3083.

[20] Environmental Protection Agency (EPA), 1994, "Sample and Velocity Traverses for Stationary Sources," EPA Method 1.

[21] Environmental Protection Agency (EPA), 1996, "Determination of Particulate Matter Emissions From Stationary Sources," EPA Method 5.

[22] Environmental Protection Agency (EPA), 1987, "Determination of Moisture Content in Stack Gases," EPA Method 4.

[23] American Society for Testing and Materials (ASTM), 2006, "Standard Practice for Controlling and Characterizing Errors in Weighing Collected Aerosols," ASTM D6552-06.

[24] International Organization for Standardization (ISO), 1993, "Guide to the Expression of Uncertainty in Measurement".

[25] American Society for Testing and Materials (ASTM), 2011, "Standard Practice for Maintaining Constant Relative Humidity by Means of Aqueous Glycerin Solutions," ASTM D5032-11.

[26] Vlasenko, A., Sjögren, S., Weingartner, E., Gäggeler, H. W., and Ammann, M., 2011, "Generation of Submicron Arizona Test Dust Aerosol: Chemical and Hygroscopic Properties," Aerosol Science and Technology, **39**(5), pp. 452-460.

[27] Kim, S. C., Wang, J., Shin, W. G., Scheckman, J., and Pui, D. Y. H., 2009, "Structural Properties and Filter Loading Characteristics of Soot Agglomerates," Aerosol Science and Technology, **43**(10), pp. 1033-1041.

[28] TSI Incorporated, 2004, "Model 3321 Aerodynamic Particle Sizer® Spectrometer." http://www.tsi.com/uploadedFiles/Product_Information/Literature/Spec_Sheets/3321.pdf

[29] Pilat, M. J. and Steig, T. W., 1983, "Size Distribution of Particulate Emissions From a Pressurized Fluidized Bed Coal Combustion Facility," University of Washington, Seattle, WA.

[30] Pilat, M. J., 1998, "Operations Manual Pilat (University of Washington) Mark 3 and Mark 5 Source Test Cascade Impactor," University of Washington, Seattle, WA.

[31] Lee, J.-K., Kim, S.-C., and Liu, B. Y. H., 2010, "Effect of Bi-Modal Aerosol Mass Loading on the Pressure Drop for Gas Cleaning Industrial Filters," Aerosol Science and Technology, **35**(4), pp. 805-814.

[32] Fairweather, M. Jones, W. P., and Lindstadt, R. P., 1992, "Predictions of Radiative Transfer from a Turbulent Reacting Jet in a Cross-Wind," Combustion and Flame, **89**(1), pp. 45-63.

[33] Woolderlink, M. H. F., 2014, "Soot Formation in Ultra-rich Turbulent Combustion of Natural Gas at Elevated Pressure," Ph.D. thesis, University of Twente.

[34] Akridis, P. and Rigopoulos, S., 2015, "Modelling of soot formation in a laminar coflow non-premixed flame with a detailed CFD-Population Balance model," Procedia Engineering, **102**, pp. 1274-1283.

[35] DeCarlo, P. F., Slowik, J. G., Worsnop, D. R., Davidovits, P., and Jimenez, J. L., 2004, "Particle Morphology and Density Characterization by Combined Mobility and Aerodynamic Diameter Measurements. Part 1: Theory," Aerosol Science and Technology, **38**(12), pp. 1185-1205.

[36] Schneider, C. A., Rasband, W. S., and Eliceiri, K. W., 2012, "NIH Image to ImageJ: 25 years of image analysis," Nat. Meth., **9**(7), pp. 671-675.

[37] American Society for Testing and Materials (ASTM), 2005, “Standard Practice for Characterization of Particles,” ASTM F1877-05.

APPENDIX A

ISOKINETIC SAMPLER ASSEMBLY AND TEST STAND DRAWINGS

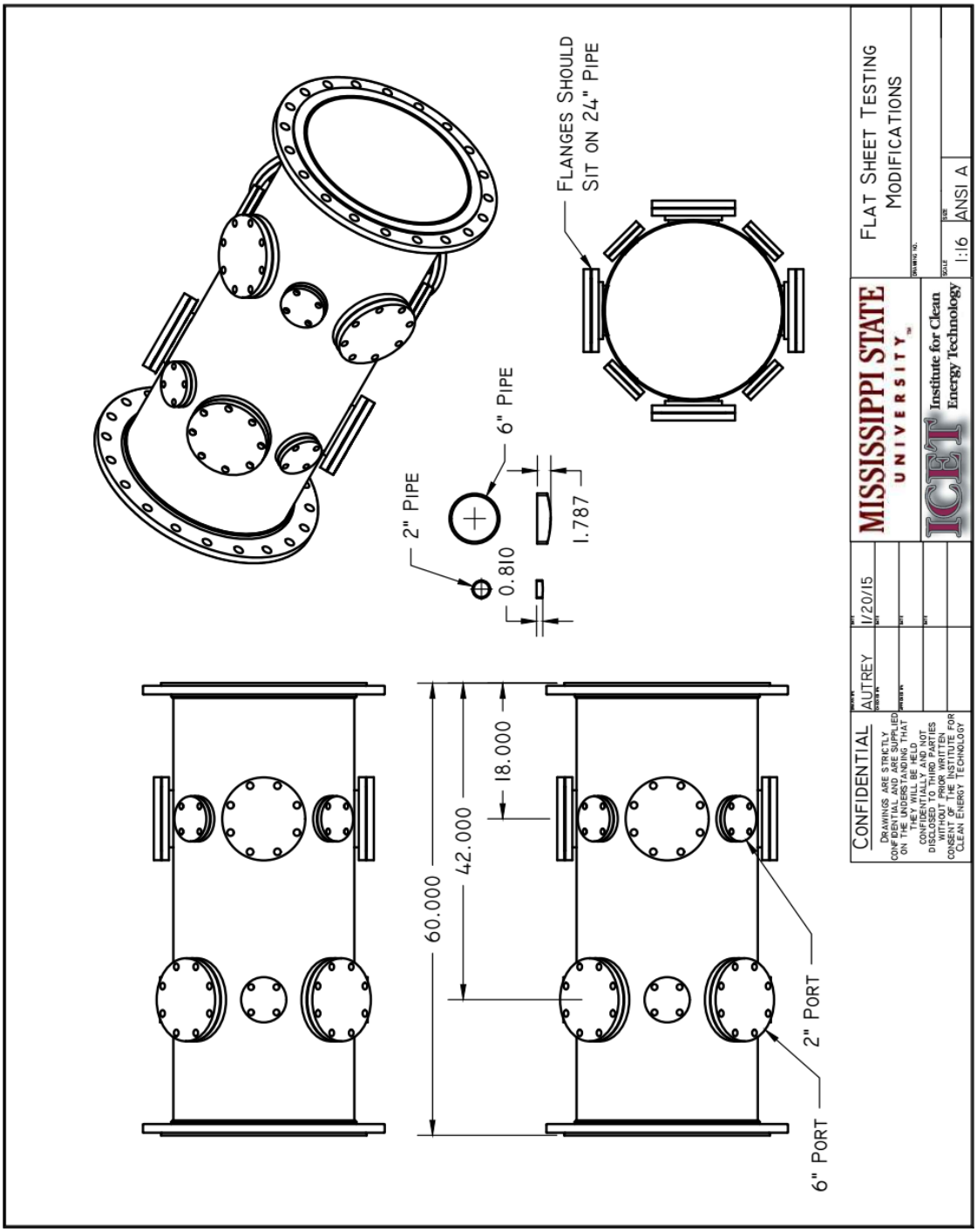

Figure A.1 CAD Drawing of the modified test duct section for the isokinetic samplers.

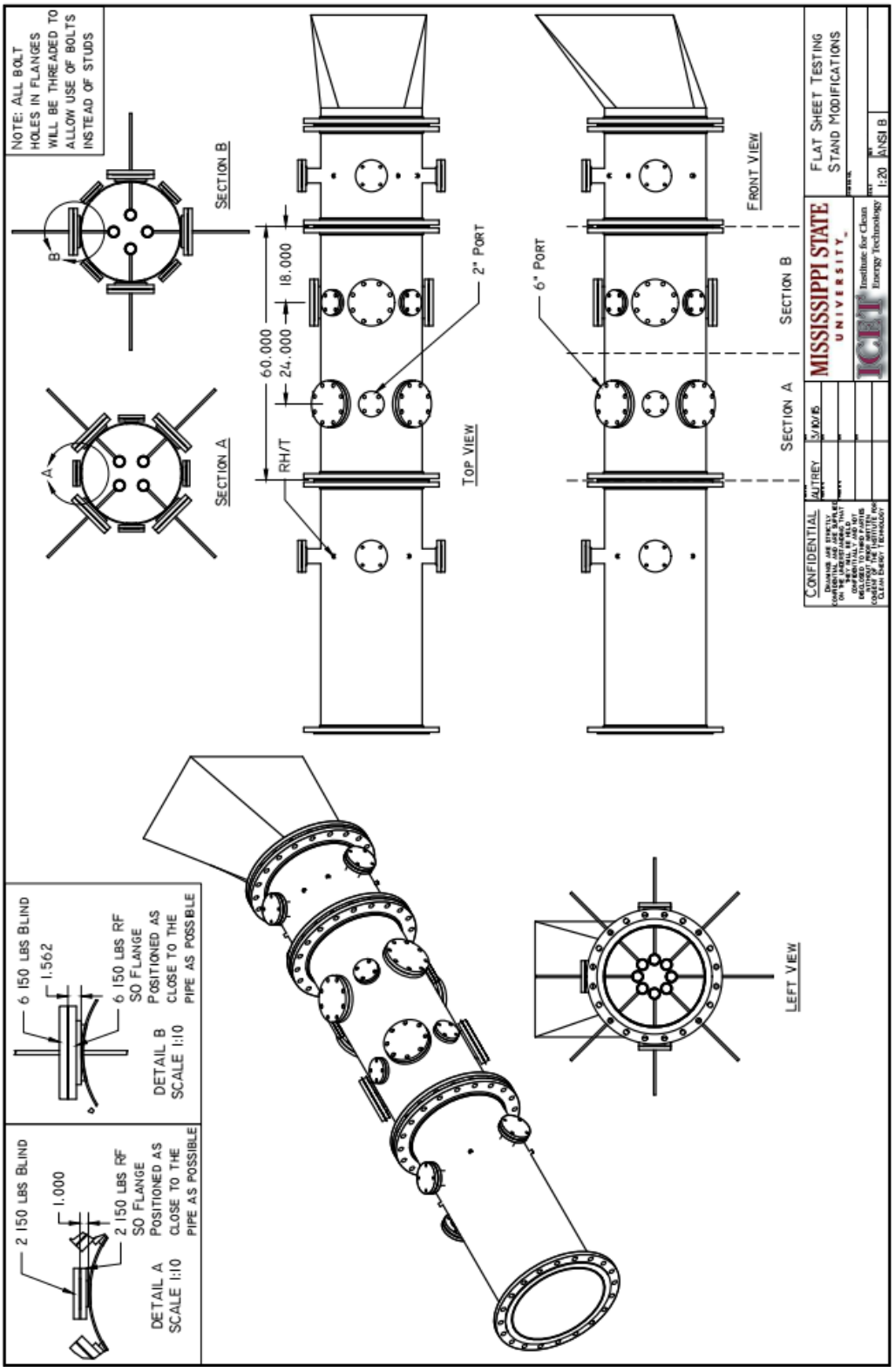

Figure A.2 CAD drawing of modified test duct section with isokinetic samplers installed.

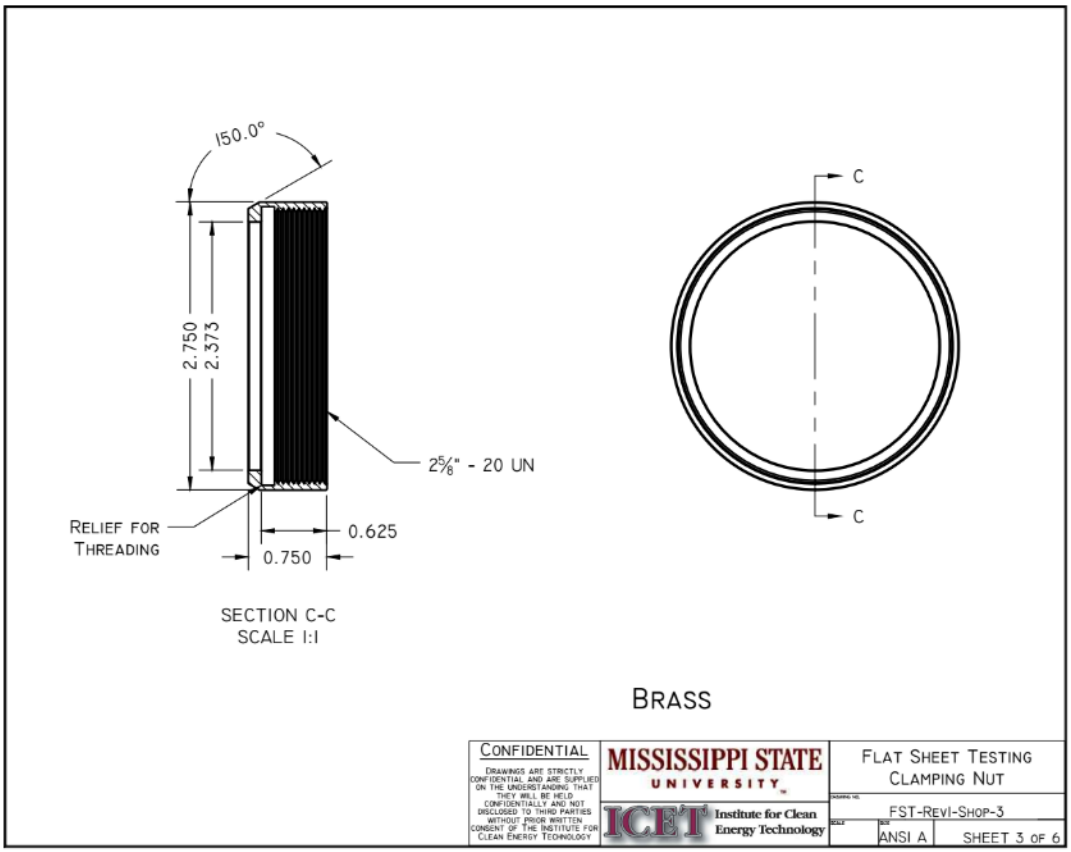

Figure A.3 CAD drawing of the knurled brass retaining collar.

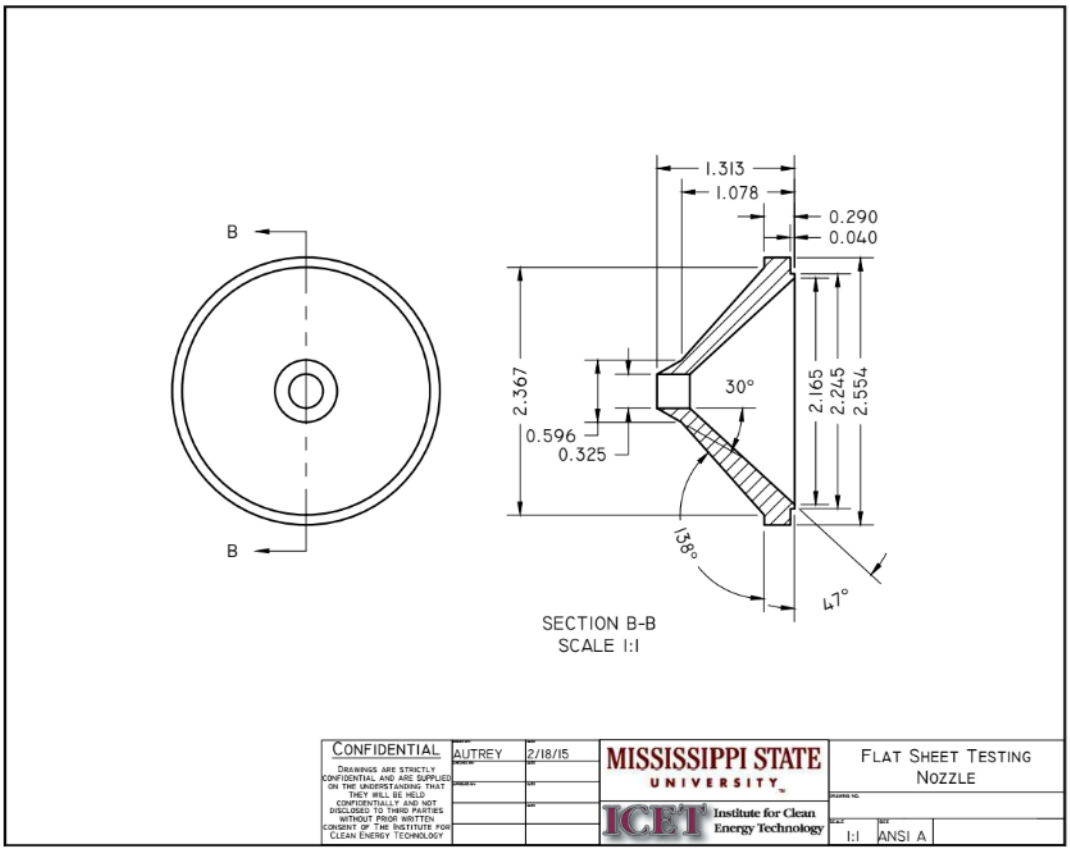

Figure A.4 CAD drawing of the isokinetic sampling nozzle.

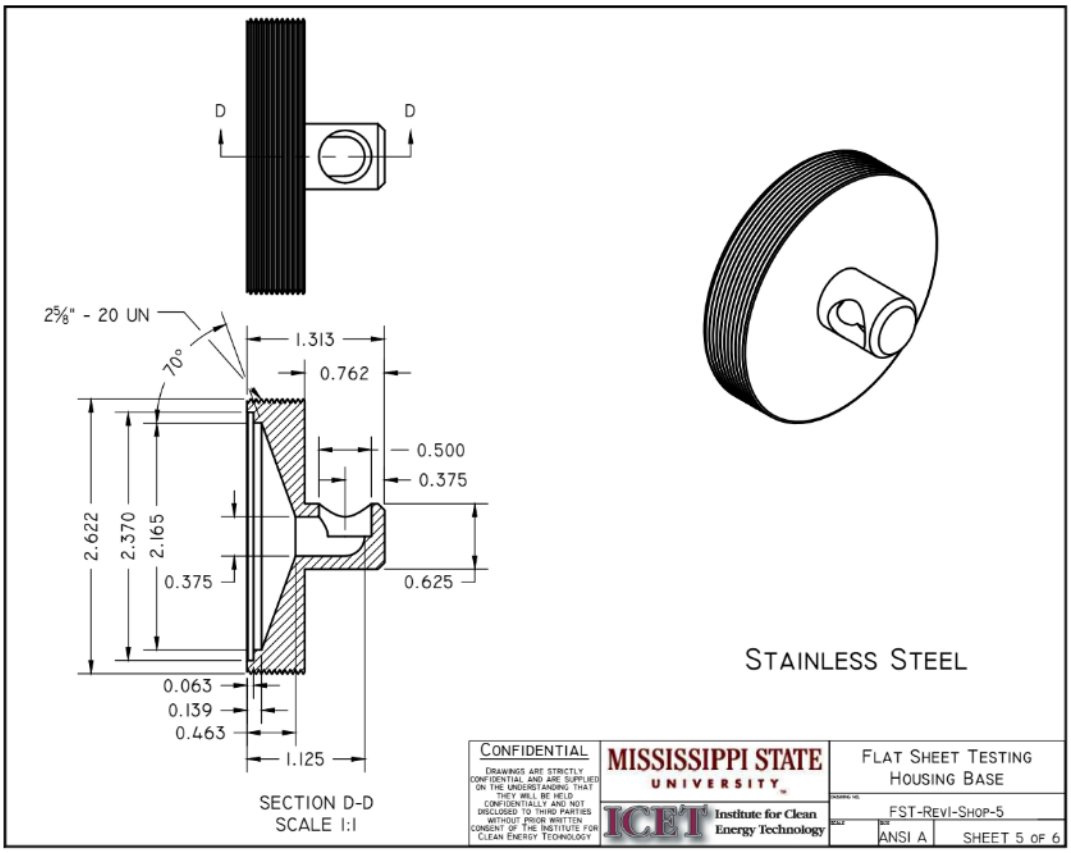

Figure A.5 CAD drawing of the isokinetic sampler base.

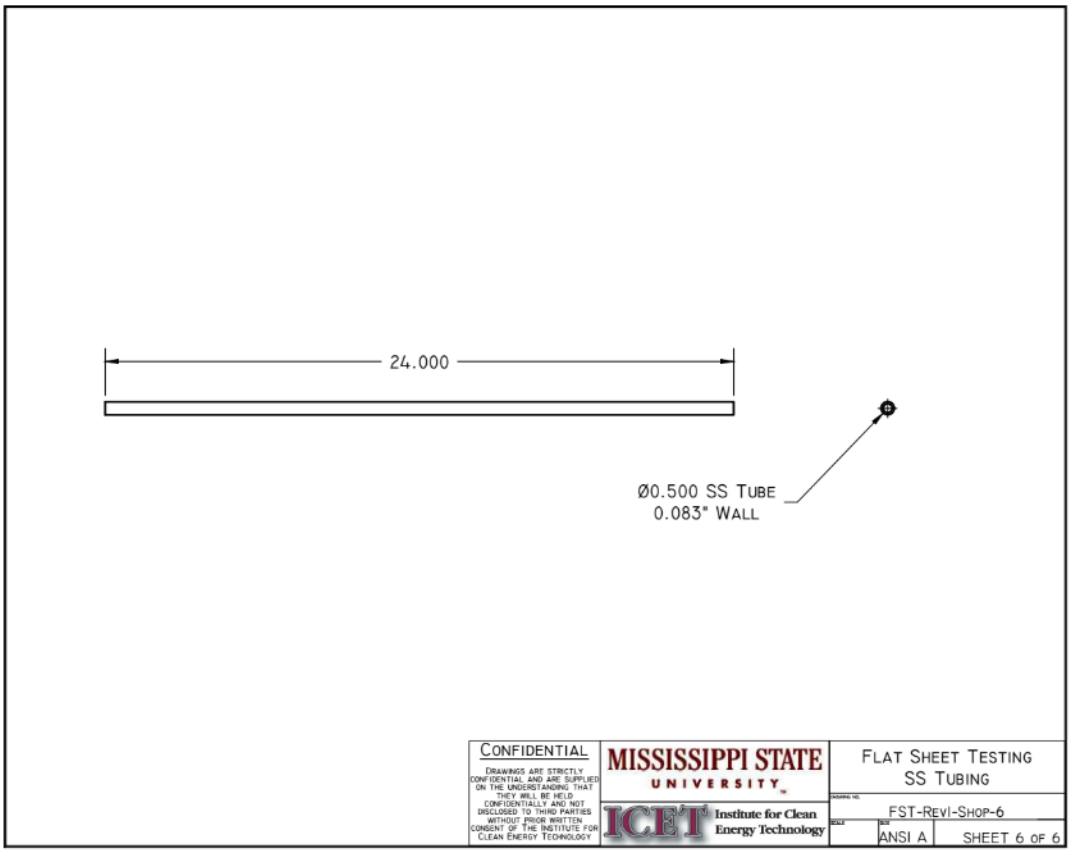

Figure A.6 CAD drawing of the stainless steel isokinetic sampler sampling stem.

Once the isokinetic sampler was assembled, the stainless-steel sampling stems were cut to sufficient length to prevent obstruction during testing.

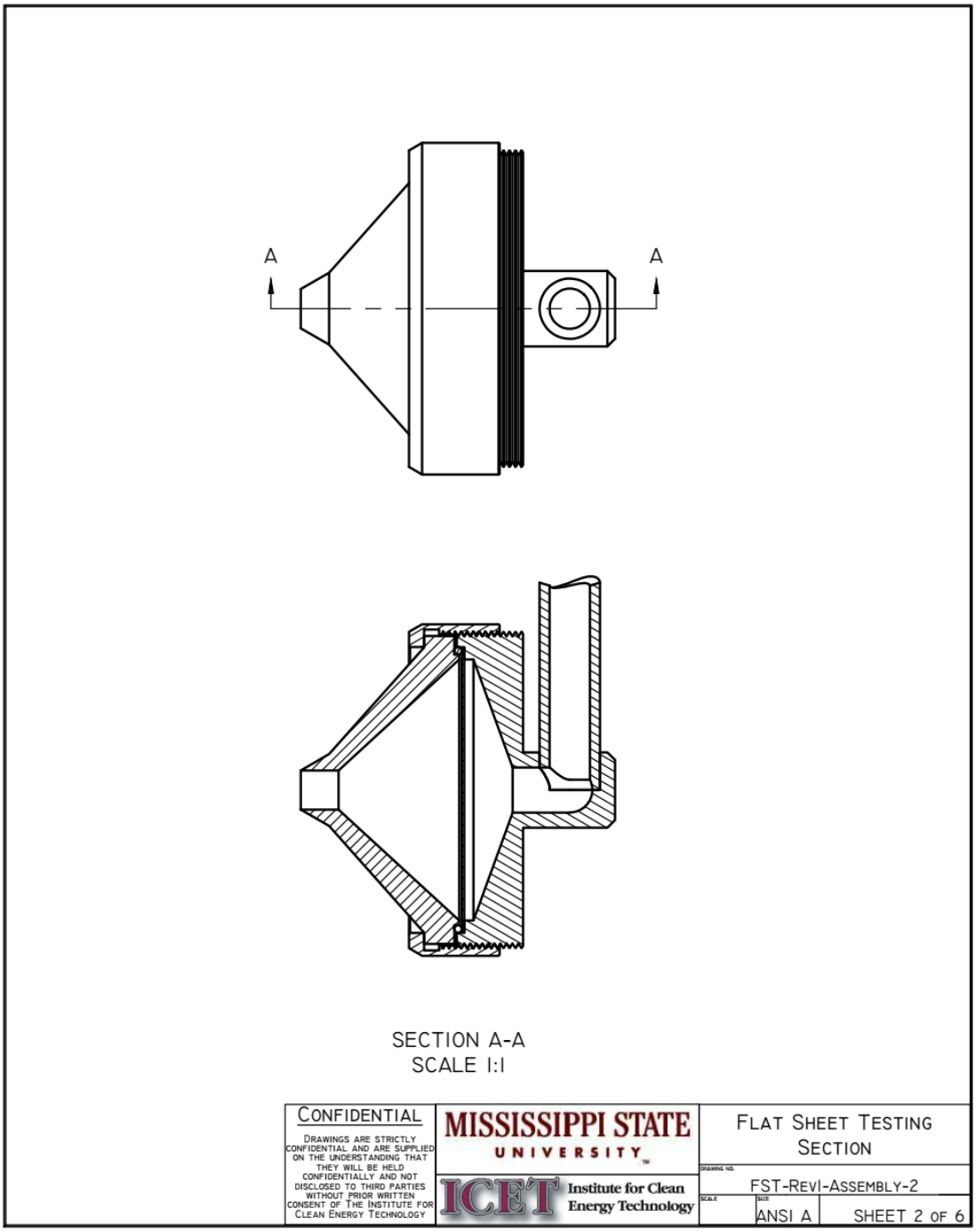

Figure A.7 CAD drawing of the isokinetic sampler assembly.

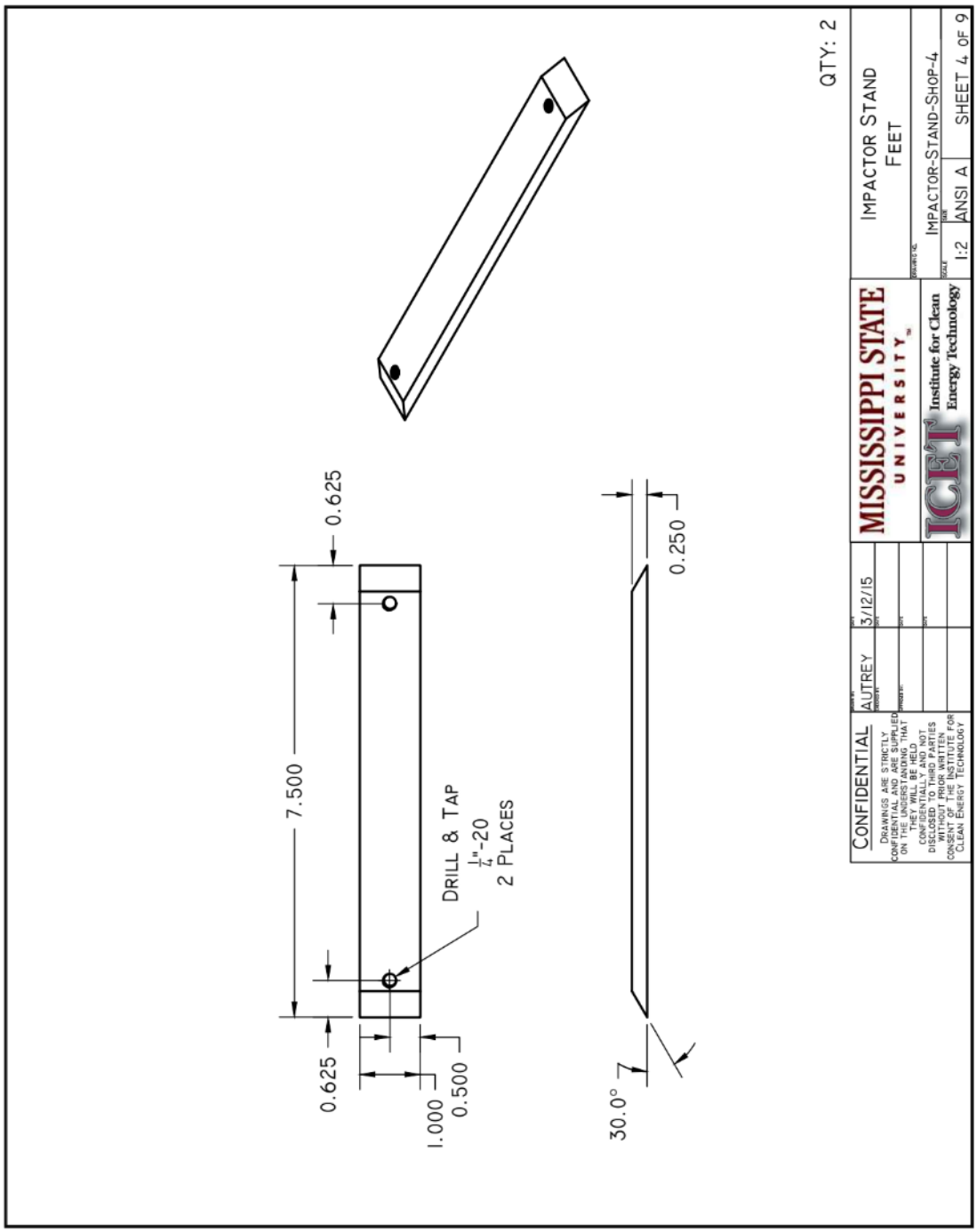

Figure A.8 CAD drawing of the Pilat impactor stand duct mounts.

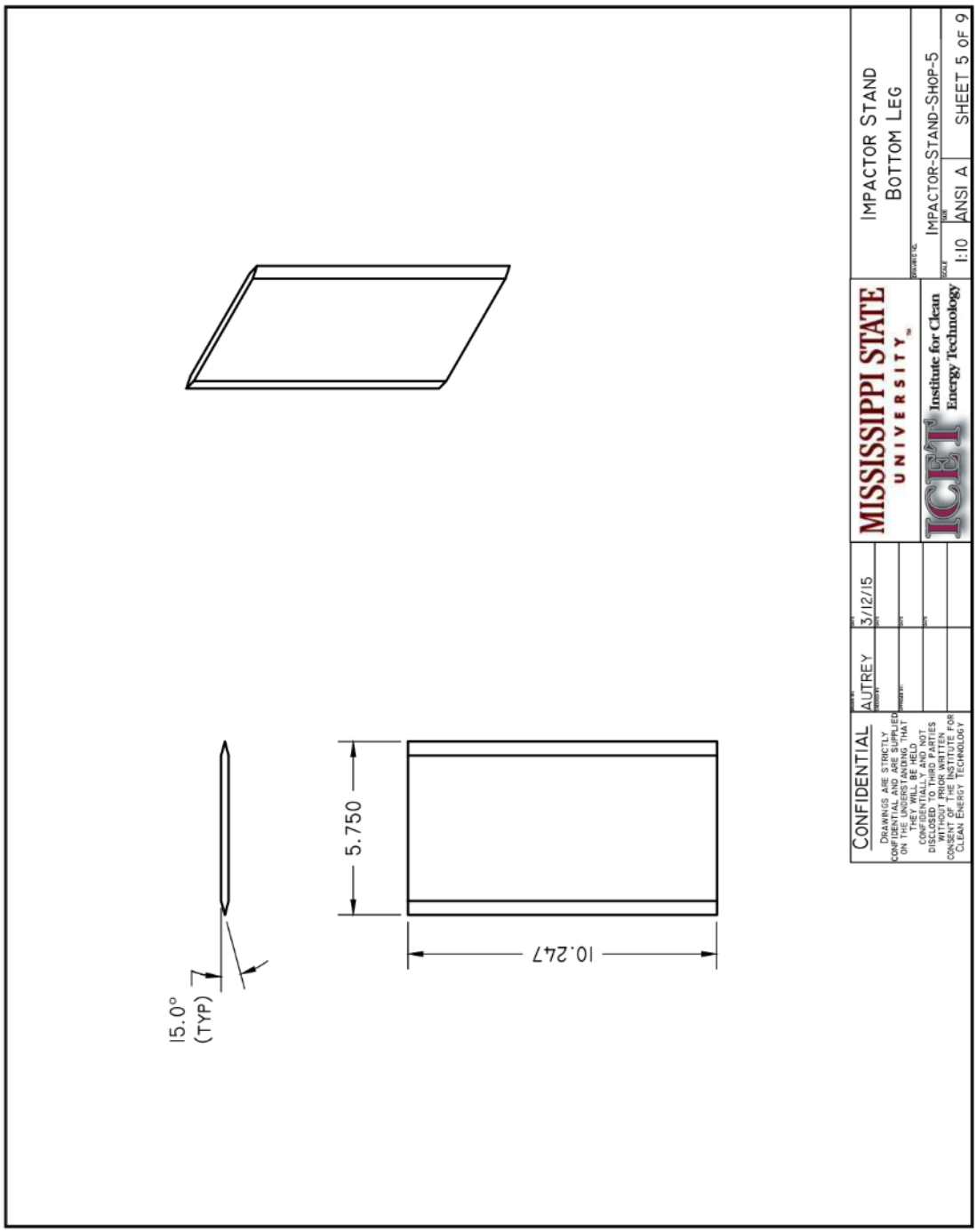

Figure A.9 CAD drawing of the vertical Pilat impactor stand legs.

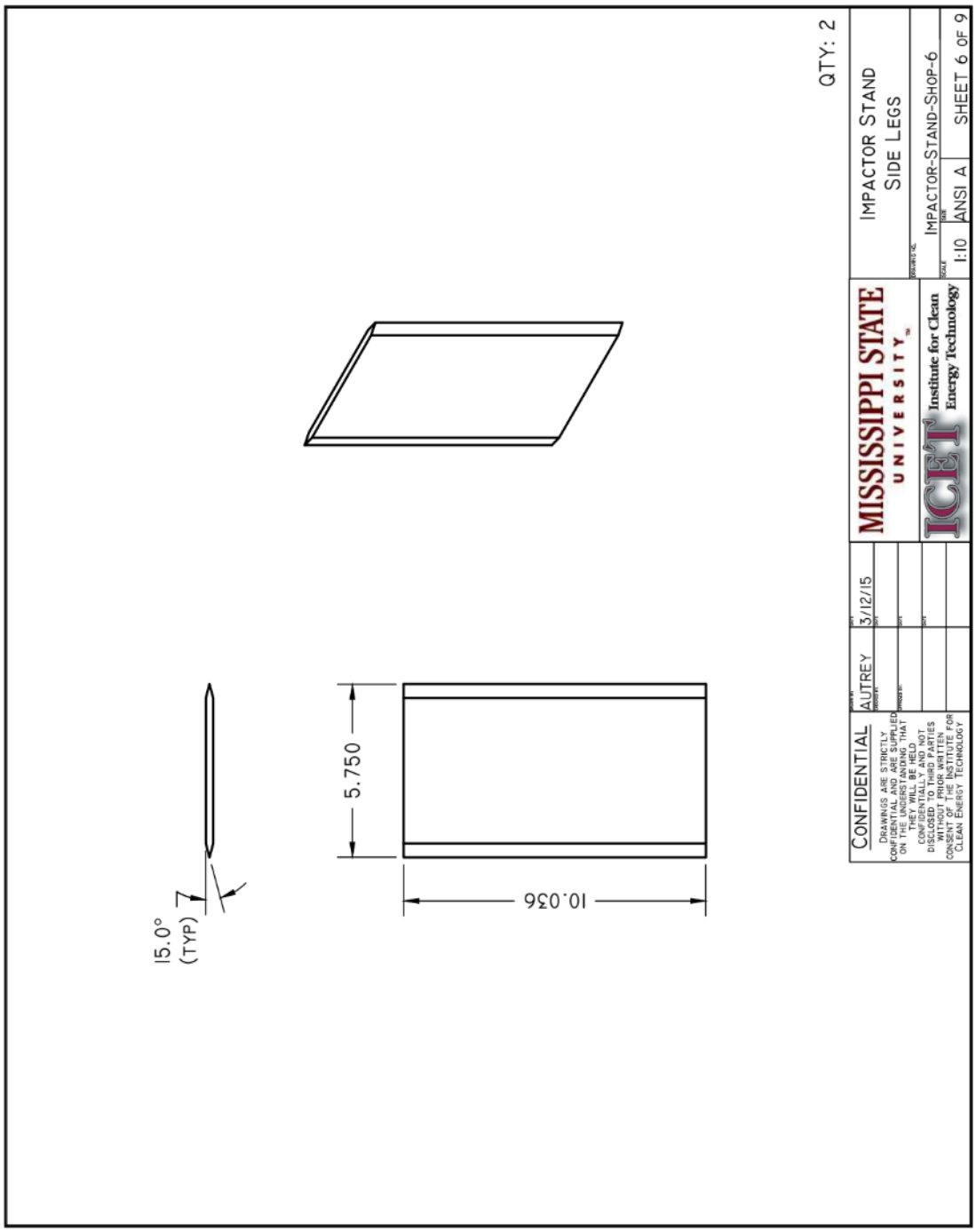

Figure A.10 CAD drawing of the horizontal Pilat impactor stand legs.

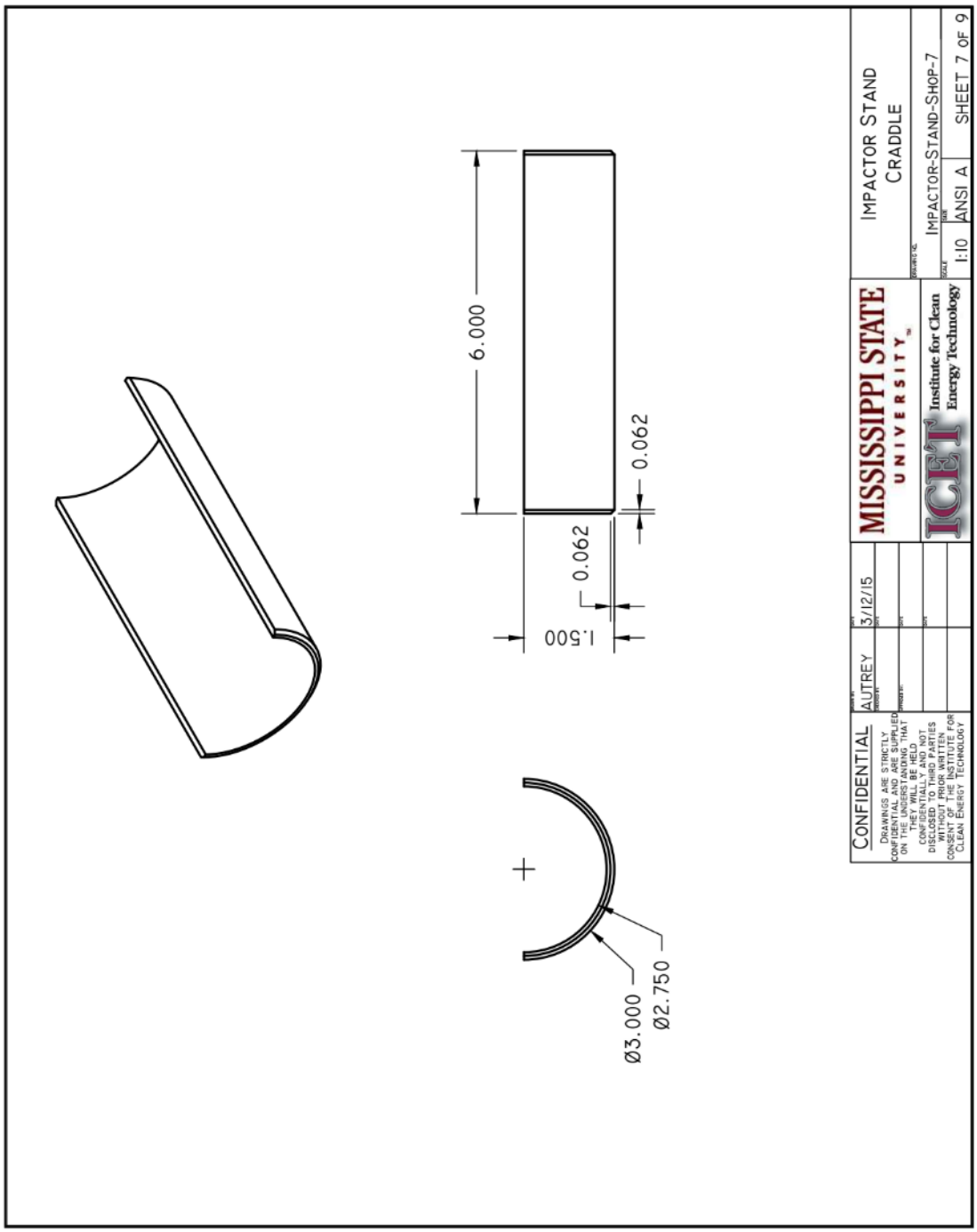

Figure A.11 CAD drawing of the Pilat impactor retaining cradle.

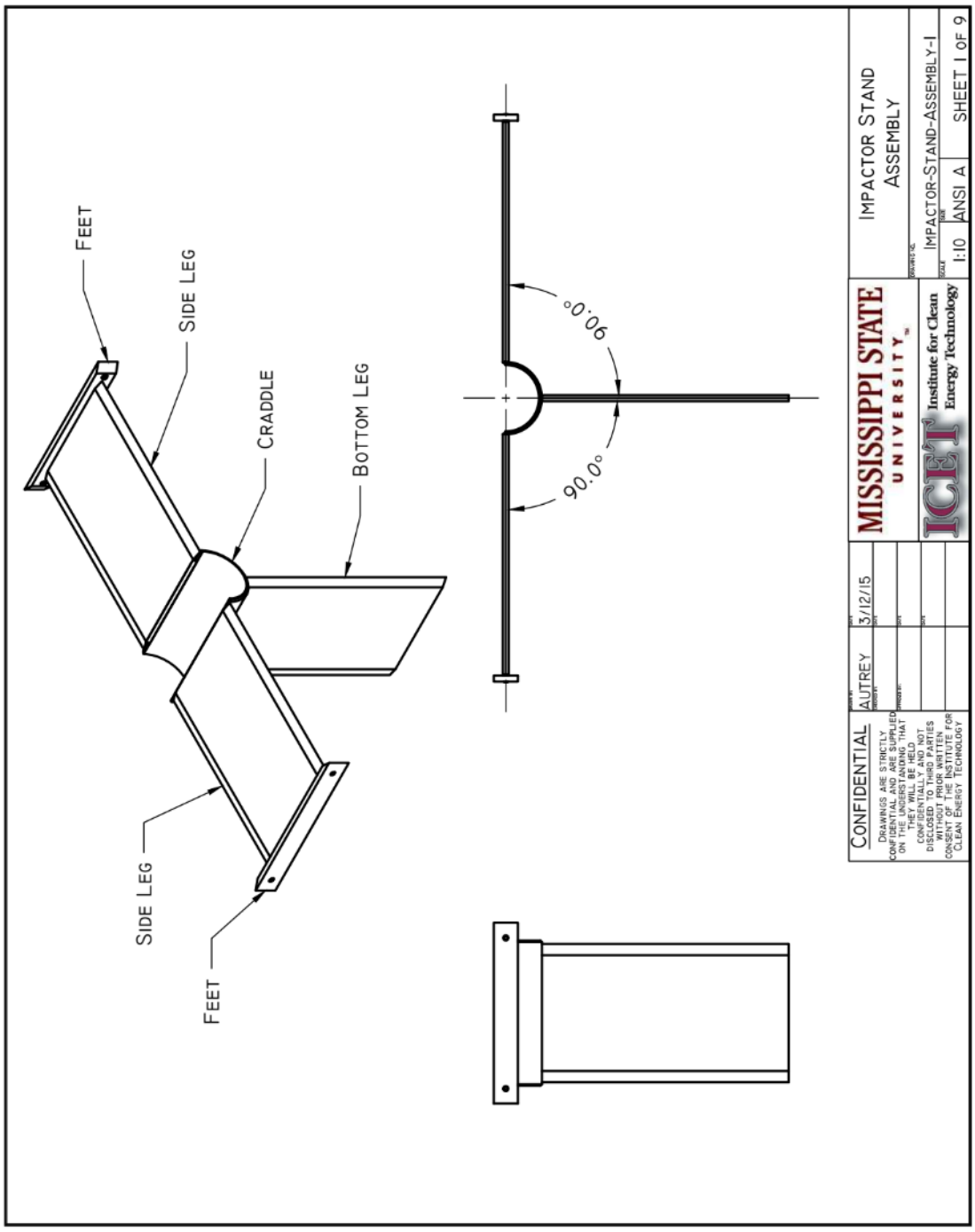

Figure A.12 CAD drawing of the Pilat impactor stand assembly.

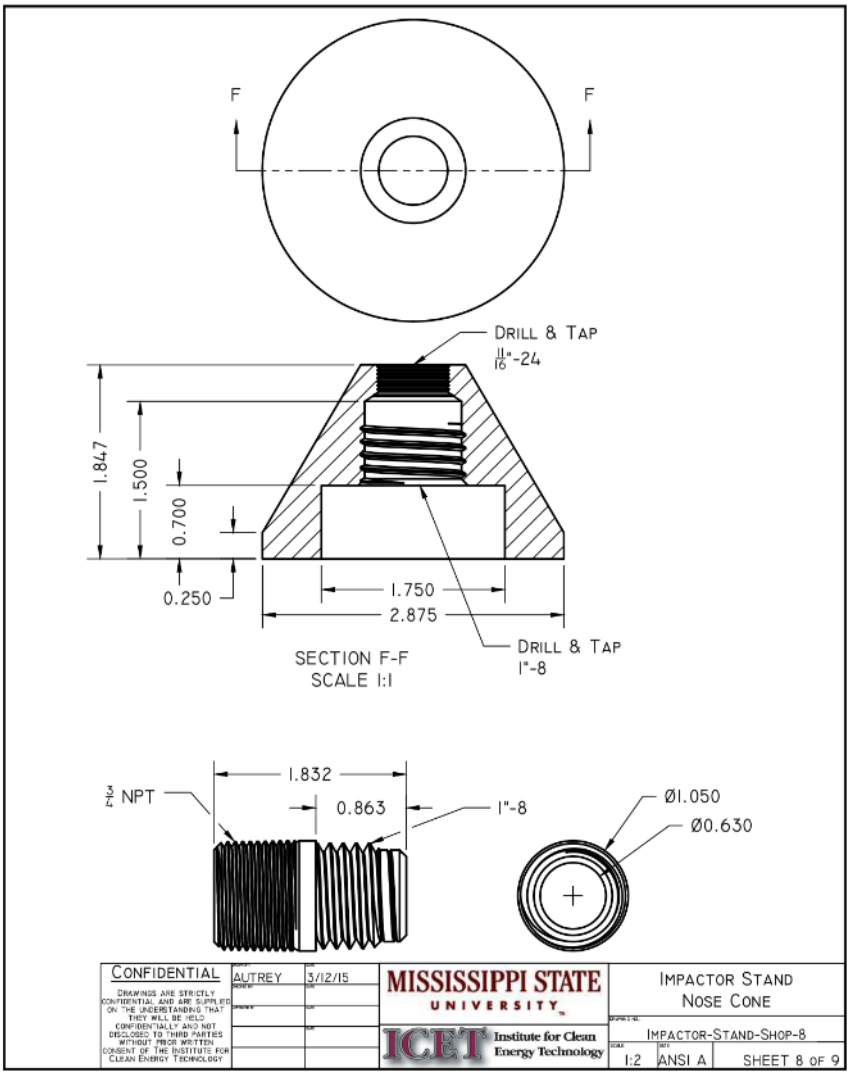

Figure A.13 CAD drawing of the Pilat impactor nose cone.

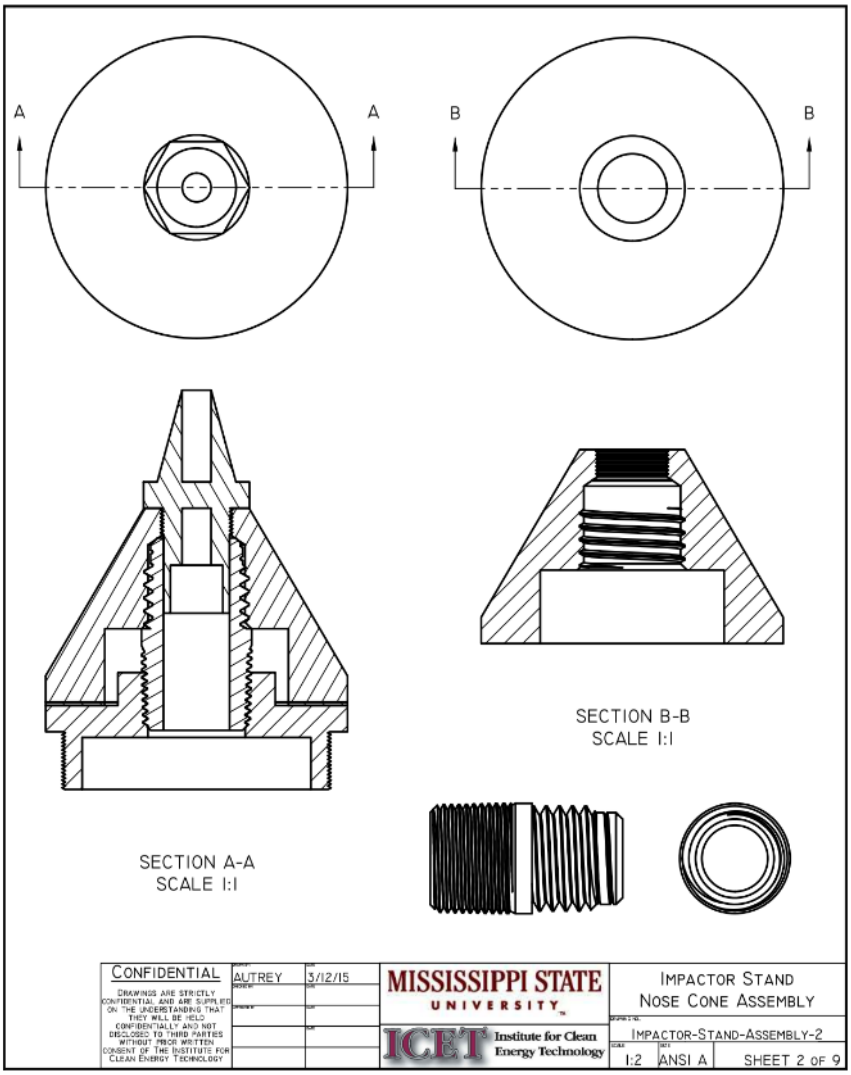

Figure A.14 CAD drawing of the Pilat impactor nose cone assembly.

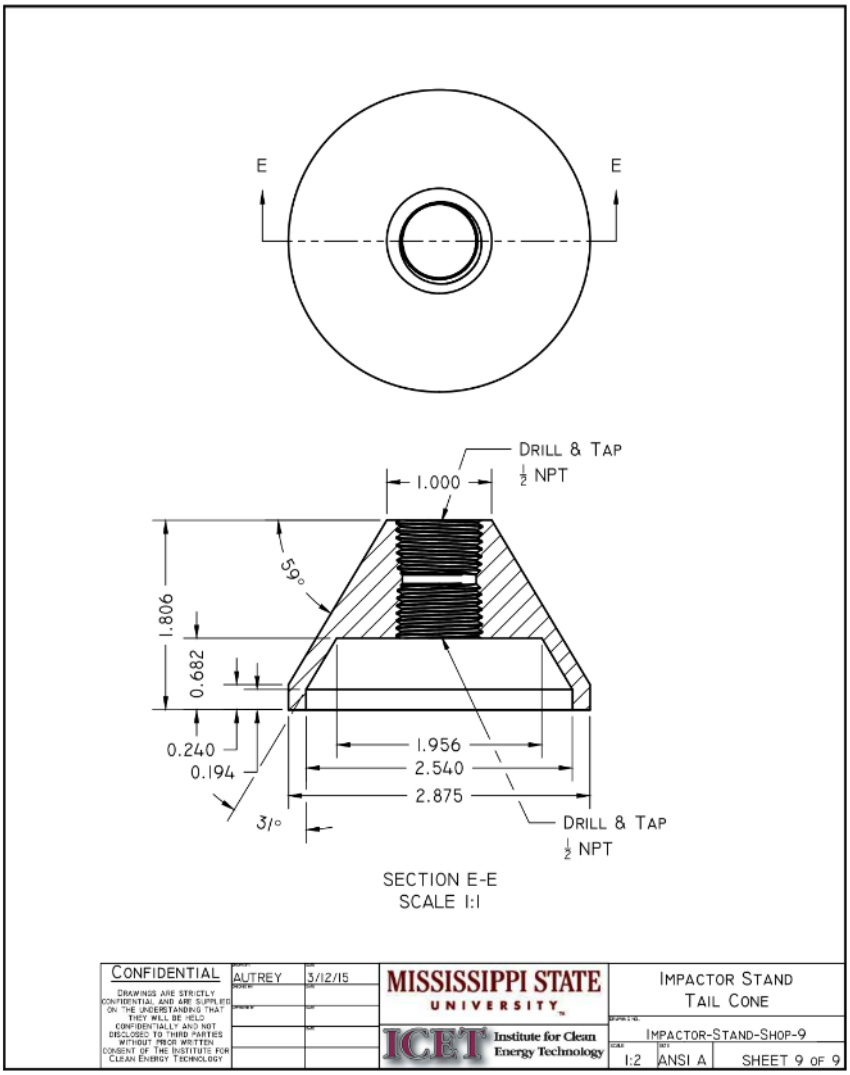

Figure A.15 CAD drawing of the Pilat impactor tail cone.

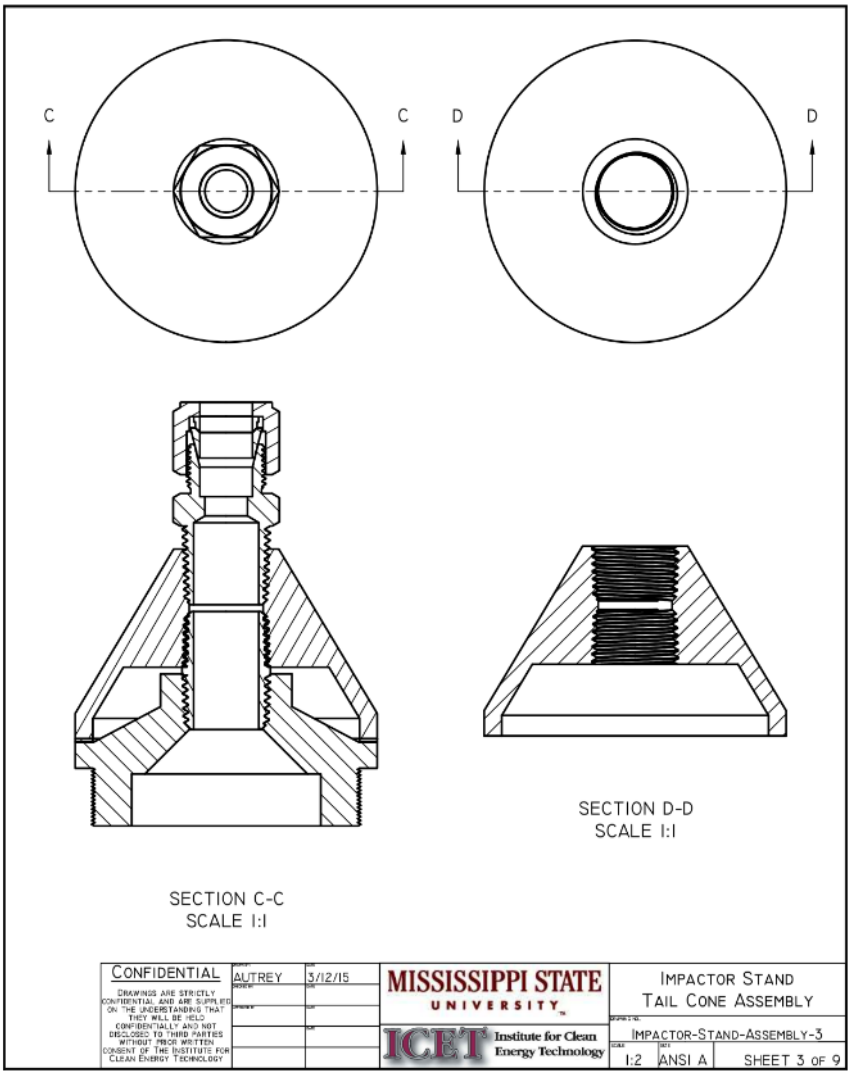

Figure A.16 CAD drawing of the Pilat impactor tail cone assembly.

APPENDIX B

MSU ICET HEPA-029 GRAVIMETRIC ANALYSIS PROCEDURE

Gravimetric Analysis of Test Stand Samples Procedure

Revision:
Effective Date is immediate upon signature approval

Prepared By: _____ 3/21/16 **Date**

Reviewed By: _____ 3/21/16 **Date**

APPROVAL: _____ 3/21/16 **Date**

REVISION HISTORY

Revision Number	Reason for Revision	Revision By
0	Initial Issue	CBR / SRP

1.0 PURPOSE

The purpose of this procedure is to provide a method for operation of the semi-micro balance used for analysis of test stand samples. These guidelines are meant to ensure quality of data and uniformity of techniques among analysts, while reducing errors and uncertainty associated with differences in sample pretreatment.

2.0 SCOPE

This procedure applies to the operation of the analytical balances used for gravimetric analysis of test stand samples. In order to reduce the errors associated with gravimetric analysis of collected aerosol samples, set procedures are devised to eliminate uncertainty due to measurable weight changes (i.e., from uncontrolled environmental effects through slow evaporation or moisture uptake) or forces which act on the weighing pan and weighing sample (i.e., from magnetism or electrostatics) which are interpreted by the balance as weight changes.

3.0 TERMS / DEFINITIONS

3.1 Semi-micro Balance- a five-digit balance whose readability includes up to 0.00001 g.

3.2 Substrate – A material that is used to collect aerosol samples for various types of testing techniques (i.e., ELPI substrates are the aluminum coupon with grease solution, Pilat susbtrates are the stainless steel prepared coupon with grease solution, Flat sheet substrates are the filter coupons for sampling).

3.3 Blank sampling media - substrates which are exposed to the same treatment and conditions as are active sampling media. Blanks are matched to each sample type.

3.4 Active sampling media - substrates which are used for sampling

3.5 Forceps – tweezers used to handle samples and place them on the balance pan.

3.6 Initial weighing effect – the effect produced by obtaining a measurement from a balance that has not been active for more than 0.5 hour. This effect may cause measurement drift and can cause errors in accuracy.

3.7 RH – relative humidity, the ratio of the water vapor density (mass per unit volume) to the saturation water vapor density, expressed in percent.

3.8 Equilibration time - time constant characterizing the approximate exponentially damped approach of the mass of an aerosol collection medium to a constant value. This time is determined to be 24 hours.

3.9 Conditioning chamber - air tight chamber which is kept at a set humidity using an aqueous glycerol solution.

3.10 Desiccator – air tight chamber which is kept at a set humidity using a desiccant.

3.11 Air buoyancy – a correction used which takes into account a supporting buoyant force on equal to the product of the mass of air it displaces and the acceleration due to gravity

3.12 Conditioning time - time required for samples to be exposed in the conditioning chamber, 24 hours.

3.13 Preconditioning time - time required for samples to be exposed to desiccating chamber. Determined to be 24 hours.

4.0 RESPONSIBILITIES

Staff with responsibilities in implementing this procedure are:

4.1 Testing Personnel

5.0 EQUIPMENT

5.1 Precalibrated semi-microbalance.

5.2 Stop watch or other timing device to observe measurement time.

5.3 Gloves and forceps to handle and transfer samples.

5.4 Hygrometer and thermometer for air density calculation, to correct for buoyancy.

5.5 Barometer for air density calculation.

5.6 Conditioning chamber with glycerol solution.

5.7 Preconditioning chamber with desiccant.

5.8 Calibrated reference weight set.

5.9 Metal spatula.

5.10 Deionized water.

5.11 Timer with second hand or stop watch to report 20 second measurement time.

6.0 SAFETY AND ENVIRONMENTAL CONCERNS

6.1 Nitrile gloves are required in the laboratory when performing gravimetric analyses and transporting samples to the laboratory.

7.0 PREREQUISITES

7.1 All personnel operating the analytical balance must be trained in accordance with ICET-QA-001.

7.2 Ensure that for each sample batch, one blank per substrate type is submitted to identical treatment (except for testing).

8.0 PROCEDURE

The Testing Personnel shall conduct the following steps:

8.1 Perform Sample Pretreatment:

8.1.1 Preconditioning of Samples

8.1.1.1 Print Attachment 1, Sample Pretreatment for Gravimetric Analysis.

8.1.1.2 Record the Run ID, Test Stand ID, Testing Dates, and whether the analysis is pre or post testing.

8.1.1.3 Record the relative humidity and temperature of the desiccator, along with time, date, serial number and calibration due date for the hygrometer.

8.1.1.4 Place all samples into the chamber for 24 hours for preconditioning.

8.1.2 Conditioning of Samples

8.1.2.1 Record the humidity and temperature of the desiccator, along with the date, time, serial number and calibration due date for the hygrometer before sample removal in Attachment 1.

8.1.2.2 Record the relative humidity and temperature of the conditioning chamber, along with the time, date, serial number and calibration due date for the hygrometer in Attachment 1.

8.1.2.3 Record the set weight of Glycerol Solution 1. The set weight is labeled on the crystallizing dish.

8.1.2.4 Remove the glycerol solution from the chamber and carefully place it on the prezeroed scale. Take care not to spill any of the contents. Record the weight of the solution in Attachment 1.

8.1.2.5 For a solution weight that differs from the labeled weight, retrieve a small quantity of deionized water in a clean beaker.

8.1.2.6 Add water to the glycerol solution dropwise and stir the solution gently using a metal spatula. Add water until the displayed weight after stirring matches the labeled weight.

8.1.2.7 Record the weight of the solution after addition in Attachment 1.

8.1.2.8 Replace Glycerol Solution 1 into the conditioning chamber, taking care not to spill.

8.1.2.9 Place all samples to be weighed into the conditioning chamber to condition for 24 hours.

8.1.2.10 Before sample removal, record the relative humidity and temperature of the conditioning chamber. Also record the date, time, serial number and calibration due date of the hygrometer.

8.1.3 Equilibration of Samples

8.1.3.1 Record the relative humidity and temperature of the glove box, along with the time, date, serial number and calibration due date for the hygrometer in Attachment 1.

8.1.3.2 Record the set weight of Glycerol Solution 2, as labeled on the crystallizing dish.

8.1.3.3 Remove Glycerol Solution 2 from the glove box and carefully place it on the prezeroed scale. Take care not to spill any of the contents. Record the weight of the solution in Attachment 1.

8.1.3.4 For a solution weight that differs from the labeled weight, retrieve a small quantity of deionized water in a clean beaker.

8.1.3.5 Add water to the glycerol solution dropwise and stir the solution gently using a metal spatula. Add water until the displayed weight after stirring matches the labeled weight.

8.1.3.6 Record the weight of the solution after addition in Attachment 1.

8.1.3.7 Replace the solution into the glove box, taking care not to spill.

8.1.3.8 Place samples in the glove box. Samples should be allowed to equilibrate by setting them inside the glove box for 30 minutes prior to weighing. Once the samples have been placed in the glove box, they must be weighed within 80 hours of placement. Samples should be placed in the glove box with their lids ajar, open to the atmosphere, for equilibration.

8.2 Perform Gravimetric Determinations:

8.2.1 Print Attachment 2A, 2B, or 2C, according to the substrate type (Pilat, ELPI, or flat sheet filter) being analyzed.

8.2.1.1 Record the test control number, testing ID and date in the upper left hand corner of the data sheet attachment. Also record whether the samples have been exposed to testing or not.

8.2.2 Conduct an Operator Precision Test

8.2.2.1 Record the date, time, operator name, Balance model, serial number, and calibration date, as well as calibration due date.

8.2.2.2 Retrieve the reference mass set and record calibration information in the data sheet.

8.2.2.3 Consult the data sheet to identify the proper reference mass to be used for the substrate type being analyzed.

8.2.2.4 Perform six successive measurements of the reference mass. Take care to ensure that the balance is properly zeroed between weighings and that the balance has stabilized before recording the readings. Place the mass carefully in the center of the balance pan and close the draft door. Allow the instability indicator to disappear (a cube in the top left hand of the display) and begin the timer. Record the result only after the instability indicator does not appear for 20 seconds.

8.2.2.5 Record the measurement results in the data sheet.

8.2.2.6 Determine the standard deviation for the set of the last five measurements and record it in the worksheet.

8.2.3 Indicate whether the standard deviation was below 0.1 with a Y or N in the data sheet.

8.2.4 When the standard deviation is above 0.1, the operator shall perform the precision test again with improved technique.

8.2.5 Record the barometric pressure using the barometer located at the entrance to the High Bay.

8.2.6 Record the relative humidity and temperature in the glove box and record the time and date.

8.2.7 Weigh each sample in the order presented in the worksheet.

8.2.7.1 Zero the balance.
8.2.7.2 Open the draft protection door and use the tweezers to wave the sample twice at a ½ inch distance from the StaticMaster Alpha Ionizer.
8.2.7.3 Place sample on the center of the balance pan.
8.2.7.4 Close the draft protection door.
8.2.7.5 Record the result only after the stabilization indicator does not appear for 20 seconds.
8.2.7.6 Repeat 8.2.7.1 – 8.2.7.5 twice, for a total of three measurements per sample.

8.2.8 Sign and date each data sheet, and have another person sign and date after review.

8.2.9 Place the data sheets with the test control document.

9.0 RECORDS

All records are considered quality records and shall be maintained and submitted to project records in accordance with ICET-QA-010, *Quality Assurance Records*.
The records for this procedure include the following:

9.1 Attachment 1 Sample Pretreatment Data Sheet
9.2 Attachment 2A Gravimetric Analysis of Pilat Samples
9.3 Attachment 2B Gravimetric Analysis of ELPI Samples
9.4 Attachment 2C Gravimetric Analysis of Flat Sheet Filter Samples

10.0 REFERENCES

10.1 Project Specific Test Plan
10.2 ASTM D6552 -06(2011) Standard Practice for Controlling and Characterizing Errors in Weighing Collected Aerosols
10.3 ISO GUM Guide to the Expression of Uncertainty in Measurement (1993)

10.4 ASTM D5032 -11 Standard Practice for Maintaining Constant Relative Humidity by Means of Aqueous Glycerin Solutions

Test Stand Designation: _____
Run ID: _____
Testing Dates: _____

Date: _____ **Time:** _____am/pm

Initial

1. Record Desiccator Conditions (Sample Preconditioning) ☐_____
   a. Relative Humidity _____
   b. Temperature _____
   c. Date _____
   d. Time _____
   e. Hygrometer Serial Number _____
   f. Hygrometer Calibration Due Date _____

2. Place Samples into Desiccator ☐_____
   Time _____
3. Precondition for 24 hours ☐_____

4. Record Desiccator Conditions (Sample Removal) ☐_____
   a. Relative Humidity _____
   b. Temperature _____
   c. Date _____
   d. Time _____
   e. Hygrometer Serial Number _____
   f. Hygrometer Calibration Due Date _____

5. Record Conditioning Chamber Conditions ☐_____
   a. Relative Humidity _____
   b. Temperature _____
   c. Date _____
   d. Time _____
   e. Hygrometer Serial Number _____
   f. Hygrometer Calibration Due Date _____

6. Replenish Glycerol Solution 1 ☐_____
   a. Record glycerol set weight _____
   b. Record glycerol actual weight _____
   c. Add water until set weight

Signature _____ Date _____ 20__
Signature _____ Date _____ 20__

d. Record new glycerol weight _____

7. Place samples into Conditioning Chamber ☐ _____
   Time _____
8. Condition for 24 hours ☐ _____
9. Record Conditioning Chamber Conditions (Sample Removal) ☐ _____
   a. Relative Humidity _____
   b. Temperature _____
   c. Date _____
   d. Time _____
   e. Hygrometer Serial Number _____
   f. Hygrometer Calibration Due Date _____
10. Record Conditions in Glove Box ☐ _____
    a. Relative Humidity _____
    b. Temperature _____
    c. Date _____
    d. Time _____
    e. Hygrometer Serial Number _____
    f. Hygrometer Calibration Due Date _____
11. Replenish Glycerol Solution 2 ☐ _____
    a. Record glycerol set weight _____
    b. Record glycerol actual weight _____
    c. Add water until set weight
    d. Record new glycerol weight _____
12. Place samples into glove box to equilibrate for 30 minutes ☐ _____

Signature _____ Date _____ 20__
Signature _____ Date _____ 20__

Operator Precision Test

Date ____________ Time ___________ Operator _________________

Balance Model ___________ Balance Serial Number _________________

Calibration Date ___________ Calibration Due ________________

Reference Mass Type ___1 g_ Reference Mass Set Serial Number _________________

Reference Mass Set Calibration Due _______________

Initial Measurement ___________ Measurement 1 ___________
Measurement 2 ______________ Measurement 3 ___________
Measurement 4 ______________ Measurement 5 ___________
Average __________ Standard Deviation __________ < 0.1 (Y/N) ______

Initial Measurement ___________ Measurement 1 ___________
Measurement 2 ______________ Measurement 3 ___________
Measurement 4 ______________ Measurement 5 ___________
Average __________ Standard Deviation __________ < 0.1 (Y/N) ______

Initial Measurement ___________ Measurement 1 ___________
Measurement 2 ______________ Measurement 3 ___________
Measurement 4 ______________ Measurement 5 ___________
Average __________ Standard Deviation __________ < 0.1 (Y/N) ______

Pilat Samples Analysis

Barometric Pressure _________________ Relative Humidity _________________

Temperature _____________ Date _________________ Time ___________

Pilat Blank B1

Measurement 1 __________ Measurement 2 __________ Measurement 3 __________

Signature ___________________ Date ______ 20__
Signature ___________________ Date ______ 20__

Pilat Stage 1

Measurement 1 _____ Measurement 2 _____ Measurement 3 _____

Pilat Blank B1

Measurement 1 _____ Measurement 2 _____ Measurement 3 _____

Pilat Blank B2

Measurement 1 _____ Measurement 2 _____ Measurement 3 _____

Pilat Stage 2

Measurement 1 _____ Measurement 2 _____ Measurement 3 _____

Pilat Stage 3

Measurement 1 _____ Measurement 2 _____ Measurement 3 _____

Pilat Stage 4

Measurement 1 _____ Measurement 2 _____ Measurement 3 _____

Pilat Stage 5

Measurement 1 _____ Measurement 2 _____ Measurement 3 _____

Pilat Stage 6

Measurement 1 _____ Measurement 2 _____ Measurement 3 _____

Pilat Stage 7

Measurement 1 _____ Measurement 2 _____ Measurement 3 _____

Pilat Stage 8

Measurement 1 _____ Measurement 2 _____ Measurement 3 _____

Pilat Stage 9

Measurement 1 _____ Measurement 2 _____ Measurement 3 _____

Pilat Stage 10

Measurement 1 _____ Measurement 2 _____ Measurement 3 _____

Pilat Stage 11

Measurement 1 _____ Measurement 2 _____ Measurement 3 _____

Signature _____ Date _____ 20__
Signature _____ Date _____ 20__

Pilat Blank B2

Measurement 1 _____ Measurement 2 _____ Measurement 3 _____

Pilat Filter Blank

Measurement 1 _____ Measurement 2 _____ Measurement 3 _____

Pilat Filter

Measurement 1 _____ Measurement 2 _____ Measurement 3 _____

Pilat Filter Blank

Measurement 1 _____ Measurement 2 _____ Measurement 3 _____

Signature _____ Date _____ 20__
Signature _____ Date _____ 20__

Operator Precision Test

Date ____________ Time ___________ Operator _________________

Balance Model ___________ Balance Serial Number _________________

Calibration Date __________ Calibration Due ________________

Reference Mass Type ___20 mg_ Reference Mass Set Serial Number _________________

Reference Mass Set Calibration Due _______________

Initial Measurement __________ Measurement 1 __________
Measurement 2 __________ Measurement 3 __________
Measurement 4 __________ Measurement 5 __________
Average __________ Standard Deviation _________ < 0.1 (Y/N) ______

Initial Measurement __________ Measurement 1 __________
Measurement 2 __________ Measurement 3 __________
Measurement 4 __________ Measurement 5 __________
Average __________ Standard Deviation _________ < 0.1 (Y/N) ______

Initial Measurement __________ Measurement 1 __________
Measurement 2 __________ Measurement 3 __________
Measurement 4 __________ Measurement 5 __________
Average __________ Standard Deviation _________ < 0.1 (Y/N) ______

ELPI Samples Analysis

Barometric Pressure _________________ Relative Humidity _________________

Temperature ____________ Date _________________ Time ___________

ELPI Blank

Measurement 1 _________ Measurement 2 _________ Measurement 3 _________

ELPI Stage 1

Measurement 1 _________ Measurement 2 _________ Measurement 3 _________

Signature ___________________ Date ______ 20__
Signature ___________________ Date ______ 20__

ELPI Stage 2

Measurement 1 _____ Measurement 2 _____ Measurement 3 _____

ELPI Stage 3

Measurement 1 _____ Measurement 2 _____ Measurement 3 _____

ELPI Stage 4

Measurement 1 _____ Measurement 2 _____ Measurement 3 _____

ELPI Stage 5

Measurement 1 _____ Measurement 2 _____ Measurement 3 _____

ELPI Stage 6

Measurement 1 _____ Measurement 2 _____ Measurement 3 _____

ELPI Stage 7

Measurement 1 _____ Measurement 2 _____ Measurement 3 _____

ELPI Stage 8

Measurement 1 _____ Measurement 2 _____ Measurement 3 _____

ELPI Stage 9

Measurement 1 _____ Measurement 2 _____ Measurement 3 _____

ELPI Stage 10

Measurement 1 _____ Measurement 2 _____ Measurement 3 _____

ELPI Stage 11

Measurement 1 _____ Measurement 2 _____ Measurement 3 _____

ELPI Stage 12

Measurement 1 _____ Measurement 2 _____ Measurement 3 _____

ELPI Stage 13

Measurement 1 _____ Measurement 2 _____ Measurement 3 _____

ELPI Blank

Measurement 1 _____ Measurement 2 _____ Measurement 3 _____

Signature _____ Date _____ 20__
Signature _____ Date _____ 20__

Operator Precision Test

Date ____________ Time ___________ Operator _________________

Balance Model ___________ Balance Serial Number _________________

Calibration Date __________ Calibration Due ________________

Reference Mass Type __1 g_ Reference Mass Set Serial Number _________________

Reference Mass Set Calibration Due _______________

Initial Measurement __________ Measurement 1 ___________
Measurement 2 _____________ Measurement 3 ___________
Measurement 4 _____________ Measurement 5 ____________
Average _________ Standard Deviation _________ < 0.1 (Y/N) ______

Initial Measurement __________ Measurement 1 ___________
Measurement 2 _____________ Measurement 3 ___________
Measurement 4 _____________ Measurement 5 ____________
Average _________ Standard Deviation _________ < 0.1 (Y/N) ______

Initial Measurement __________ Measurement 1 ___________
Measurement 2 _____________ Measurement 3 ___________
Measurement 4 _____________ Measurement 5 ____________
Average _________ Standard Deviation _________ < 0.1 (Y/N) ______

Flat Sheet Filter Samples Analysis

Barometric Pressure _________________ Relative Humidity _________________

Temperature ____________ Date _________________ Time ___________

Filter Blank

Measurement 1 _________ Measurement 2 _________ Measurement 3 _________

Filter 1

Measurement 1 _________ Measurement 2 _________ Measurement 3 _________

Signature __________________ Date ______ 20__
Signature __________________ Date ______ 20__

Filter 2

Measurement 1 _____ Measurement 2 _____ Measurement 3 _____

Filter 3

Measurement 1 _____ Measurement 2 _____ Measurement 3 _____

Filter 4

Measurement 1 _____ Measurement 2 _____ Measurement 3 _____

Filter 5

Measurement 1 _____ Measurement 2 _____ Measurement 3 _____

Filter 6

Measurement 1 _____ Measurement 2 _____ Measurement 3 _____

Filter 7

Measurement 1 _____ Measurement 2 _____ Measurement 3 _____

Filter Blank

Measurement 1 _____ Measurement 2 _____ Measurement 3 _____

Signature _____ Date _____ 20__
Signature _____ Date _____ 20__

APPENDIX C

MSU ICET MTE-008 MARK 5 PILAT IMPACTOR READINESS AND OPERATION

Mark 5 Pilat Impactor Readiness and Operation

Implementation Date:
Effective Date is Immediate upon Approval Signature

Prepared By: _____ 10/17/16 **Date**

Reviewed By: _____ 10/17/16 **Date**

APPROVAL: _____ 10/17/16 **Date**

REVISION HISTORY

Revision Number	Reason for Revision	Revision By
2	Revised historical procedure to include comments from shakedown testing with Bechtel	RJ
3	Facilitate Gravimetric Analysis procedure and incorporated comments from Bechtel after document submittal	SRP
4	Incorporate comments from Bechtel	SRP & JAW
5	Revised to incorporate comments from Bechtel after document submittal	JAW

1.0 PURPOSE

The purpose of this procedure is for readying and correctly using the Pilat Mark 5 Cascade Impactor.

2.0 SCOPE

This procedure covers the steps necessary for readying and using the Pilat Mark 5 Cascade Impactor for filter testing. All impactor measurements are considered commercial grade measurements, and do not meet the requirements of ICET's NQA-1 program.

3.0 TERMS / DEFINITIONS

None

4.0 RESPONSIBILITIES

Personnel with responsibilities for implementing this procedure are:

4.1 Test Stand Operator(s)/Testing Personnel

5.0 SAFETY AND ENVIRONMENTAL CONCERNS

5.1 Safety glasses and steel toed boots are required to be worn by testing personnel in the high bay during the Large Scale Filter Testing.

5.2 Hearing protection is required if other testing is being performed in the high bay that requires hearing protection.

5.3 Testing personnel are required to wear dosimeters if SR-90 sources are installed in any of the large scale filter test stands.

6.0 EQUIPMENT

NOTE:

Measuring and Test Equipment (M&TE) used to collect data during performance of this procedure is required to be within the current calibration cycle as evidenced by an affixed calibration label and be capable of the desired range.

6.1 Pollution Control Systems Corp. Mark 5 Pilat Impactor

6.2 Nylon gloves

6.3 Grease brush

6.4 XS2002S Mettler Toledo balance
6.5 AT261 Mettler Toledo Analytical Balance
6.6 Glove box
6.7 Tweezers
6.8 Safety glasses
6.9 Teflon tape
6.10 Desiccator
6.11 Stainless Steel Substrates
6.12 Type Two Water
6.13 Drierite
6.14 Ultrasonic Bath
6.15 Oven
6.16 Mass Flow Controller

7.0 PREREQUISITES

7.1 All personnel operating the RLSTS and instrumentation contained therein shall be trained in accordance with ICET-QA-001.
7.2 Ensure all personnel performing this procedure have signed and initialed the laboratory notebook being used with this procedure.

8.0 PROCEDURE

Testing personnel shall:

8.1 Pretest preparations of the Pilat Mark 5 Cascade Impactor
8.1.1 Preparation of Substrates, Jet Stage, and Collection Plate Assembly
8.1.2 Before preparing the Pilat Mark 5 Cascade Impactor, determine the correct assembly for the testing conditions using Table 1. Acceptable percent isokinetic is ±10% of 100%.

Table 1. Impactor nozzle and flowrate selection.

Test Stand Flow Rate	Impactor Flow Rate	Inlet nozzle	Percent Isokinetic
2000 cfm	0.31 cfm	5/16 inch	109.7 %
1200 cfm	0.31 cfm	3/8 inch	94.5%

8.1.2.1 Ensure that all parts have been cleaned of any dirt and soiling material and inspect the stages for plugged jets by holding the stages up to a light and ensuring that light is seen through each of the jet stage holes.

8.1.2.2 Check the O-rings for any damage or corrosion and replace if necessary.

8.1.2.3 Ensure the stainless steel substrates are clean and have been thoroughly dried. The substrates shall be in numbered petri dishes, 1 to 11 in the desiccator. The number 1 substrate shall be a solid stainless steel foil and the rest shall be donut in shape. Include a blank of each type and place them in labeled petri dishes. The solid blank shall be labeled B1 and the donut B2.

8.1.2.4 Using the small arch punch in the lab, cut two filter coupons out of the sheet of extra HEPA media. One shall be used as the backup filter coupon in the Pilat and the other shall be the blank for the weighing procedure. Place these into labeled petri dishes F and BF. Place in the pre-conditioning chamber with the petri dishes open.

8.1.2.5 Wearing a pair of nylon gloves and grounding bracelet, remove the top of a petri dish and grease the impaction surface of the substrate with the Apiezon L grease and toluene mixture using the provided grease brush. Do not cake on or leave clumps of grease. There shall be a thin smooth layer after application. Repeat for each substrate, including blanks.

8.1.2.6 Bake the substrates at 85°C for 30 minutes and place the substrates and backup filter coupons in the desiccation chamber with the petri dishes open.

8.1.2.7 Condition and weigh the samples according to Gravimetric Analysis procedure HEPA-029. NOTE: This procedure may take up to 72 hours to complete.

8.1.2.8 Gather the impaction jet stages and the inlet and outlet end caps of the Pilat Mark 5 Cascade Impactor in the glove box.

8.1.2.9 Starting from the outlet end cap, place the filter support, metal screen, and filter collar into the outlet end cap respectively.

8.1.2.10 Place a collection plate with the number 11 substrate on top of that.

8.1.2.11 Next place an O-ring and the number 11 jet stage.

8.1.2.12 Repeat steps 8.1.1.11 and 8.1.1.12 with the number 10 substrate and jet stage and continue in that pattern until the primary impaction plate and number 1 substrate have been properly placed. Be careful not to tip over the impaction stage assembly as this shall start over the process and damage the substrates and jet stages.

8.1.2.13 After the primary collection plate and number 1 substrate have been placed, slide on and fasten the Pilat Mark 5 Cascade Impactor sheath and then screw on the inlet end cap and inlet nozzle.

8.1.2.14 Place a protective cap over the impactor inlet to prevent particle entry when not operating.

8.1.3 Preparation of condensate container

8.1.3.1 Record in Lab Notebook

8.1.3.1.1 Balance Serial Number, Model, calibration date, and calibration due date.

8.1.3.2 Ensure that the condensate container is clean.

8.1.3.3 Allow the water collection container to dry.

8.1.3.4 Weigh the condensate container with the XS2002S Mettler Toledo Balance, record the mass, and then close the top on the container.

8.2 Impactor Loading Procedure for the Pilat Mark 5 Cascade Impactor

8.2.1 Once the Pilat Mark 5 Cascade Impactor has been correctly assembled and the test stand has been prepared for testing, insert the Pilat impactor onto its mount upstream of the in-duct coupon sampling section of the test stand and remove the protective inlet cap. This shall be done before inserting the flat sheet samples.

8.2.2 Ensure that the Pilat Impactor is facing upstream and parallel to the ducting.

8.2.3 Attach the black conductive sampling tube to the outlet of the Pilat impactor that is facing towards the filter housing.

8.2.4 Ensure the water chiller is running.

8.2.5 Ensure the air line is connecting the sample probe from the Pilat Impactor to the heat exchanger that removes moisture from the air stream.

8.2.6 Ensure the mass flow controller is in calibration, plugged in and the vacuum hose is properly attached.

8.2.7 Ensure test filter media area is entered on the test stand control computer.

8.2.8 Once these steps are complete the Pilat Impactor is ready for testing.

8.2.9 Ensure the Readiness and Operation Datasheet is completed.

8.2.10 Once ready to begin sampling, measure the Barometric pressure and turn the pump on.

8.2.11 Once sampling with the Pilat Impactor is finished turn the pump off.

8.3 Impactor Unloading Procedure for the Pilat Mark 5 Cascade Impactor

8.3.1 Ensure that the in-duct coupon sampling port #2 on the in-duct coupon sampling section of the test stand has been removed.

8.3.2 Reach into the in-duct coupon sampling section of the test stand through the second in-duct coupon sampling port and remove the black conductive tubing from the outlet of the Pilat Mark 5 Cascade Impactor assembly.

8.3.3 Carefully remove the Pilat impactor from its mount and attach the protective inlet cap. Do not drop or bump the impactor assembly on the ducting or other objects in the highbay.

8.3.4 Place the Pilat impactor assembly in a safe location where it shall not roll around or fall off of a surface.

8.3.5 Detach the condensate container from the heat exchanger.

8.3.6 Carry both the Pilat impactor assembly and the condensate container to the lab for disassembly and weighing.

8.4 Sample Analysis Measurement

8.4.1 Condensate container

8.4.1.1 Record in lab notebook

8.4.1.1.1 Balance Model

8.4.1.1.2 Serial Number

8.4.1.1.3 Calibration Date

8.4.1.1.4 Calibration Due Date

8.4.1.1.5 Final mass of condensate container, filters, and blanks.

8.4.1.2 Weigh and record mass of the water inside the condensate container.

8.4.2 Pilat impactor assembly

8.4.2.1 Take the Pilat impactor assembly to the laboratory and put on nitrile gloves and the grounding bracelet.

8.4.2.2 While holding the Pilat impactor assembly upright, carefully remove the inlet nozzle.

8.4.2.3 Carefully remove the jet stage sheath. Do not tilt the assembly to either side during this step as the jet stages may fall over and damage the samples and impactors.

8.4.2.4 One by one remove the jet stages and impaction plates with the substrates on them and place to the side.

8.4.2.5 With a clean pair of tweezers remove the stainless steel substrates and back up filter and place in the correctly numbered petri dishes.

8.4.2.6 Carefully move the petri dishes to a shelf in the dessication chamber. Be sure to group them with the blanks created earlier.

8.4.2.7 During conditioning, rinse the impaction plates, jet stages, and inlet and outlet nozzles under running water to remove residual aerosol from the previous test. Dispose of and replenish the bath as needed. The jet stages and impaction plates are washed separately for 20 minutes at 60° C each for greater cleaning performance.

8.4.2.8 Condition and weigh the samples according to Gravimetric Analysis procedure HEPA-029. NOTE: This procedure may take up to 72 hours to complete. After the substrates and filters have been weighed, the substrates can be washed in the ultrasonic bath in Lab 284 and the filters can be disposed of if noticeable imperfections are present.

8.4.2.9 After washing the substrates, place them in clean petri dishes for the next test.

8.4.2.10 Enter in the recorded values from the test into the Pilat Impactor Data Sheet, print off the results, and attach to the Pilat Mark 5 Cascade Impactor Readiness and Operation Datasheet.

8.5 Additional samples for electron microscopy to be completed upon request.

8.5.1 Select suitable substrate with low background noise.

8.5.2 Prepare substrates for use in impactor stages using hole punches.

8.5.3 No weighing is required.

8.5.4 Run Pilat impactor for 10 minutes to collect a very light sample of aerosol for analysis.

9.0 RECORDS

All records are considered quality records and shall be maintained and submitted to project records in accordance with ICET-QA-010, *Quality Assurance Records*. The records included in this procedure include the following:

9.1 Pilat Mark 5 Cascade Impactor Readiness and Operation Datasheet

9.2 Laboratory Notebook

10.0 REFERENCES

10.1 Operations Manual Pilat (University of Washington) Mark 3 and Mark 5 Source Test Cascade Impactor

10.2 EPA Reference Method 1 "Sample and Velocity Traverse for Stationary Sources"

10.3 EPA Reference Method 2 "Determination of Stack Gas Velocity and Volumetric Flow Rate (Type S Pitot Tube)"

10.4 EPA Reference Method 5 "Determination of type Particulate Emissions from Stationary Sources"

10.5 ICET-QA-010, *Quality Assurance Records.*

11.0 ATTACHMENTS

11.1 Pilat Mark 5 Cascade Impactor Readiness and Operation Datasheet

Attachment 1

Pilat Mark 5 Cascade Impactor Readiness and Operation Datasheet

1. ID/Serial No. of filter to be tested _____
2. Test date _____
3. Run ID No. _____

Notes:

_____
_____
_____
_____
_____
_____
_____
_____
_____
_____
_____
_____
_____
_____
_____

_____	_____	_____	_____
Operator Name (Print)	Initials	Operator Signature	Date

APPENDIX D

MSU ICET HEPA-RLSTS-15 ISOKINETIC SAMPLER ASSEMBLY REMOVAL AND INSTALLATION

In-duct Coupon Particle Loading Test System (ICTS) Sampler Housing Removal and Installation

Implementation Date:
Effective Date is Immediate upon Approval Signature

Prepared By: John Wilson — 5/20/16 **Date**

Reviewed By: [signature] — 5/20/16 **Date**

APPROVAL: [signature] — 5/20/16 **Date**

REVISION HISTORY

Revision Number	Reason for Revision	Revision By
0	Initial Issue after shakedown testing with Bechtel	JAW
1	Updated to incorporate comments from Bechtel after document submittal	JAW
2	Incorporated comments from Dr. Bergman section 7.4.1 and MSU comments.	JAW

1.0 PURPOSE

The purpose of this procedure is to ensure proper preparation of samples for in-duct coupon sampling with flat sheet media and proper installation and removal of the in-duct coupon samplers in the Radial Flow Large Scale Test Stand (RLSTS).

2.0 SCOPE

This procedure involves the in-duct coupon sampler preparation and the installation and removal of the flanges onto the duct section of the RLSTS.

3.0 TERMS / DEFINITIONS

3.1 ICTS – In-duct Coupon Particle Loading Test System
3.2 RLSTS – Radial Flow Large Scale Test Stand
3.3 PPE – Personal Protective Equipment (see 5.0 and 6.0)

4.0 RESPONSIBILITIES

Staff with responsibilities for implementing this procedure are:
4.1 Test Stand Operator(s)/Test Personnel

5.0 EQUIPMENT

5.1 Safety Glasses
5.2 Work Gloves
5.3 Dual ratcheting combination wrench
5.4 8 inch diameter gaskets (4)
5.5 Numbered petri dishes (7)
5.6 Clean shop towel
5.7 Clean tweezers
5.8 Nitrile gloves

6.0 SAFETY AND ENVIRONMENTAL CONCERNS

6.1 Aerosol hazards are present in the high bay. Powdered aerosols, dust, test aerosols, etc. Safety glasses are required in the high bay during testing.
6.2 Personal dosimeters are required for testing personnel in the high bay when sources are installed in the neutralizer section of any test stand.

6.3 Steel toed boots or shoes are required for testing personnel working in the high bay.
6.4 Hearing protection is required if work is being performed with the impact wrench in the high bay or if the fan on the resistance to liquid pressure test stand is in operation.
6.5 If the RLPTS or the FI test stand are in use, hard hats are required past the signage.
6.6 Work gloves are required while attaching and detaching bolts from the RLSTS.

7.0 PREREQUISITES

7.1 All personnel operating the RLSTS and instrumentation contained therein shall be trained in accordance with ICET-QA-001.
7.2 All personnel shall be familiar with this procedure, HEPA-RLSTS-015.

8.0 TEST SYSTEM REMOVAL AND INSTALLATION PROCEDURE.

Test stand operators /test personnel shall:

8.1 Preparation of the ICTS sampling flanges

8.1.1 Ensure that the in-duct coupon sampling cones are free of visible aerosol contamination. Wipe down the exterior, interior, and the sampling port of the nozzle with a clean shop towel.
8.1.2 Ensure that the coupon holder is free of aerosol contamination. If the aerosol bypassed the in-duct coupon media, clean the coupon support screen and check the downstream vacuum tube for aerosol contamination.
8.1.3 Clean the O-ring by wiping with a clean shop towel and check for any imperfections prior to re-using.
8.1.4 If coupon support screen was removed for cleaning, place back into sampler base.
8.1.5 Wear nitrile gloves prior to handling the in-duct coupon media samples located in the numbered petri dishes.
8.1.6 Using a pair of clean tweezers, remove a coupon and carefully place into the sampler base. Ensure that the coupon is properly centered to prevent vacuum leak or unintended aerosol bypass. Ensure coupon is placed in sampler with the corresponding number to the petri dish the coupon was removed from. Take photo of the media sample on the sampler. See Figure 1 for example of in-duct coupon on the sampler.

8.1.7 Using the tweezers, place the O-ring onto the coupon, ensuring that the O-ring is properly centered.

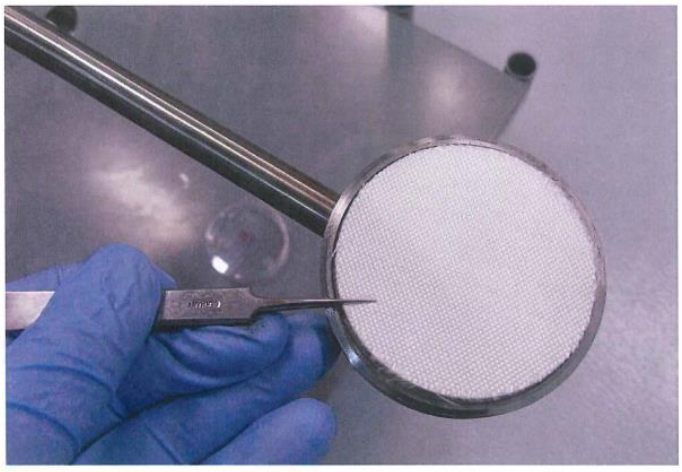

Figure 1. Installing in-duct coupon on sampler

8.1.8 Carefully place the in-duct coupon sampling cone on top of the O-ring and take precaution that the knife-edge does not deform or cut into the O-ring when placing.

8.1.9 Screw on the knurled retaining collar onto the sampling base until the collar is snug to secure the in-duct coupon sampling cone.

8.1.10 Repeat Steps 8.1.6 through 8.1.9 on sampling flanges two through four.

8.2 Leak check of the in-duct coupon sampler

8.2.1 Connect the end of the sampler to one of the in-duct coupon vacuum lines.

8.2.2 Set the flow rate on the corresponding mass flow controller to _____ (This corresponds to 5 ft/min face velocity)

8.2.3 Verify that the dP on the in-duct coupon is the same as the dP of the corresponding media tested in the vertical test stand at the same face velocity.

8.3 Installation of the ICTS sampling flanges

8.3.1 Ensure all personnel participating in the ICTS installation are wearing the proper PPE.

8.3.2 Unlock the correct holding rack's wheel locks by pressing down on the "OFF" levers on two wheels.

8.3.3 Move the holding rack closer to the RLSTS ducting to be properly attached to the upstream section containing the ports for the sampling flanges.

8.3.4 For sampler one, place the gasket on the top port and slowly lower the sampling flange. Ensure that the sampling cone is facing upstream. The locations of the samplers on the test duct are shown in Figure 2.

8.3.5 The sample locations are as follows: Sample 1 is on the top, Sample 2 faces the water tank, Sample 3 is on the bottom and sample 4 faces the RLPTS.

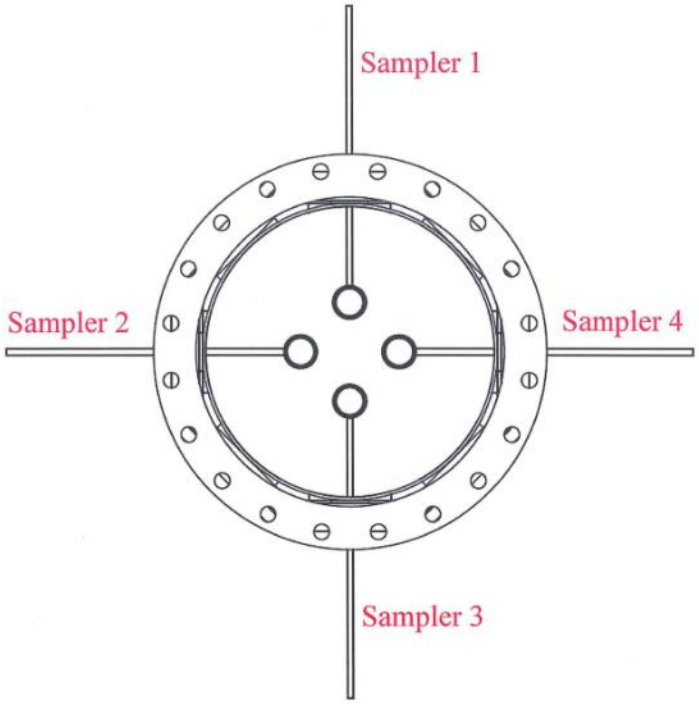

Figure 2. Sampling Section with Sampler Locations.

8.3.6 There is a mark on the outside of the flange showing the direction (Figure 3).

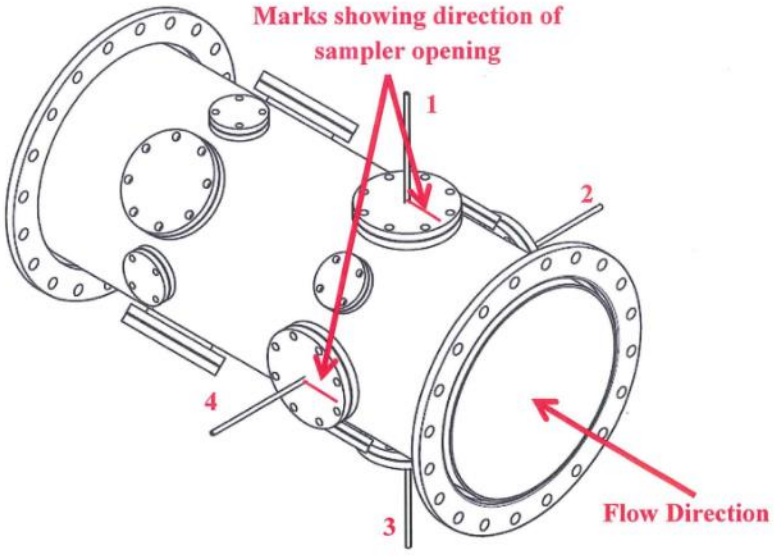

Figure 3. ICTS Testing Section

8.3.7 For samplers two and four, place two bolts on bottom of the sampling flange and slide a gasket into place. Be careful not to rotate the sampling cones during installation. Ensure the sampling cones are facing upstream.

8.3.8 For sampler three, the bottom duct, place a gasket between the flange and the duct, and thread the bolts to retain the flange in place. Ensure the sampling cone is facing upstream.

8.3.9 Snugly tighten the four bolts onto the flange using the dual ratcheting combination wrench.

8.3.10 Slide the vacuum tubing onto the stainless steel sampler tubes and tighten nut to secure in place. See Figure 4 for picture of vacuum tubing on the end of the sampler.

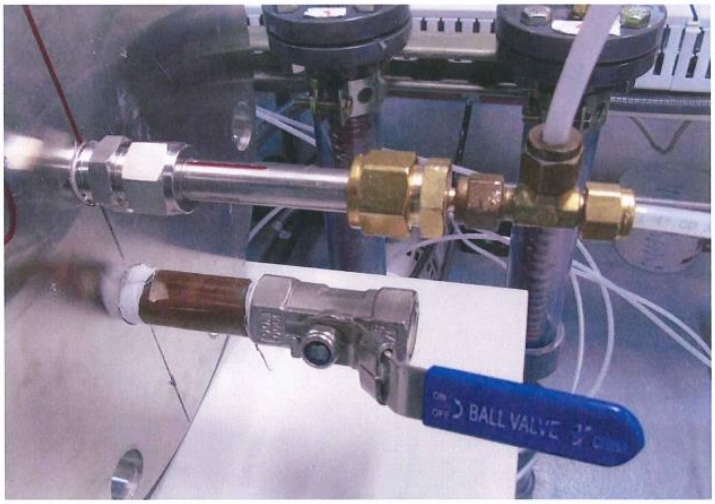

Figure 4. Vacuum tubing attached to end of sampler.

8.4 Ensure the ICTS is already installed on the RLSTS test stand. Figure 5 shows the location of the ICTS on the test stand.

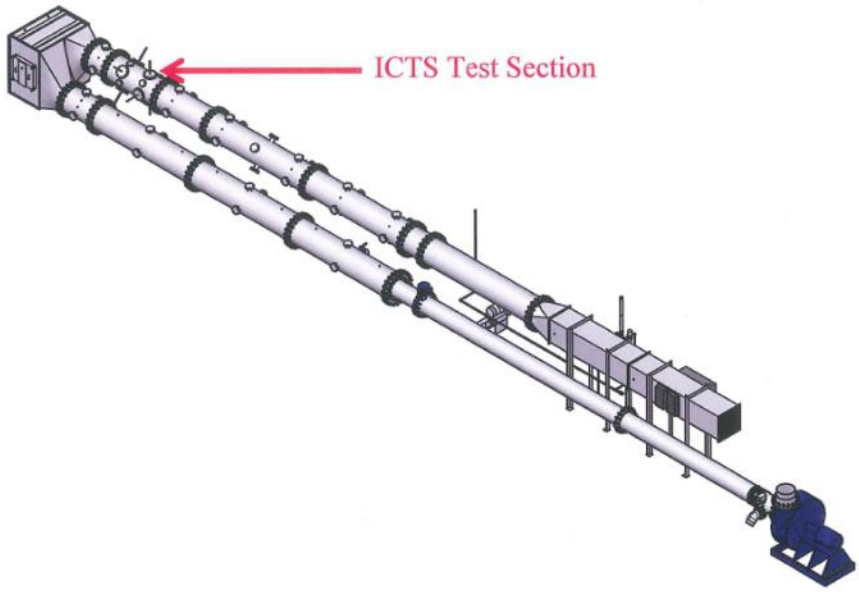

Figure 5. Location of the ICTS Section of the Test Duct.

8.5 Removal of ICTS sampling flanges

8.5.1 Ensure that all personnel participating in the ICTS removal procedure are wearing the proper PPE.

8.5.2 Ensure the vacuum pump connected to the ICTS is off.

8.5.3 Remove the vacuum line connected to each sampling tube.

8.5.4 Using the dual ratcheting combination wrenches found in the highbay, loosen and remove all bolts holding the ICTS flanges to the RLSTS ducting using an opposing clockwise pattern ensuring that one half of the bolts are not removed before the other.

8.5.5 With assistance of personnel holding the flange, carefully remove the bolts holding the flanges in place. Remove and place each ducting gasket to the side and out of the way of potential damage.

8.5.6 Place the sampling flanges in numerical order (from left to right) on the holding rack with in-duct coupon sampling nozzles facing upwards to prevent confusion.

8.5.7 Using an appropriate number of testing personnel, safely move the sampling flanges to an appropriate location in the highbay out of the way of testing.

8.5.8 Lock the holding rack's wheels by pressing down on the "ON" levers on two wheels.

8.6 Removal of the in-duct coupon samplers

8.6.1 Ensure that the in-duct coupon sampling cones are free of visible aerosol, capable of contaminating the specimen inside the sampler.

8.6.2 If aerosol contamination is visible, wipe down the exterior of the in-duct coupon sampling cone with a clean shop towel.

8.6.3 Carefully unscrew the knurled collar holding the in-duct coupon sampling cone in place. See Figure 6 for picture of the knurled collar.

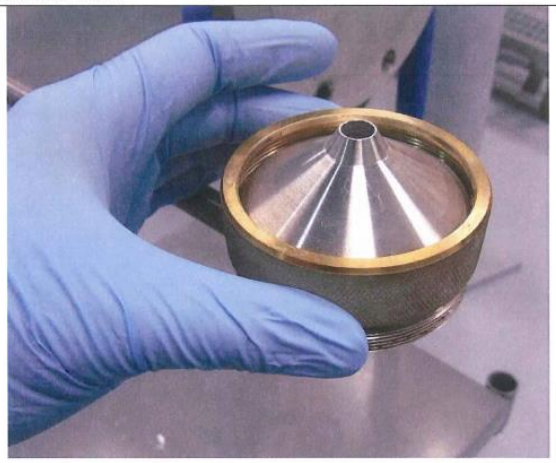

Figure 6. Installing knurled collar for the in-duct sampler.

8.6.4 Remove the collar and set it aside.
8.6.5 Wear nitrile gloves while handling the loaded specimen.
8.6.6 Slowly lift the in-duct coupon sampling nozzle and place aside.
8.6.7 Remove O-ring with tweezers.
8.6.8 Using a pair of clean tweezers, carefully remove the original media coupon. Take extra precaution to prevent the disturbance of the filter cake.
8.6.9 Open a petri-dish with its corresponding sampler number and place inside the dish. See Figure 7 for a picture of the numbered petri dish.

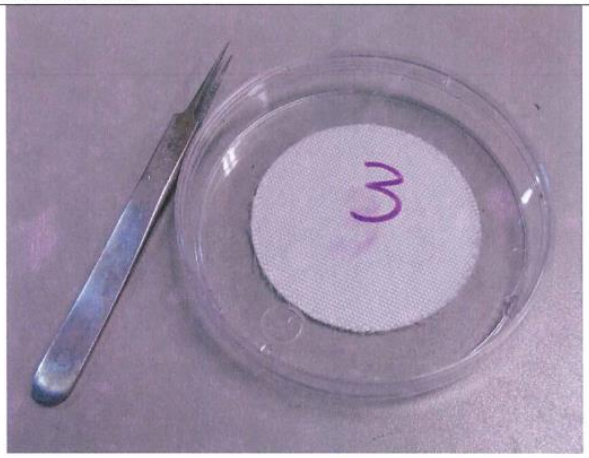

Figure 7. Numbered petri dish for in-duct coupons.

8.6.10 Cover the dish and place aside for conditioning at ambient conditions and weighing.

8.6.11 Samples need to be cut and analyzed for deposit height and depth penetration.

8.7 After testing is complete save pictures from camera of in-duct coupons to filter specific drive.

9.0 RECORDS

All records are considered quality records and shall be maintained and submitted to project records in accordance with ICET-QA-010, *Quality Assurance Records*.

The records produced by this procedure include the following:

9.1 Test Notebook

9.2 Test Control Document

10.0 REFERENCES

10.1 None

11.0 ATTACHMENTS

11.1 None